

Heterotrimeric G-protein Interactions and Activation in Chemokine Receptor 5 Signalling

Jason Stuart Kerr

**A Thesis Presented for the Degree of Doctor of
Philosophy at the University of East Anglia,**

Norwich, UK

April 2010

©This copy of the thesis has been supplied on the condition that anyone who consults it is understood to recognise that its copyright rests with the author and that no quotation from the thesis, nor any information derived there from, may be published without the author's prior, written consent.

Table of Contents

TABLE OF CONTENTS	1
LIST OF FIGURES	4
ABSTRACT	7
ABBREVIATIONS	8
PUBLICATIONS	12
CONFERENCE AND POSTER ABSTRACTS	12
ACKNOWLEDGEMENTS	14
CHAPTER ONE	15
INTRODUCTION	15
1.1 G-PROTEIN COUPLED RECEPTORS	15
1.1.2 <i>CCR5 Structure and Function</i>	18
1.1.2.1 Extracellular Domains.....	21
1.1.2.2 Intracellular Domains	22
1.1.2.3 CCR5 Chemokine Ligands	23
1.1.3 <i>Heterotrimeric G-Protein Structure</i>	25
1.2 DOWNSTREAM EFFECTORS OF G-PROTEINS	30
1.2.1 <i>Gα subunit signalling</i>	30
1.2.2 <i>G$\beta\gamma$ Subunit Signalling</i>	33
1.2.3 <i>G-protein Mediated Calcium Release</i>	34
1.2.4 <i>G-protein mediated cAMP Regulation</i>	36
1.2.5 <i>CCR5 Mediated Cytoskeleton Reorganisation</i>	37
1.2.6 <i>G-protein Interactions with Other Signalling Pathways</i>	38
1.3 METHODS TO INFER AND MONITOR PROTEIN-PROTEIN INTERACTIONS	40
1.3.1 <i>Indirect Methods</i>	40
1.3.1.1 Small Interfering Ribonucleic Acids	41
1.3.2 <i>Direct methods</i>	42
1.4 FLUORESCENCE AND BIOLUMINESCENT RESONANCE TRANSFER	44
1.4.1 <i>Fluorescence proteins for FRET</i>	45
1.4.2 <i>Living System FRET measurements</i>	46
1.4.3 <i>Bioluminescence Resonance Energy Transfer</i>	48
1.5 <i>Aims and Hypothesis</i>	49
CHAPTER TWO	50
MATERIALS AND METHODS	50
2.1 CELL CULTURE	50
2.1.1 <i>Routine Conditions</i>	50
2.2 CALCIUM FLUX MEASUREMENTS.....	52
2.2.1 <i>Fura-2 loading</i>	52
2.2.2 <i>Ratiometric Measurement of Calcium Release</i>	53
2.3 SPECTROPHOTOMIC AND STATISTICAL DATA ANALYSIS	53
2.3.1 <i>Calcium Flux Analysis</i>	54
2.3.2 <i>FRET and BRET Analysis</i>	54
2.3.3 <i>Concentration Response Curve Fitting and Analysis</i>	55
2.4 FLUORESCENCE MICROSCOPY	56
2.4.1 <i>Slide Preparation for CCR5 and Fusion Protein Visualisation</i>	56
2.4.2 <i>siRNA Transfection Visualisation</i>	57
2.5. CLONING AND MOLECULAR BIOLOGY TECHNIQUES	58

2.5.1 Plasmids.....	58
2.5.2 Primers.....	58
2.5.3 Transformation of DH5 α	59
2.5.4 Plasmid Isolation (analytical).....	59
2.5.4.1 Plasmid isolation (amplification)	60
2.5.4 Plasmid Digestion	61
2.5.5 DNA Separation and Purification.....	61
2.5.5 Polymerase Chain Reaction	62
2.5.6 Phosphatase Treatment of Sequences	62
2.5.7 Purification of DNA after Enzymatic reactions	63
2.5.8 Ligation.....	63
2.6 TRANSFECTION	63
2.6.1 Transfection of DNA.....	63
2.6.2 Transfection of siRNA	64
2.6.3 Transfection Reagents and Volumes	64
2.7 WESTERN BLOTTING.....	65
2.7.1 Protein Extraction and Preparation	65
2.7.2 SDS-PAGE Gel Electrophoresis and Protein Transfer	65
2.7.3 Immunoblotting and Development.....	66
2.7.4 Antibodies for Immunoblotting	67
2.8 CAMP MEASUREMENT	68
CHAPTER THREE	69
CREATION AND CHARACTERISATION OF CELLS STABLY EXPRESSING TAGGED G-PROTEINS	69
3.1 INTRODUCTION.....	69
3.2 RESULTS.....	71
3.2.1 Creation of Plasmids for HEK.CCR5 Stable Expression	73
3.2.2 Selection of Stable Single Expression HEK.CCR5	75
3.2.3 Characterisation of Stable HEK.CCR5 Single Transfectants	76
3.2.4 Creation of HEK.CCR5 EYFP-G β_1 G α_{i2} -ECFP	78
3.2.5 Characterisation of Dual Fluorescence HEK.CCR5	79
3.3.1 Creation of Plasmids for Stable Expression in CHO.CCR5	84
3.3.2. Selection of Stable Single Expression Cell Lines	87
3.3.3 Characterisation of CHO.CCR5 Stable Single Transfectants.....	89
3.3.4 Creation and Characterisation of CHO.CCR5 Stably expressing pcDNA6/V5-His:G α_{i2} -ECFP/pZeo SV2:EYFP-G β_1	91
3.4 DISCUSSION	95
CHAPTER FOUR	103
MONITORING HETEROTRIMER ACTIVATION BY CCR5 WITH FRET	103
4.1 INTRODUCTION.....	103
4.2 RESULTS.....	105
4.2.1 Sodium Butyrate Treatment of CHO.CCR5.Y/C	106
4.2.2 Fluorescent Emission in Following CCL3 Stimulation	108
4.2.3 CHO.CCR5.Y/C Exhibit variation in their FRET Ratio	110
4.2.4 Kinetics of G α_{i2} Activation by CCR5	112
4.3 DISCUSSION	120

CHAPTER FIVE	127
DEVELOPMENT OF A BRET ASSAY TO MEASURE $G\alpha_{i2}$ $G\beta_1$ INTERACTION	127
5.1 INTRODUCTION	127
5.2 RESULTS	129
5.2.1 <i>Creation of pcDNA3.1:hrLuc-$G\alpha_{i2}$</i>	129
5.2.2 <i>Optimisation of hrLuc Transient Transfection</i>	130
5.2.3 <i>Dual Transient Transfection</i>	131
5.2.4 <i>Substrate Kinetics and BRET</i>	133
5.3 DISCUSSION	136
CHAPTER SIX	140
THE IMPACT OF MUTANT FORMS OF $G\alpha$ ON CCR5 SIGNALLING	140
6.1 INTRODUCTION	140
6.2 RESULTS	143
6.2.1 <i>The Expression of DNM $G\alpha_{i2}$, CAM $G\alpha_{i2}$, and $G\alpha_{12}$ Result in Increased Basal Calcium Levels.</i>	143
6.2.1.1 <i>The Expression of DNM $G\alpha_{i2}$, CAM $G\alpha_{i2}$, and $G\alpha_{12}$ Effect Speed and Quantity of CCL3 Stimulated Calcium Mobilisation</i>	145
6.2.2.1 <i>Effects of systematic knockdown of $G\alpha$ subunits</i>	147
6.2.2.2 <i>$G\alpha_{i2}$ is not Involved in CCR5 Mediated Calcium Mobilisation</i>	149
6.2.2.3 <i>Knockdown of $G\alpha_q$ Increases CCL3 Potency but not Efficacy</i>	149
6.2.2.4 <i>Combination Knockdown Results in a Decrease in Efficacy</i>	152
6.3 DISCUSSION	155
CHAPTER SEVEN	163
SMALL MOLECULE INTERFERENCE OF $G\beta\gamma$ SUBUNITS	163
7.1 INTRODUCTION	163
7.2 RESULTS	165
7.2.1 <i>Gallein Enhances CCR5 Mediated Calcium Release</i>	165
7.2.1.2 <i>Gallein Treatment Results in Enhanced CCL3 Efficacy but not Potency</i>	166
7.2.2 <i>Gallein's Effects are not Cell Type Specific</i>	167
7.2.3 <i>Gallein Treatment Increases resting cAMP Levels</i>	169
7.3 DISCUSSION	171
CHAPTER EIGHT	177
SUMMARY	177
8.1 EXPLORING G-PROTEIN INTERACTIONS WITH RESONANCE ENERGY TRANSFER	177
8.2 INTERFERENCE OF CCR5 G-PROTEIN SIGNALLING	180
8.3 SMALL MOLECULE DISRUPTION OF G-PROTEIN INTERACTIONS	182
8.4 CROSSTALK IN CCR5 SIGNALLING PATHWAYS	183
8.5 CONCLUSIONS	184
REFERENCES	186

List of Figures and Tables

CHAPTER ONE

Figure 1.1.	Schematic Representation of CCR5	18
Figure 1.2.	2D Schematic Representation of CCR5	20
Table 1.1.	Chemokine Receptors and their Ligands	24
Figure 1.3.	Protein Explorer Model of G α i	26
Figure 1.4.	Protein Explorer Model of G β γ	28
Table 1.2.	Activators and Inhibitors of Adenylyl Cyclase	32
Figure 1.5.	CCR5 Signalling Pathways	39
Figure 1.6.	Absorbance and Fluorescence Spectra for ECFP and EYFP	47

CHAPTER TWO

Table 2.1.	Combinations of Filters Used for Different Experimental Procedures	55
Table 2.2.	Antibodies Used for CCR5 Immunofluorescent Staining	57
Table 2.3.	Primers Details	58
Table 2.4.	Reagents and Ratios for Plasmid DNA Transfections	64
Table 2.5.	Reagent and Ratios for siRNA Transfections	64
Table 2.6.	Primary Antibody Details	67
Table 2.7.	Secondary Antibody Details	67

CHAPTER THREE

Table 3.1.	Stable Cell Lines Created and the Plasmids Used	70
Figure 3.1.	Schematic Representations of the Plasmids Produced and Transfected.	72
Figure 3.2.	Stable Cell Line Images	75
Figure 3.3.	Stable Cell Line Concentration Response Curves	77
Table 3.2.	Log EC ₅₀ Values for HEK.CCR5.Y/C.	79
Figure 3.4.	Characterisation of HEK.CCR5.Y/C.	83
Figure 3.5.	Fluorescent Microscopy Images of HEK.CCR5.Y/C.	83
Figure 3.6.	Schematic Representations of the Plasmids Produced and Transfected	85
Figure 3.7.	Analytical Digests of pZeo SV2:EYFP-G β 1.	86
Figure 3.8.	Analytical Digests of pcDNA6/V5-his: G α i2-ECFP	86
Figure 3.9.	Fluorescent Microscope Images of Single Stable Transfectants	88
Figure 3.10.	Concentration Response Curves for CHO.CCR5 Single Transfectants	90
Figure 3.11.	Characterisation of CHO.CCR5 Y/C	93
Figure 3.12.	Fluorescent Microscopy Images of CHO.CCR5 Y/C.	94

CHAPTER FOUR

Table 4.1.	Buffer Composition and CHO.CCR5 Autofluorescence	105
Figure 4.1.	Fluorescence Measurement NaBu Treated Cell Populations	107
Table 4.2.	Fluorescence Values for CHO.CCR5 and CHO.CCR5.Y/C	107
Figure 4.2.	Emission Traces for CHO.CCR5.Y/C	109
Figure 4.3.	FRET Ratio Measurements	111
Figure 4.4.	FRET Measurement of G α i2 β 1 γ Dissociation	113
Figure 4.5.	FRET Measurement of Pertussis Toxin Treated CHO.CCR5.Y/C	114
Figure 4.6.	NaBu Effect on FRET Ratios in CHO.CCR5.Y/C	116
Figure 4.7.	FRET Measurement of Mastoparan Treated CHO.CCR5.Y/C	117
Figure 4.8.	Mastoparan Prestimulation FRET Ratios	119

CHAPTER FIVE

Figure 5.1.	Expression of rLuc-G α i2 in CHO.CCR5	130
Figure 5.2.	Expression Levels of rLuc and EYFP in CHO.CCR5	132
Figure 5.3.	Luminescence and Fluorescence Levels Following.	133
Table 5.1.	Proportional Emission of Transiently Transfected CHO.CCR5	134
Figure 5.4.	Proportional Emission of Double Transfected CHO.CCR5	135

CHAPTER SIX

Figure 6.1.	Effect of Transient Transfection of DNM and CAM	144
Figure 6.2.	DNM and CAM effect on CCR5 Mediated Calcium Flux	145
Figure 6.3.	DNM and CAM Effect on Rapidity of Calcium Flux	146
Figure 6.4.	Calcium Mobilisation after G α Knockdowns	148
Table 6.1.	Corresponding Values for Figure 6.4.	148
Figure 6.5.	Western Blots Showing Protein Expression for CCR5 and G α i2..	150
Figure 6.6.	Concentration Response Curve for HeLa RC-49 G α i2 Knockdown	150
Figure 6.7.	Western Blots Showing Protein Expression for CCR5 and G α q.	151
Figure 6.8.	Concentration Response Curve for HeLa RC-49 G α q Knockdown..	151
Figure 6.9.	Concentration response Curve for HeLa RC-49 G α q/G α i1 Knockdown.	153
Table 6.2.	Knockdown Induced Changes to CCL3 efficacy and potency in HeLa RC-49 cells	154

CHAPTER SEVEN

Figure 7.1.	Gallein Effect on CCR5 Mediated Calcium Release.	165
Figure 7.2.	Gallein Increases CCL3 Efficacy Through the CHO.CCR5 Receptor.	166
Figure 7.3.	Gallein Increases CCL3 Stimulated Calcium Mobilisation	167
Figure 7.4.	Gallein Increases CCL3 Efficacy Through the CCR5 Receptor	168
Figure 7.5.	Gallein Increases Resting Levels of cAMP in HeLa RC-49	169
Table 7.1.	Gallein induced changes to CCL3 concentration response	170
Figure 7.6.	Schematic of Cellular Interactions Leading to Calcium Mobilisation and Potential Sites that Gallein may Interfere With	176

Abstract

Activation of the G-protein coupled receptor (GPCR) chemokine receptor 5 (CCR5) has been shown to result in activation of the $G\alpha_i$ family of heterotrimeric G-proteins. However, little is currently known about the temporal characteristics of G-protein heterotrimer activation by CCR5. Furthermore, this simplistic model does not account for the range of changes CCR5 activation brings about. Recent evidence suggests that GPCRs may be able to signal through numerous permutations of heterotrimer.

In order to assess G-protein activation and interaction with CCR5 functional stably transfected cell lines were created expressing $G\alpha_{i2}$ fused to ECFP and $G\beta_1$ fused to EYFP. The interaction of these constructs was confirmed by measuring fluorescent resonance energy transfer (FRET). Stably transfected cells exhibited a FRET ratio of 2.63% ($\pm 0.345\%$, $n=3$) over that of control cells. Following CCR5 stimulation with CCL3, $G\alpha_{i2}\beta_1\gamma$ activation could be monitored in real time, in whole cell populations, on a fluorescent plate reader by monitoring FRET emissions. This assay system represents a novel approach to measuring G-protein activation which can be used as a foundation to build more powerful FRET based assays. Measurement of G-protein interactions was further investigated by BRET based studies.

Transfection of dominant negative and constitutively active G-proteins alongside siRNA knockdown of G-proteins revealed that CCR5 is capable of signalling through other members of the $G\alpha_i$ family, with strikingly similar efficacy and potency to CCL3 stimulation. Dual knockdown of $G\alpha_i$ subunits and $G\alpha_q$ resulted in much attenuated calcium release following CCL3 stimulation, providing evidence that CCR5 may functionally couple to several types of G-proteins. Findings also support the theory that GPCRs can participate in domain swapping in order to rescue function.

Treatment with gallein resulted in higher resting cytosolic cAMP but did not prevent CCR5 mediated inhibition of cAMP production. Gallein treatment also resulted in significant increases in calcium release following CCR5 activation, highlighting $G\beta\gamma$ as a potential target for modulating CCR5 signalling events. Data herein emphasize the complexity of GPCR signalling, and also provide a foundation for exploring GPCR signalling using fluorescence resonance energy transfer methods in the future.

Abbreviations

AC	Adenylyl Cyclase
AGS8	Activator of G-protein Signalling 8
ATP	Adenosine Triphosphate
B ₂ -AR	Beta 2 Adrenergic Receptor
BiFC	Bimolecular Fluorescence Complementation
BRET	Bioluminescent Resonance Energy Transfer
Ca ²⁺	Calcium
CaM	Calmodulin
CAM	Constitutatively Active Mutant
CAF	Calcium Flux Buffer
cAMP	Cyclic Adenosine MonoPhosphate
cE	Calculated Efficacy
CIP	Calf Intestinal Phosphatase
CCR5	Chemokine Receptor 5
cDNA	Complementary Deoxyribonucleic Acid
CHO	Chinese Hamster Ovary
CHO.CCR5	Chinese Hamster Ovary Expressing Chemokine Receptor 5

CHO.CCR5.Y/C	Chinese Hamster Ovary Expressing Chemokine Receptor 5 and $G\alpha_{i2}$ -ECFP, EYFP- $G\beta_1$
DAG	Diacylglycerol
DAPI	4',6-diamidino-2-phenylindole
DNM	Dominant Negative Mutant
DMEM	Dulbecco's Modified Eagle Medium
DMSO	Dimethyl Sulphoxide
ECFP	Enhanced Cyan Fluorescent Protein
EDTA	Ethylenediaminetetraacetic acid.
EYFP	Enhanced Yellow Fluorescent Protein
FAD	Flavin Adenine Dinucleotide
FAK	Focal Adhesion Proteins
FCS	Fetal Calf Serum
FRET	Fluorescent Resonance Energy Transfer
Fura2AM	Acetoxymethyl 2-[5-[bis[(acetoxymethoxy-oxo-methyl)methyl]amino]-4-[2-[2-[bis[(acetoxymethoxy-oxo-methyl)methyl]amino]-5-methylphenoxy]ethoxy]benzofuran-2-yl]oxazole-5-carboxylate.
G418	Geneticin
GDP	Guanine Diphosphate
GFP	Green Fluorescence Protein

GTP	Guanine Triphosphate
GPCR	G-protein coupled receptor
GRK	G-Protein Receptor Kinase
HBSS	Hank's Balanced Salt Solution
HEK	Human Embryonic Kidney
HeLa	Helen Lane derived cell line
HEPES	2-[4-(2-hydroxyethyl)piperazin-1-yl]ethanesulfonic acid
IBMX	Isobutylmethylxanthine
IP3	Inositol 1,4,5-trisphosphate
IP3R	Inositol 1,4,5 trisphosphate receptor
JAK	Janus Kinase
NaBu	Sodium Butyrate
NADPH	Nicotinamide Adenosine Dinucleotide Phosphate
PBS	Phosphate Buffered Saline
PCA	Protein Complementation Assays
PDE	Phosphodiesterase
PH	Pleckstrin Homology
PI3K	Phosphoinositide 3-Kinase
PIP2	Phosphatidylinositol 4,5-bisphosphate

PIP3	Phosphatidylinositol (3,4,5)-trisphosphate
PKA	Protein Kinase A
PKC	Protein Kinase C
PLC	Phospholipase C
PTEN	Phosphatase and Tensin Homolog
PTX	Pertussis Toxin
RCF	Relative Centrifugal Force
RGS	Regulator of G-protein Signalling
RISC	RNA Induced Silencing Complex
ROS	Reactive Oxygen Speices
rLuc	Renilla Luciferase
RPM	Revolutions per Minute
siRNA	Small Interferring RiboNucleic Acid
SOCs	Store-Operated Calcium Channels
STAT	Signal Transducers and Activator of Transcription
TAE	TRIS Acetate EDTA Buffer
TM	Transmembrane
TRITC	Tetramethyl Rhodamine Iso-Thiocyanate
Y2H	Yeast Two Hybrid

Publications

CCR5 internalisation and signalling have different dependence on membrane lipid raft integrity, Clara Moyano Cardaba, **Jason S. Kerr**, Anja Mueller (2008) Cellular Signalling 20:1687-1694.

Conference and Poster Abstracts

School of Biology Research Colloquium, Poster Presentation.

Detection of G-protein Activation using FRET. **Jason S. Kerr** and Anja Mueller, The School of Biological Sciences, University of East Anglia, United Kingdom, July 2007

The Post Graduate Showcase, Poster Presentation and Oral Presentation.

Talking Cells. **Jason S. Kerr**, The Forum, Norwich, United Kingdom, September 2008.

Winner, Vice-Chancellors Award for a Research Presentation

The School of Chemical Sciences and Pharmacy Post Graduate Symposium, Poster Presentation

Exploring CCR5 Multiplicity. **Jason S. Kerr** and Anja Mueller, John Innes Conference Centre, Norwich, United Kingdom, September 2008. **Winner, Best Poster**

The 3rd Focused Meeting on Cell Signalling, British Pharmacological Society, Poster Presentation

Functional Selectivity of CCR5 Interaction with Heterotrimeric G-proteins, **Jason S. Kerr** and Anja Mueller, University of Leicester, United Kingdom, April 2009

34th Federation of European Biosciences Congress, Life's Molecular Interactions, Poster Presentation.

Functional Selectivity of CCR5 Interaction with Heterotrimeric G-proteins, **Jason S. Kerr** and

Anja Mueller, Prague, Czech Republic, July 2009

Acknowledgements

I'd like to express my appreciation for the help and support I have received from my supervisor, Anja Mueller, and my friend and colleague Clara Moyano-Cardaba. I would like to thank the school of Chemical Sciences and Pharmacy for providing the funding that made my tenure as a Ph.D. student possible.

I have discovered the Ph.D. process to be a lonely at times, but along the way have found solace in other like minded individuals who were able to share their experiences, advice, and more importantly, provide good company in the pub. Thank you to Peter Sidaway, Colin Kay, Neil Sparshott, Megan Murray, the UEA Squash Club 2007-2008, and again, Clara Moyano for fulfilling that important role.

A colossal acknowledgement of my gratitude must go to Zoe Remsbery, who as well as teaching me about the gothic novel and dramatic devices used in Educating Rita, has also taught me to appreciate the correct use of the comma, helped me make written sense of my scientific ideas and provided unparalleled support for me throughout the Ph.D. process – Thank you.

Finally, it gives me vast pleasure to thank my mum and brother for helping to make me who I am. They have both provided me with a library of life experiences and good advice that has helped me to succeed and achieve.

Chapter One

Introduction

1.1 G-Protein Coupled Receptors

G-protein coupled receptors (GPCR) are a diverse family of transmembrane receptor proteins that work in concert with guanine nucleotide regulated proteins (G-proteins) (Oldham *et al.*, 2007). GPCRs play important roles in cellular signalling networks involving processes such as neurotransmission, cellular metabolism, secretion, cellular differentiation and growth, inflammatory and immune responses, smell, taste and vision (McCudden *et al.*, 2005). This superfamily of proteins is of importance in understanding many human diseases, and has been proved to be one of the most attractive targets for drug development and targeting (Henry, 2004). The breadth of physiological activities controlled by GPCRs is, in part, due to the wide range of ligands that interact with receptors of this class, as well as the number of different G-proteins to which they can be coupled. GPCRs status as a major class of receptor linked to signalling proteins that modulate a variety of biological functions, make them an attractive target for drugs. All members of the GPCR superfamily possess seven transmembrane (TM) spanning α helices with an extra cellular N-terminus and an intracellular C-terminus. The seven TM region of the receptor are bundled together in a circular fashion to help facilitate ligand recognition and binding (Kristiansen, 2004). Each receptor has alternating intra and extra cellular loops which can vary in length depending on the receptor type. The three extracellular loops and the N-terminus are important for ligand specificity and binding, the intracellular loops and C-terminus are thought to be responsible for G-protein specificity (Moller *et al.*, 2001), β -arrestin binding (Tohgo *et al.*, 2003) and G-protein activation (Oppermann, 2004). These

obvious structural differences allow for variation in the outcome of intracellular signalling and allow ligand specificity to be carried through to G-protein binding.

Recent crystallographic studies of the β_2 -adrenergic receptor (β_2 -AR) have helped shed light upon the receptor architecture and the conformational changes associated with activation of G-proteins following ligand binding. The exceptional work carried out in the crystallation of the human β_2 -adrenergic receptor (PDB 2RH1) (Cherezov *et al.*, 2007) has given insight into the function of type A GPCRs other than rhodopsin. To facilitate crystallization and produce a high resolution structure, T4 lysozyme was fused in place of the 3rd intracellular loop (fig 1.1). The β_2 -AR has a fold composed of seven TM helices forming a helical bundle. Helices II, V, VI, and VII each have a proline induced kink along the span of the TM, which are thought to facilitate structural rearrangements required for G-protein activation (Yohannan *et al.*, 2004). In addition to the 7TM domain β_2 AR has a short extracellular α -helix and an intracellular helix termed helix VIII; believed to be common in all type A GPCR (Katragadda *et al.*, 2004).

Comparison of β_2 -AR with rhodopsin reveals several minor differences in architecture of the helical bundle. Namely, the extracellular portions of helices I and III are angled away from the receptor, helix IV is translated away from the centre of the receptor, helix V is translated closer to the centre of the receptor, and helix VI angles away from the receptor on the cytoplasmic face. These structural differences may arise due to a difference in ligand binding properties (Cherezov *et al.*, 2007).

Structural studies of rhodopsin β_2 -AR and form the basis for understanding the mechanisms of G-protein activation by GPCR. It is believed that ligand binding to a type A GPCR results in an outward movement of helix VI, thereby opening an intracellular crevice (Farrens *et al.*, 1996) and breaking the ionic lock, believed to prevent G-protein activation, located between helix III and VI (Bhattacharya *et al.*, 2008).

The amount of ligands capable of activating GPCR is staggeringly large, natural ligands include photons, hormones, neurotransmitters, and molecules ranging from small peptides to large proteins. Binding of a GPCR to other GPCRs or small molecules has also been shown to modulate/potentiate the binding and activation characteristics of GPCR (Milligan, 2003). Once GPCR has bound ligand its effects are mediated by the modulation of a series of second messengers. The increase or decrease in these second messengers leads to intracellular responses which underlie the physiological responses of the particular tissue or organ.

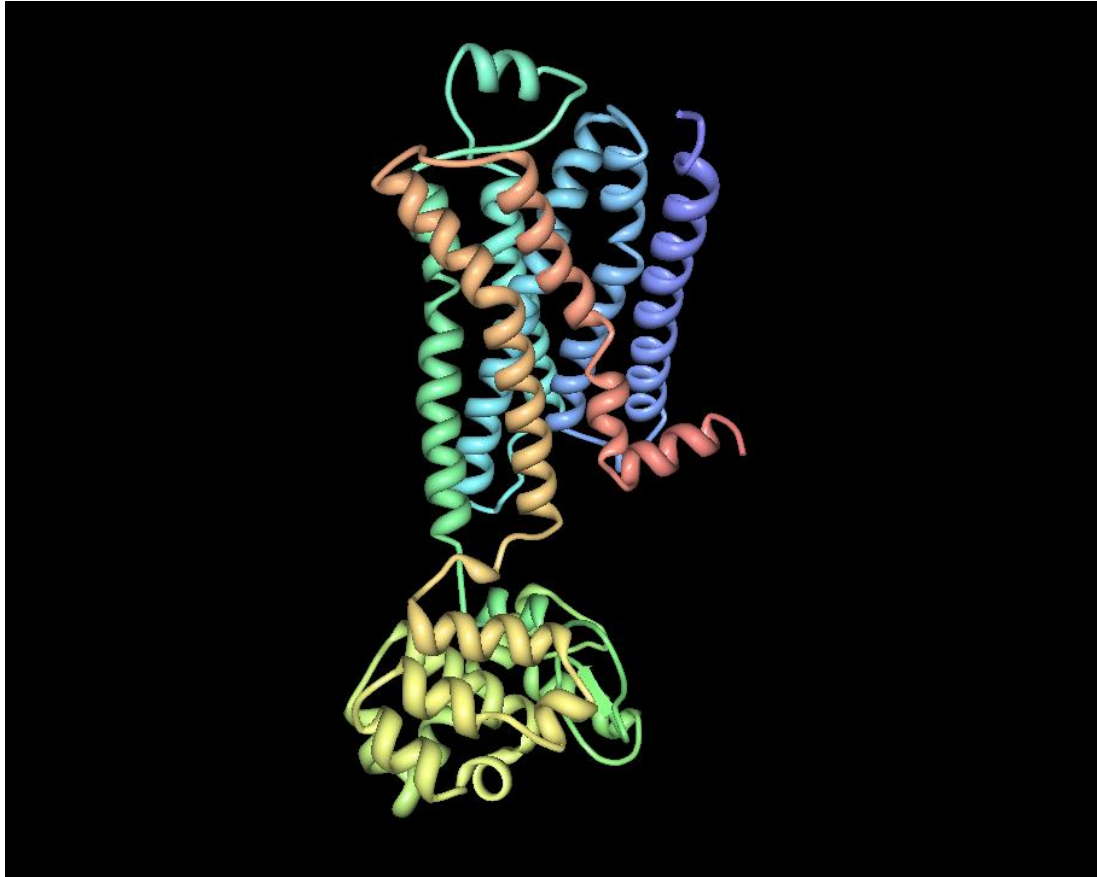


Figure 1.1 Model of β_2 AR-T4L. T4 lysozyme was inserted in the third intracellular loop to facilitate crystallization, shown here as the predominantly yellow structure, the seven TM helical bundle is coloured blue to red, with helix I and helix VIII being blue and red, respectively. PDB accession ID 2RH1 (Accessed 12/03/10). Adapted from Cherezov *et al.* using Jmol viewer. (Cherezov *et al.*, 2007)

1.1.2 CCR5 Structure and Function

The GPCR superfamily has been categorised into 6 different classes (A-F), as defined by the GPCRDB classification scheme (Bettler *et al.*, 2003). Class A GPCR, the largest of the GPCR superfamily classes, share significant homology to rhodopsin and are further sub-classified into subfamilies on the basis of their phylogenetic relationship (Joost *et al.*, 2002). Based on this classification CCR5 is classed as an A1 receptor, alongside other chemokine receptors. All chemokine receptors share a similar structural design with all receptors being between 340 to 370 amino acids in length, CCR5 has 352 residues, with similar C- and N-terminus structural motifs that confer ligand, signalling, and trafficking specificity to a particular receptor (Figure 1.2) (Oppermann, 2004).

CCR5 is predominantly expressed on lymphocytes, monocytes, macrophages and dendritic cells in the immune system (Martin *et al.*, 1999). It is also expressed on primary and secondary lymphoid organs and in the central nervous system (Bajetto *et al.*, 2002). CCR5 binds several chemokines with high affinity including CCL3, CCL4, CCL5 and CCL8 (Onuffer *et al.*, 2002), all of which bring about cytoskeletal changes in lymphocytes and macrophages. Recent studies in CCR5 deficient mice show very limited defects in cell mediated immune processes, however absence of CCR5 has been implicated in allograft rejection (Dehmel *et al.*, 2009). CCR5 constitutes the main functional co-receptor for M-tropic HIV-1 strains and humans deficient in functional CCR5, a subpopulation that expresses a mutant form CCR5 containing a 32 residue deletion, termed CCR5- Δ 32, have a reduced rate of HIV progression (Huang *et al.*, 1996) with no other ill effects. CCR5 has also been implicated in the activation of T_H1 helper cells (Galli *et al.*, 2001) West Nile virus susceptibility (Lim *et al.*, 2006) and arthritis (Pokorny *et al.*, 2005). The redundancy CCR5 exhibits, coupled with its high homology to many other physiologically important GPCR make it a good candidate to study GPCR signalling interactions.

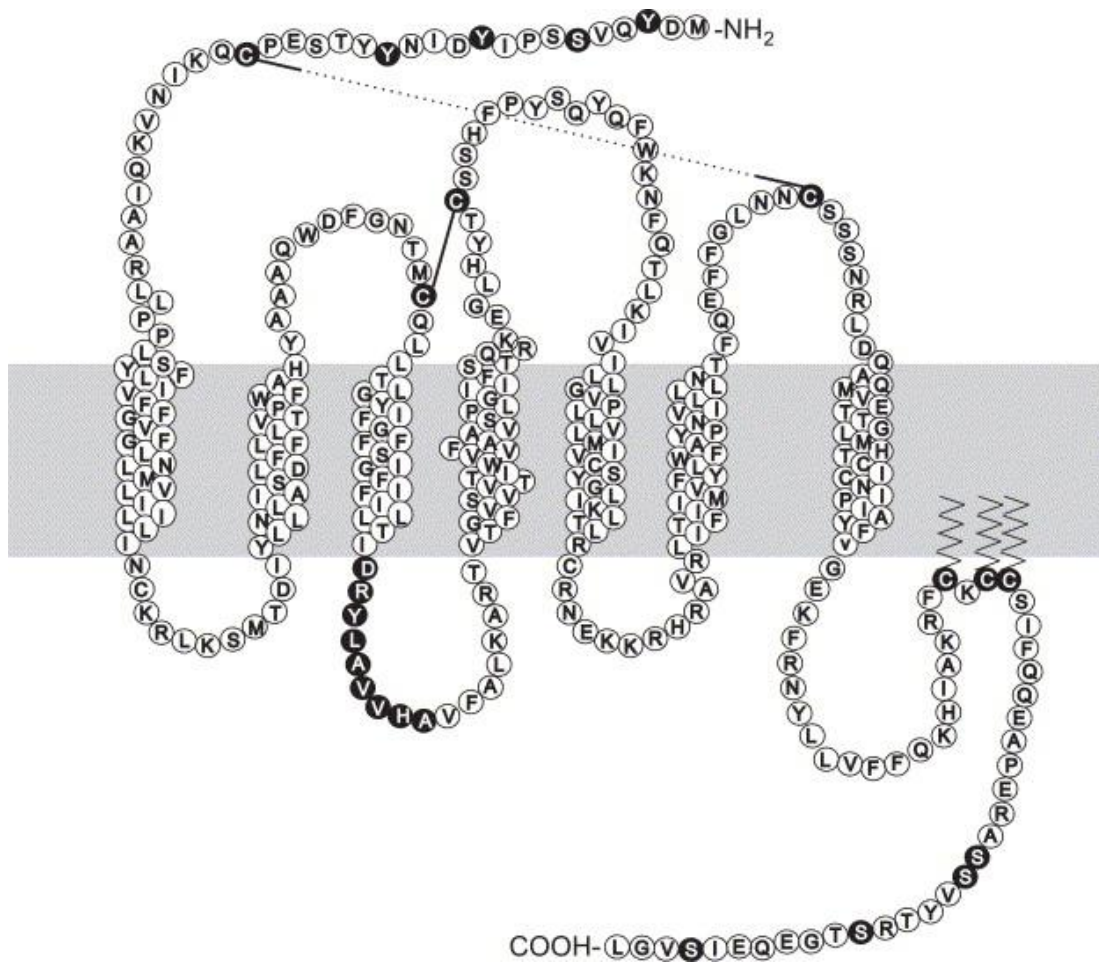


Figure 1.2 Schematic representation of CCR5 showing the 2-dimensional conformation of CCR5. The plasma membrane is represented by the grey shaded area, conserved residues and those important amino for receptor function are highlighted. Of special importance to CCR5 are the two extracellular disulphide bridges, signified by the dashed and solid line, which are believed to hold the receptor in a conformation capable of binding specific chemokine ligands and the DRYLAVVHA motif, located intracellularly, which is conserved between all members of the chemokine receptor family. Residues critical for receptor function are shown as filled circles. (Oppermann, 2004)

1.1.2.1 Extracellular Domains

The four extracellular loops of CCR5 each contain a cysteine residue that forms disulphide linkages between extracellular domains two and three, and one and four. These disulphide bonds hold the receptor in a conformation capable of allowing ligand access to the binding pocket and consequently binding chemokine (Blanpain *et al.*, 1999). Comparatively, a typical class A GPCR contain only two cysteine residues in the extracellular domains which form a disulfide bond that links the first and second extracellular loops (Savarese *et al.*, 1992). Mutation to these conserved cysteine residues results in a decrease in receptor function due to impaired ligand binding (Wess *et al.*, 2008). In addition to this conserved disulphide bridge, all chemokine receptors have two additional cysteines located in the N-terminal domain and the third extracellular loop. These extra cysteines are thought to form a second disulfide bond, which confers an additional structural restriction on the GPCRs conformation that contributes to its stability (Baggiolini *et al.*, 1997).

Ligand specificity in CCR5 is conferred by the second extracellular loop. Studies comparing the binding properties of CCR5 and CCR2b, the chemokine receptor with the highest similarity to CCR5, showed that the region with the lowest homology was responsible for ligand specificity in CCR5 (Habasque *et al.*, 2002). However, ligand specificity for chemokine receptors is not only defined by the second extracellular domain, CCR1 binding to ligand, for example, is reported to be mediated by the third extracellular loop (Monteclaro *et al.*, 1996)

1.1.2.2 Intracellular Domains

The intracellular structure of CCR5 contains four loops, allowing binding of downstream signalling elements and β arrestin. It appears the first intracellular loop is completely dispensable for the correct function of the receptor, as the creation of five TM CCR5, having had the first and second TM domains removed, resulted in a fully functional chemokine receptor (Ling *et al.*, 1999). The second intracellular loop contains a –DRY residue motif that is highly conserved between all class A GPCR (Rovati *et al.*, 2007). The –DRY motif is responsible for keeping the receptor in its inactive ground state; upon activation the arginine residue undergoes a conformational shift resulting in the formation of an active receptor (Cotecchia *et al.*, 2002). Within the chemokine receptor family this highly conserved –DRY motif is extended to include further residues resulting in a conserved –DRYLAVHA motif across the chemokine receptor family (Oppermann, 2004). This second loop motif has been implicated in G-protein association with the receptor (Shibata *et al.*, 1996) as well as playing a role β -arrestin binding to the receptor (Bennett *et al.*, 2000). Although the third intracellular loop has been implicated in β -arrestin binding in other class A GPCR, this is not the case for CCR5 which contains an unusually short and positively charged third intracellular domain (Huttenrauch *et al.*, 2002). No apparent functional use has been published for the third intracellular loop in CCR5. However, mounting evidence suggests that the sequence in a GPCRs third intracellular loop may be important for G protein specificity (Beqollari *et al.*, 2009). The fourth intracellular loop is formed by post translational palmitoylation of three cysteine residues and their association with the inner leaflet of the plasma membrane; it has been shown to be essential to receptor trafficking (Blanpain *et al.*, 2001) and acts as a docking site for G-Protein Receptor Kinases (GRK) and Protein Kinase C (PKC) to bind to and phosphorylate serine, threonine and tyrosine residues on the intracellular domains.

1.1.2.3 CCR5 Chemokine Ligands

Chemokines are leukocyte activating peptides that facilitate migration to affected areas by stimulating actin cytoskeleton rearrangements and the degranulation of cells expressing chemokine receptors (Mackay, 2001). Synthesis of chemokines occurs in monocytes and macrophages, they are released in response to physical damage or pathogen challenge to the body, and approximately 50 chemokines are known to exist to date. The principle target for chemokines is bone marrow derived immune system cells (Mackay, 2001)

There are four families of classification that chemokines can fall in to; each family is dependent on amino acid sequence, specifically, based on the configuration of cysteine residues at the N terminus. The families are; CC – two adjacent cysteines, CxC two cysteines separated by a single amino acid, C – a single cysteine residue and C₃C – two cysteines separated by three amino acids (Thelen, 2001).

Ligand binding to CCR5 is thought to occur as a two-step process. Firstly, the chemokine core binds to the exposed N-terminal via post-translationally sulphonated tyrosines (Zlotnik *et al.*, 2000). These tyrosines are situated in a positively charged milieu; sulphonation increases the negative charge, thus increasing the affinity for chemokine binding. The chemokine also binds to adjacent regions on the second extra-cellular loop, it is this interaction that confers ligand specificity (Samson *et al.*, 1997). The free amino terminal end of the chemokine can then bind to the third membrane helix, causing conformational change to CCR5, thus, activating the receptor (Blanpain *et al.*, 1999). This process is the method used by chemoattractant leukocyte receptor systems (Farzan *et al.*, 1999). However, different chemokines require different structural determinants to bind. This ensures that there is not a one size fits all binding method. The configuration of CCR5 lends

itself to predominantly binding to CCL3, CCL4 and CCL5 as well several other chemokines (Table 1.1), whereas CCR4, for example, binds predominately to CCL17 and CCL22 (Navenot *et al.*, 2001). There are four described isoforms of CCL3 (CCL3, CCL3L1, CCL3(5–70), CCL3(2–70)), which differ in their ability to bind and activate CCR5 (Mueller *et al.*, 2006). CCL3L1, also known as LD78 β , is a naturally occurring non allelic variant of CCL3. This isoform has been shown to be more potent than CCL3, a proline residue at position 2 is believed to confer this enhanced potency (Nibbs *et al.*, 1999). Although not as potent as CCL3L1 some studies have shown CCL3(2–70) to be as efficacious as CCL3L1. These studies have led to the conclusion that binding and activation of chemokine receptors by chemokines is dependent upon the N-terminus of the chemokine (Mueller *et al.*, 2006).

Receptor	Ligand
CCR1	CCL3, CCL5, CCL7, CCL8, CCL13-16, CCL23
CCR2	CCL2, CCL7, CCL8, CCL13
CCR3	CCL11, CCL5, CCL7, CCL8, CCL13, CCL15, CCL24, CCL26
CCR4	CCL17, CCL22
CCR5	CCL3, CCL4, CCL5, CCL8, CCL14
CCR6	CCL20
CCR7	CCL19, CCL21
CCR8	CCL1, CCL4, CCL17
CCR9	CCL25
CCR10	CCL26-28
CXCR1	CXCL8
CXCR2	CXCL1-3, CXCL5-8
CXCR3	CXCL9-11
CXCL13	CXCL12
CXCR5	CXCR4
CX3CL1	CXCL16
CX3CR1	CXCR6
XCR1	XCL1, XCL2

Table 1.1 Chemokine Receptors and their Ligands. Many chemokine receptors have overlapping specificity for chemokines. Table adapted from IUPHAR-DB (Harmar *et al.*, 2009)

1.1.3 Heterotrimeric G-Protein Structure

G-proteins are made up of three different subunits α , β , and γ . The heterotrimeric G-proteins are typically classified into four families, based on sequence homology of the $G\alpha$ subunit, they are: $G\alpha_i$, $G\alpha_s$, $G\alpha_q$, and $G\alpha_{12/13}$ (Simon *et al.*, 1991). Crystal structures have been solved for at least one member of each family and have allowed structural characterisation of the $G\alpha$ subunit (Figure 1.3). The $G\alpha$ subunit consists of two domains; a GTPase domain, and α helical domain. The GTPase domain is conserved in all members of the G-protein superfamily, and is responsible for GTP hydrolysis and contains residues involved in $G\beta\gamma$ and effector binding. This domain also contains three flexible loops, termed switch regions 1-3, which undergo conformational changes upon GTP binding and hydrolysis (Mixon *et al.*, 1995). The helical domain is composed of six α helices that form a lid over the GTP binding site, burying the core of the protein (Coleman *et al.*, 1994).

Upon GDP displacement and GTP binding the GTPase domain undergoes a number of conformational changes in switch regions I-III, resulting in decreased affinity for the $G\beta\gamma$ subunit and an increase for cellular effectors (Lambright *et al.*, 1996). The classical view is that then the $G\alpha$ subunit dissociates from the $G\beta\gamma$ subunit and activates its effectors, however this has recently been questioned, by demonstrating that some G-protein heterotrimers signal without dissociating (Bunemann *et al.*, 2003). The helical domain also contains a fourth switch region that undergoes a nucleotide dependent conformational change (Mixon *et al.*, 1995). Switch IV has been shown to form a binding region for GoLoco motifs found in regulator of G-protein signalling proteins (RGS) (Kimple *et al.*, 2002).



Figure 1.3 Protein Explorer model of $G\alpha_i$ demonstrating the deep binding cleft into which GTP (ball and stick model) binds. Switch regions are located around the β -sheet formation. PDB Accession ID 1TAD. Adapted from McCudden *et al.* using protein explorer. (McCudden *et al.*, 2005)

Interaction between $G\alpha$ and $G\beta\gamma$ is believed to be modulated by an α helix formed by the extended N terminal of $G\alpha$. The N terminal of $G\alpha$ units has 26-36 residues, of which the first 23 in $G\alpha$ have been shown, in a heterotrimeric conformation, to form an α helix. The helix interacts with the $G\beta\gamma$ subunit, thus connecting them through ionic interactions. The helix is believed to form as a consequence of the N terminal myristate imposing conformational rigidity on the amino terminus (Preininger *et al.*, 2008).

The $G\beta$ subunit forms a structurally stable functional heterodimer with the $G\gamma$ subunit that does not dissociate unless denatured (Schmidt *et al.*, 1992). There are five $G\beta$ known units and 12 known $G\gamma$ units (Fletcher *et al.*, 1998) this suggests a large number of possible permutations for the $G\beta\gamma$ subunit. Most combinations do form and become functional dimers. However, there are some exceptions; for example $G\beta_2$ cannot pair with $G\gamma_1$ (Spring *et al.*, 1994). It has also been noted that some combinations have greater affinity for specific receptors for example $G\beta_1\gamma_1$ binds with higher affinity to rhodopsin than other potential combinations (McCudden *et al.*, 2005).

All $G\beta\gamma$ subunits contain seven tryptophan-aspartic acid sequences that repeat approximately every 40 residues, which form small anti parallel β strands (Neer *et al.*, 1994). This feature causes the $G\beta$ subunit to adopt a propeller shape formation, known also as a torus-like structure (Figure 1.3). The dimerous structure of the $G\beta\gamma$ unit is stabilised by the $G\gamma$ subunit forming two α -helices. The C terminus helix interacts with the torus-like structure, binding to blades five and six, while the N terminus helix forms a coiled coil with the $G\beta$ N-terminus (Sondek *et al.*, 1996).

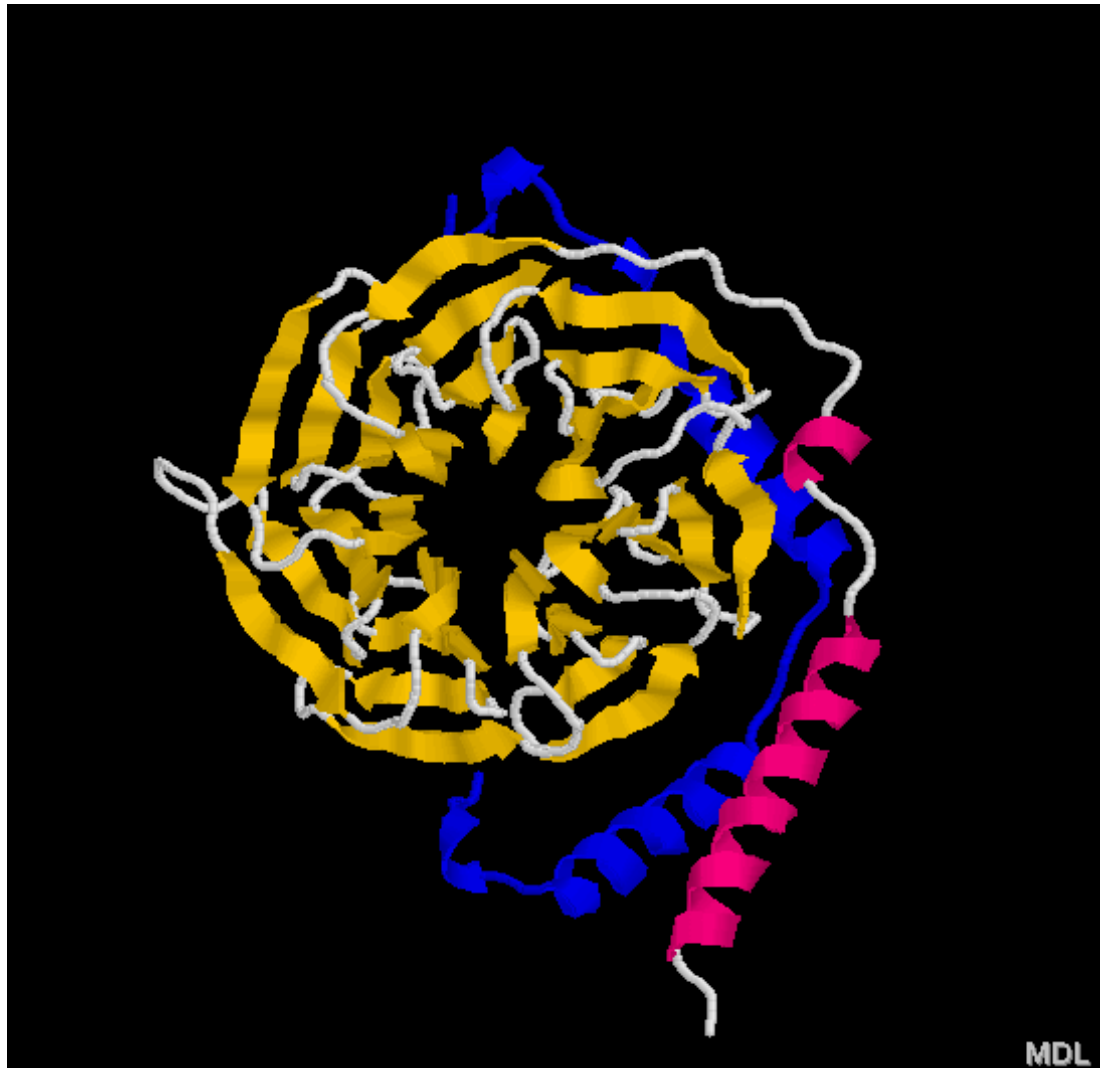


Figure 1.4 The $G\beta_1\gamma_1$ subunit, the torus structure of the β unit is clearly visible, the γ subunit is coloured in blue, its two α -helices bind to the β unit to stabilise the dimer. PDB Accession ID 1TBG. Adapted from McCudden et al. using protein explorer.(McCudden *et al.*, 2005)

The G $\beta\gamma$ interacts primarily at a hydrophobic pocket formed by switches I and II on G α and five of the seven blades of the G β subunit. On formation of the heterotrimer the G $\beta\gamma$ subunit significantly alters the conformation of G α (Wall *et al.*, 1995). Unlike the G α subunit the G $\beta\gamma$ subunit does not undergo a conformational change in order to activate it. Instead the active sites of the G $\beta\gamma$ unit are partially shared with the binding site for G α . Therefore, classical G-protein theory suggests G $\beta\gamma$ is unable to signal whilst bound to G α (Sondek *et al.*, 1996). However this notion has recently been brought into question with the discovery of AGS proteins capable of activating signalling through the G $\beta\gamma$ subunit without causing dissociation of the heterotrimer (Yuan *et al.*, 2007).

1.2 Downstream effectors of G-proteins

The different classes of $G\alpha$ subunit, once active, target different effectors dependent on their structural determinants. Structural differences between G-proteins result in targeting to, and the activation of, different downstream effectors (Skiba *et al.*, 1996; Sprang, 1997). Activation or inhibition of other downstream effectors can also be achieved by interactions with the $G\beta\gamma$ subunit. Activation of CCR5 results in the targeting of several effectors (Figure 1.4)

1.2.1 $G\alpha$ subunit signalling

The activation of $G\alpha_q$ leads to the activation of the enzyme phospholipase C (PLC). To date there have been 12 mammalian PLC isoforms that can be divided into five isotypes based upon functional and structural characteristics; PLC- β , PLC- δ , PLC- γ , PLC- ϵ , and PLC- ζ . More recently a new phospholipase has been identified (PLC- η) which is calcium dependent and mainly expressed in nerve cells (Hwang *et al.*, 2005a; Hwang *et al.*, 2005b). All mammalian PLC contain X and Y catalytic domains as well as regulatory domains and require calcium for their activation. PLC- β is the only isotype that is activated by the action of $G\alpha_q$ binding. The activation of PLC- β results in the breakdown of the phospholipid phosphoinositol bisphosphate (PIP2) to the lipophilic compounds diacylglycerol (DAG) and inositol triphosphate (IP3).

The activation of $G\alpha_s$ leads to the stimulation of adenylyl cyclase (AC) whereas, in classical models of G-protein signalling, activation of the $G\alpha_i$ subunit leads to inhibition of AC activity. AC activation results in an increase of the of the second messenger cyclic adenosine monophosphate (cAMP), which is responsible for the regulation of a plethora of

further proteins. Structurally, the AC complex consists of an N-terminal domain, two transmembrane clusters, each consisting of six α -helices, and two cytoplasmic loops, termed C1 and C2. It is here, within these cytoplasmic loops, that the active site is located and catalysis of ATP to cAMP occurs (Tesmer *et al.*, 1997b). There are ten known isoforms of AC discovered in humans, each isoform has a slightly different expression profile and different protein association profile. Most tissues and cell types can express more than one isoform of AC, but expression is tightly regulated. Different isoforms are inhibited and activated in different ways, providing cells with a method to respond diversely to similar stimuli (Patel *et al.*, 2001). For example AC V is directly inhibited by $G\alpha_i$ whereas AC II is not (Patel *et al.*, 2001). AC I can be inhibited by $G\beta\gamma$ subunits whereas AC II and AC VII are stimulated by $G\beta\gamma$ (Taussig *et al.*, 1994b). It is important to note, that while it is widely accepted that activation of the $G\alpha_i$ subunit results in inhibitory effects upon AC, the associated $G\beta\gamma$ subunit can actually activate several isoforms (see Table 1.2) including AC VII (Watts *et al.*, 1997). The specific expression pattern of AC isoforms is not completely characterised, however, there is strong evidence that in human neutrophils isoforms III, VI, VII, and IX are predominantly expressed (Mahadeo *et al.*, 2007).

AC Isoform	Activators	Inhibitors
I	$G\alpha_s, Ca^{2+}/CaM$	$G\alpha_i, G\beta\gamma, CaM$ Kinase IV
II	$G\alpha_s, G\beta\gamma, PKC$	P-Site analogues
III	$G\alpha_s, Ca^{2+}/CaM$	CaM Kinase III, P-Site analogues
IV	$G\alpha_s, G\beta\gamma$	P-Site analogues
V	$G\alpha_s, PKC$	$G\alpha_i, G\beta\gamma$
VI	$G\alpha_s,$	$G\alpha_i, PKA, PKC$
VII	$G\alpha_s, G\beta\gamma, PKC$	P-Site analogues
VIII	$G\alpha_s, Ca^{2+}/CaM$	P-Site analogues
IX	$G\alpha_s$	P-Site analogues
Soluble	HCO_3^-	?

Table 1.2 Comparison of activators and inhibitors of adenylyl cyclase. Table adapted from T.B. Patel *et al* (2001).

1.2.2 Gβγ Subunit Signalling

In recent years, knowledge of the roles heterotrimeric G proteins in cellular signalling has dramatically increased. Originally, the Gβγ dimer was thought to be necessary mainly for the inactivation of Gα subunits, allowing them to reassociate with the receptor for subsequent rounds of signalling. Thus, Gβγ was viewed as a negative regulator of Gα signalling. The first evidence for a direct role of Gβγ dimers in signalling came in 1987 when purified Gβγ subunits from bovine brain were shown to activate a cardiac potassium channel normally activated by muscarinic cholinergic receptor following acetylcholine release (Logothetis *et al.*, 1987). We now know that Gβγ subunits can modulate many effectors via direct interaction that are also regulated by Gα subunits, including Kir3 potassium channels, as well as PLCβ (Guo *et al.*, 2003), phosphatidylinositol 3-kinase (PI3K)(Neves *et al.*, 2002), and isoforms of adenylyl cyclase (Taussig *et al.*, 1994a). These Gβγ functions have been investigated heavily in recent years and many interactions have been shown to result in an increase in cytosolic calcium levels (Robishaw *et al.*, 2004).

Investigations into Gβγ targets have revealed that the interaction between Gβγ and Ca²⁺ channels is direct. To prove this observation, Gβγ was overexpressed in various cell lines and shown to inhibit calcium channel activity (Herlitze *et al.*, 1996), whereas the overexpression of proteins that bind Gβγ, acting as scavengers of free Gβγ, were shown to suppresses this effect (Kammermeier *et al.*, 2000). Currently, the mechanism by which Gβγ interacts with its downstream effectors is not entirely clear. Many of Gβγ effectors contain pleckstrin homology domains (PH); however, not all PH domain-containing proteins interact with Gβγ, making prediction of interactions difficult. Currently there are few studies into the critical residues involved in Gβγ interactions. However, the Gβ₁γ₂ interaction with the PH domain of GRK2 has been elucidated(Tesmer *et al.*, 1997a), and residues important for

GIRK channels have also been identified (He *et al.*, 2002). This information may help deduce further G $\beta\gamma$ -effector interactions in the future. Recent studies have also implicated the G $\beta\gamma$ subunit as a mediator of cross talk between pathways (Kumar *et al.*, 2007; Zagar *et al.*, 2004)

1.2.3 G-protein Mediated Calcium Release

Following chemokine binding and stimulation of a chemokine receptor, the cytosolic concentration of free calcium can increase by 10 fold that of normal basal levels (Berridge *et al.*, 2000). The most well studied pathways regarding G-protein mediated calcium release is the G α_q pathway. When G α_q associated receptors are activated, the PLC- β pathway is triggered resulting in PLC β catalysed increases in IP3 from membrane anchored Phosphatidylinositol 4, 5-bisphosphate (PIP2). Free IP3 then diffuses into the cytoplasm from the inner plasma membrane leaflet resulting in the activation of with IP3 receptors (IP3R) located on the ER. The IP3R are a family of calcium release channels located on the endoplasmic reticulum, stimulation of these receptors results in the release of pooled calcium from the ER to the cytosol (Foskett *et al.*, 2007). The overall mechanisms controlling the IP3R are complex and diverse, but the underlying principles of activation are the same; once IP3 binds the receptor a conformational change occurs causing the receptor 'gate' to open, allowing the passage of calcium through a newly formed pore in the membrane. The release of calcium from the ER results in further downstream signalling events, one of which causes the modification of IP3 to either inositol 1,4-bisphosphate or inositol 1,3,4,5-tetrakisphosphate. These changes to IP3 and calcium levels act as a negative feedback loop, resulting in a loss IP3 binding and phosphorylation of the receptor and consequently its subsequent deactivation (Bugrim, 1999).

The classical calcium signalling pathway involves activation of $G\alpha_q$ linked receptors leading to the activation of PLC- β and subsequent production of IP3 is not the only mechanism by which GPCR can stimulate calcium release. The $G\beta\gamma$ subunit plays an equally central role in mediating intracellular calcium flux. When the $G\alpha_q$ subunit is activated the $G\alpha$ and $G\beta\gamma$ can target different downstream effectors. The conformation of free $G\beta\gamma$ does not differ to $G\beta\gamma$ when bound to the $G\alpha$ subunit (Sondek *et al.*, 1996) suggesting that the $G\alpha$ subunit acts as a negative regulator of $G\beta\gamma$ interactions. $G\beta\gamma$ subunits have been shown to directly interact with calcium signalling machinery within a cell and it has been proposed that IP3 receptors can be activated directly by $G\beta\gamma$ subunits (Zeng *et al.*, 2003). Studies on the alpha 2A adrenergic receptor proved that the $G\beta\gamma$ subunits from activated $G\alpha_i$ heterotrimers are directly responsible for the stimulation of PLC- β and the release of calcium (Dorn *et al.*, 1997). There are also reports that free $G\beta\gamma$ subunits may also activate or enhance the activity of $G\alpha_q$ (Quitterer *et al.*, 1999). It is suggested that $G\alpha_q$ activation by $G\beta\gamma$ is facilitated by $G\beta\gamma$ promoting $G\alpha_q$ activation by accelerating the receptor stimulated GTP-binding (Quitterer *et al.*, 1999). Studies have also shown that the activity of calcium ion channels can be potentiated or modulated by $G\beta\gamma$ binding (Dascal, 2001; Herlitze *et al.*, 1996).

Following the initial rapid increase in cytosolic calcium by IP3 receptors there is a second slower phase involving extracellular calcium entry, believed to be necessary for maintenance of ER calcium stores (Parekh *et al.*, 2005). The entry of extracellular calcium is known as capacitative calcium entry (Berridge, 1995). The emptying of ER calcium serves as a trigger for a message that travels to the PM, resulting in activation of store-operated channels (SOCs) allowing the movement of calcium from high concentration to low; Extracellular calcium is approximately at a 10,000 fold concentration across the PM (Parekh

et al., 2005). Activation of SOCs leads to the long-term increase in cytosolic calcium concentration, which in turn replenishes intracellular stores. The mechanism for this second phase that couples ER calcium store depletion with calcium entry into the cell is not yet fully understood.

1.2.4 G-protein mediated cAMP Regulation

The cytosolic concentration of cAMP in a cell is kept at a relatively low concentration; extracellular signals can cause cAMP levels to increase by more than 20 fold within seconds of GPCR activation. The basal level of cAMP in a cell is kept low by cAMP phosphodiesterase activity which hydrolyses cAMP to adenosine 5'-monophosphate (AMP) (Conti *et al.*, 2003). Binding of PTX sensitive $G\alpha_i$ subunits to AC is specified by a post translational N-terminal acylation, and results in a lowering of the intracellular cAMP concentration (Taussig *et al.*, 1994b). Binding of $G\alpha_s$ subunits occurs at a different site to $G\alpha_i$ and results in an increase of cAMP - thus, AC is under dual control and turnover of substrate can be fine tuned by levels G-protein binding (Simonds, 1999).

Increases in cAMP concentration results in further downstream effects mediated by cAMP-dependent Protein Kinase A. Phosphorylation of specific residues on a target protein allows regulation of their function and PKA is also responsible for phosphorylation, and the consequent deactivation, of GPCRs. PKA is a holoenzyme made up of four subunits; two catalytic and two regulatory. The regulatory subunits undergo a conformational change following the binding of cAMP, allowing them to dissociate from the catalytic subunits resulting in active PKA. The relationship between cAMP and adhesion of leukocytes is not well understood. However, recent studies suggest that lowering of cAMP may be

physiologically relevant and facilitate the migration of dendritic cells towards lymph nodes, and inhibit firm adhesion of other leukocytes (Burzyn *et al.*, 2002).

1.2.5 CCR5 Mediated Cytoskeleton Reorganisation

Ultimately, the activation of CCR5 leads to chemotaxis of a cell along a chemotactic gradient towards areas that have a high concentration of chemokine. Movement of the cell is brought about by the reorganisation of its cytoskeleton. The main effectors involved in initiating chemotaxis of the cell are predominantly under the control of G $\beta\gamma$ subunit targeting (Neptune *et al.*, 1997).

Upon G-protein heterotrimer activation G $\beta\gamma$ binds to and activates PLC β , ultimately, resulting in intracellular calcium mobilisation. The subsequent calcium influx activates PKC, which goes on to phosphorylate the fourth intracellular loop of CCR5, setting in motion desensitisation mechanisms. PLC β activation also results in the MAPK pathway becoming activated which up regulates gene transcription for cytokine production (Lee *et al.*, 2003). However, studies in mice have shown this pathway to be dispensable for chemotaxis (Li *et al.*, 2000). In contrast, mice deficient in PI3K showed severe defects in leukocyte chemotaxis (Hirsch *et al.*, 2000).

Upon activation, CCR5 has been shown to activate PI3K- κ as well as RhoA resulting in the formation of lamellipodia. RhoA is a member of the Rho family of small GTPases, a family which also includes Rac and Cdc42. Their activation results in the co-ordinated rearrangement of the actin cytoskeleton, which determines cell polarity, adhesion and motility (Oppermann, 2004). The focal adhesion proteins (FAK), FAK and Pyk2, are also

activated following CCR5 stimulation, these two proteins play an important role in cell motility and spreading (Ganju *et al.*, 1998). Activation of FAK and Pyk2 also results in the activation of integrins by binding to their cytoplasmic face, promoting cell adhesion and migration (Hecht *et al.*, 2003).

Evidence has recently emerged demonstrating that GPCR do not only rely on classical G-protein signalling pathways to signal. Work by Mueller *et al.* demonstrated the ability of Janus Kinase2/ Signal Transducers and Activator of Transcription (JAK/STAT) pathways to be activated upon CCR5 stimulation in the presence of PTX, an inhibitor of $G\alpha_i$ signalling (Mueller *et al.*, 2004a). This suggests CCR5 can activate JAK2 in a G-protein independent manner. G protein independent activation of the JAK2/STAT pathway through a GPCR has also been demonstrated by Marrero *et al.* who showed that angiotensin via the AT1 receptor activates the JAK2/STAT pathway (Marrero *et al.*, 1995).

1.2.6 G-protein Interactions with Other Signalling Pathways

For some time now the notion of discrete signalling pathways working independently towards bringing about physiological changes has been questioned. There is accumulating evidence that GPCR signalling pathways work as highly regulated cell specific networks, with proteins working in concert to bring about changes (Gurevich *et al.*, 2008). Although research into this area is plentiful, describing interactions in a mechanistic fashion is proving to be difficult in living systems. Recently crosstalk between CCR5 and the neurokinin-1 receptor has been described, which results in enhanced chemotaxis of macrophages (Chernova *et al.*, 2009). However, finding a definite model of cross-talk

between GPCRs and G-proteins is difficult. Compounds that inhibit one part of a pathway may also affect other signalling pathways thus complicating mechanistic studies.

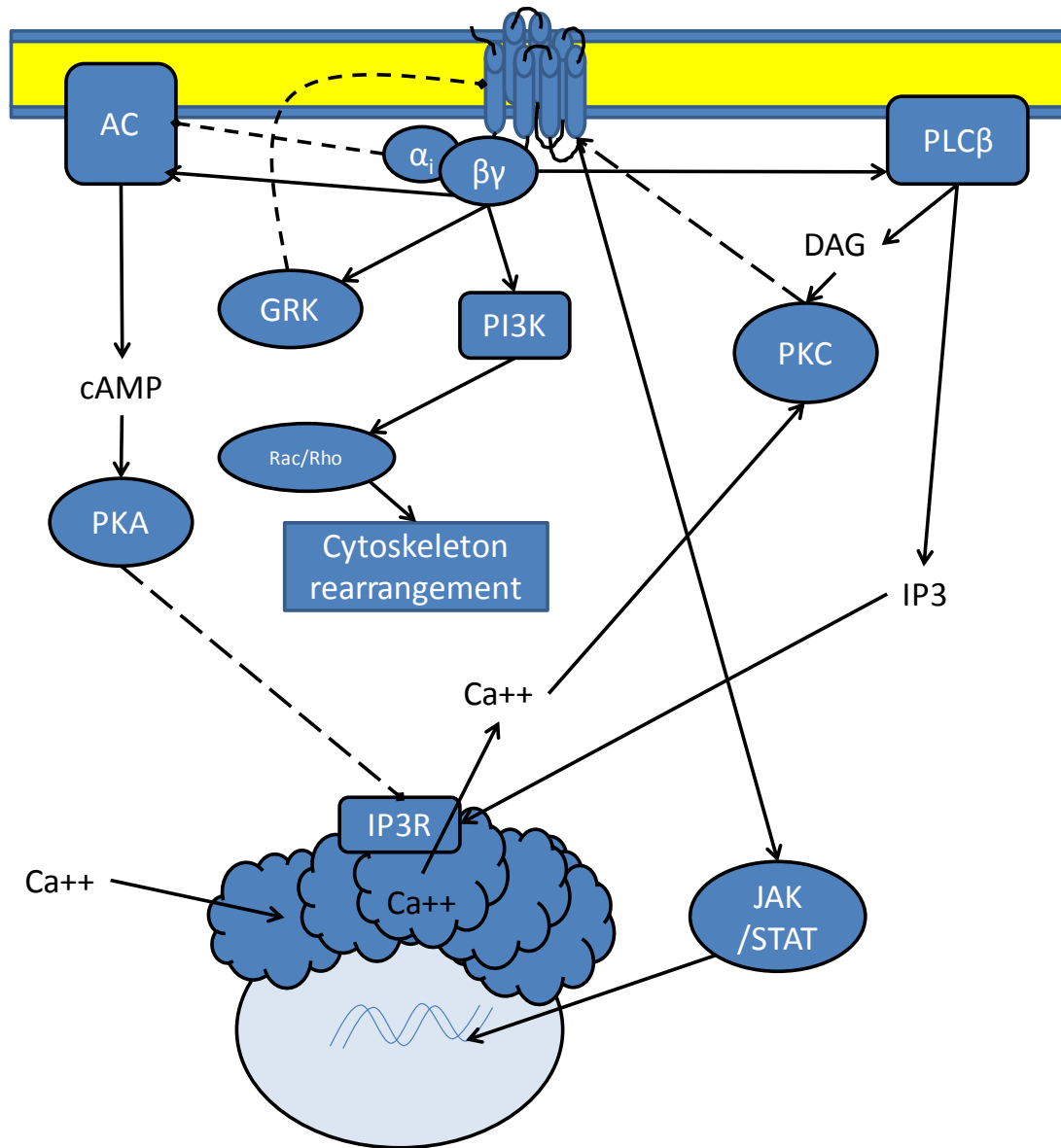


Figure 1.5 Activation of CCR5 by binding of chemokine results in the activation and inhibition of several signalling pathways. $G\alpha_i$ subunits inhibit adenylyl cyclase resulting in the reduction of cAMP production. $G\beta\gamma$ targets several pathways, ultimately resulting in the release of cytosolic stores of calcium, cytoskeleton rearrangement and the formation of lamellipodia, and desensitisation of the active receptor.

1.3 Methods to Infer and Monitor Protein-Protein Interactions

The protein-protein interactions that underpin the correct function of the cell were for so long invisible by ordinary scientific methods; interactions were inferred on the basis of indirect assay systems and putative interactions. However, the fundamental importance of understanding the mammalian interactome has led to the development of a plethora of direct assay methods capable of identifying protein-protein interactions. Each method has its own strengths and weaknesses, especially with regard to the sensitivity and specificity of each method. These strengths and weaknesses need to be taken into account when creating a suitable assay to measure interactions. In the interest of brevity it is not possible to discuss all methods at our disposal, however, the key methodologies for investigating G-protein heterotrimer interactions will be discussed here.

1.3.1 Indirect Methods

Indirect methods rely on measuring the physiological changes brought about from the activation of a protein of interest. In the case of CCR5 stimulation, the activation of the $G\alpha_q$ family of heterotrimers results in a reduction of cAMP, an increase in IP3 production and cytosolic calcium release. Measurement of calcium release is one of the most common in-cell measurements used to assess GPCR activity. The release of calcium following GPCR stimulation can be attributed typically to $G\alpha_q$ or the $G\beta\gamma$ subunits of an active heterotrimer acting on downstream effectors. Changes in intracellular calcium can be measured with ion-sensitive dyes, whose excitation and emission properties change dependent on whether or not they have bound calcium – One such widely used dye is Fura-2 AM.

Accurate measurement of cAMP and IP3 in a cellular system has, until recently, relied upon the radioactive labelling of such molecules. Traditionally the measurement of cAMP relied

upon the use of ^{125}I -cAMP. Cells of interest are lysed and the cytosol used to determine the AMP concentration by using cAMP antibodies and ^{125}I -labeled cAMP in a competition binding assay. Free cAMP from the sample competes with the radiolabeled cAMP and thus reduced antibody-coupled radioactivity, the amount of radioactivity left in the assay mixture following thorough washing is inversely proportional to the concentration of cAMP in the sample. Similar methods are employed to measure levels of IP3, where the incorporation of ^{32}P ions into IP3 and a competitive capture assay is undertaken to determine IP3 concentrations. The biggest drawback to these methods is the associated safety concerns when handling radioactivity and the need for specialist equipment. Recently it has become possible to perform cAMP assays using a bioluminescence assay based on the principle that cAMP stimulates PKA activity, decreasing the available ATP in assay solutions, leading to decreased light production in a coupled luciferase reaction.

The addition of compounds that have been proven to prevent certain interactions, such as PTX catalysed ribosylation acting on $G\alpha_i$ subunits to prevent the active conformation, combined with the use of these assays can yield information about the protein-protein interactions involved in certain cellular responses. However, as the results are inferred from the measurement of second messengers downstream of initial interactions, there is an undefined margin for error.

1.3.1.1 Small Interfering Ribonucleic Acids

The use of small interfering ribonucleic acids (siRNA), coupled with the measurement of second messengers is another way that protein-protein interactions can be inferred. siRNA is a short sequence of double stranded RNA that complements a section of the genetic sequence involved in coding for a protein of interest. Predesigned synthesised siRNA is

freely available to purchase, and can be easily introduced into cells. Once inside the cell, the siRNA undergoes strand separation and are integrated into the RNA induced silencing complex (RISC). The antisense strand of the siRNA then binds its complementary mRNA sequence, which results in the targeted destruction of the mRNA and thus active protein (Matranga *et al.*, 2005). By effectively removing the protein of interest from the cell, its effects can be measured, allowing its protein-protein interactions to be inferred. In combination with direct methods of measuring interactions, such as immunoprecipitation, siRNA can help categorically confirm interactions.

1.3.2 Direct methods

Direct methods of measuring protein-protein interactions have flourished in the post genomic era, due to newly discovered genes without characterised functions. Identifying and understanding the interactions of these proteins plays an important part in helping decipher their function. Many of these developed methods can also help identify the kinetics of interactions and the cellular location.

The major breakthrough in screening for protein-protein interactions was made by the creation of the yeast 2 hybrid (Y2H) system (Fields *et al.*, 1989). Briefly, the Y2H system works by relying on the modular structure of transcription factors in yeast. By splitting a particular transcription factor into two halves and fusing them to two proteins of interest, termed the bait and prey, its function would only be restored if the proteins of interest interacted. This technique was limited to protein interactions in the nucleus. But the principle of fusing complementary portions of proteins to bait and prey was transferable and extended to allow measurements of interactions in other locations (Piehler, 2005).

Built on the back of the Y2H system, protein complementation assays (PCA), using proteins other than transcription factors revolutionised interactome studies. By tagging prey and bait proteins with complementary portions of enzymes, fluorophores or ubiquitin, the interactions of many more proteins could be measured. The ubiquitin system has been applied successfully to identify interactions that occur between membrane proteins using reporter proteins (Thaminy *et al.*, 2004), methods using split enzymes such as lactamase have also been employed for this purpose (Galarneau *et al.*, 2002). However, both systems rely on reporters that are time shifted from the actual event of interaction and may require incubation with a substrate. These issues can be overcome by tagging bait and prey proteins with two halves of a GFP. Bimolecular fluorescence complementation (BiFC) has been successfully used in many applications, and recently has been exquisitely used to identify the interactions between the G β and γ subunits *in vivo* (Hynes *et al.*, 2008).

Although Y2H and PCA methods are adequate for identifying interactions, more instantaneous methods are required to assess the kinetics and localisation of these interactions in living cells. Two similar methods currently exist that fulfil these criteria, they are fluorescence resonance energy transfer (FRET) and bioluminescence resonance energy transfer (BRET). These techniques, unlike the Y2H system, are currently fairly cumbersome and require expensive equipment, such as powerful confocal microscopes. However, with the recent development of plate readers capable of measuring FRET and BRET signals, the experimental processes could potentially be simplified and streamlined into a high throughput screening (HTS) system.

1.4 Fluorescence and Bioluminescent Resonance Transfer

Fluorescence resonance energy transfer (FRET) is the transfer of electron excitation energy from a donor fluorophore to an acceptor fluorophore. When a donor fluorophore is excited with suitable mono-chromatic light, its excitation energy can be transferred non-radiatively, that is to say without the appearance of a photon, to an acceptor fluorophore by means of intermolecular long range dipole-dipole interactions (Forster, 1949).

FRET can be thought of as a molecular yardstick, allowing the interactions between molecules and proteins to be measured, provided they are labelled with suitable fluorophores. It is important to note that the efficiency of FRET energy transfer is inversely proportional to the sixth power of the distance between donor and acceptor fluorophores (Maki *et al.*, 1976). This means the ability to transfer energy between fluorophores rapidly decreases over distance. The effective range for FRET to occur over is 1-10 nm dependent on experimental conditions (dos Remedios *et al.*, 1995). Interestingly, this distance is within the extent of conventional protein dimensions and similar to those of multimeric protein complexes observed in biological systems (New *et al.*, 2003).

Technological advances in light microscopy imaging, combined with the availability of genetically encoded fluorescent proteins have provided the tools necessary to assess the temporal protein associations inside living cells (Heim *et al.*, 1996). Interactions between adequately labelled proteins can be monitored by observing the emission of the acceptor fluorophore in a system; the detection of acceptor fluorophore emission indicates a level of donor-acceptor interaction. Ideally, emission of the acceptor fluorophore does not overlap with the emission of the donor allowing for easy quantification of the interaction. Workable FRET pairs need to include sufficient separation in excitation spectra for selective

stimulation of the donor, an overlap greater than 30% between the emission spectrum of the donor and the excitation spectrum of the acceptor to obtain efficient energy transfer, and reasonable separation in emission spectra between donor and acceptor fluorophores to facilitate independent measurement of the fluorescence of each fluorophore (Pollok *et al.*, 1999). In biological systems the most commonly used donor-acceptor pair is enhanced cyan fluorescence protein and enhanced yellow fluorescence protein, both derivatives of green fluorescence protein (GFP).

1.4.1 Fluorescence proteins for FRET

GFP was first described in the jellyfish *Aequorea Victoria* in 1955 and was subsequently extracted, purified and identified as a protein in 1962 (Shimomura *et al.*, 1962). However, its use in molecular biology did not begin outright until 1994 when it was successfully cloned and expressed (Chalfie *et al.*, 1994). Adjustments to GFP's excitation and emission spectra were made shortly after this breakthrough providing more robust fluorophores for use in molecular biology. Fluorescence is dependent upon a region of the protein that forms an imidazolidinone ring; the residues serine 65, tyrosine 66, and glycine 67. Mutating residues in close proximity to this imidazolidinone ring skews the absorbed and emitted wavelengths of GFP resulting in variations of GFP (Kretsinger, 2005). Various mutations have resulted in the development of Cyan FP, Yellow FP, Red FP, Saffron FP, Blue FP as well as many more minor variations. Many factors affect the ability of protein pairs to behave as FRET pairs, special consideration must be given to the amount of spectral overlap between the fluorophores, the distance between them, and the quantum yield of the donor protein. Many pairings have been tried since the inception of the FRET technique, one pair which satisfies all these requirements is ECFP and EYFP. Consequently, ECFP and EYFP has become one of the most widely utilised donor acceptor pairs for protein-protein interaction studies.

The excitation wavelength of EYFP overlaps with the emission wavelength of ECFP (Figure 1.5) allowing FRET to occur without too much overlap with its emission spectra with the emission spectra of EYFP (Gryczynski, 2005).

1.4.2 Living System FRET measurements

Measurements of many protein-protein interactions by FRET have been conducted in intact cells. Some examples of interactions that have been studied by FRET are GPCR dimerisation studies, β -arrestin binding to GPCRs, and protein folding interaction with chaperones (Rye, 2001). The introduction of FRET for the study of G-protein activation in intact cells begun in *Dictyostelium* (Janetopoulos *et al.*, 2001) and was later utilised in other systems including yeast (Yi *et al.*, 2003) and mammalian systems (Azpiazu *et al.*, 2004; Bunemann *et al.*, 2003). Currently, the majority of this work has been performed with the use of confocal microscopy equipment, and until recently there was not an adequate plate reader system capable of measuring the fast kinetics seen in G-protein activation in a FRET based assay (Talbot *et al.*, 2008)

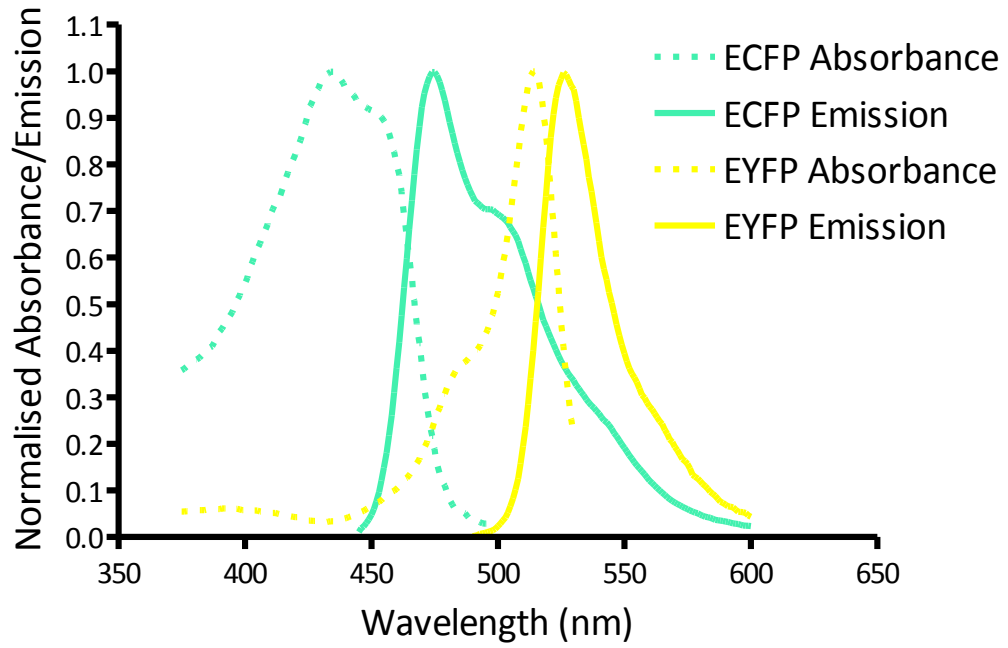


Figure 1.6 Normalised absorbance and emission spectra for ECFP and EYFP. The emission spectra of ECFP has substantial overlap with the absorbance spectra of EYFP absorbance, resulting in the non radiative transfer of energy to EYFP, resulting in EYFP fluorescence following ECFP excitation, when ECFP is within 10 nm.

1.4.3 Bioluminescence Resonance Energy Transfer

Bioluminescence is a naturally occurring form of chemiluminescence where energy is released by a chemical reaction in the form of light emission. This natural phenomenon can be used to investigate protein-protein interactions in living systems in the same way as FRET. By replacing the donor fluorophore used in FRET with a protein capable of producing light in a chemiluminescent way a more sensitive system can be created.

In nature, the sea pansy *Renilla reinformas*, along with other aquatic organisms respond to mechanical stimulation with the release of calcium from intracellular stores, which results in an indirect stimulatory effect upon its species specific luciferase – renillia luciferase (rLuc). Light is produced from rLuc by the catalysis of coelenterazine with ATP and oxygen to coelenteramide, on its own this results in emission at approximately 480 nm. However, GFP is located closely and energy is transferred by resonance energy transfer resulting in a spectral shift to 520 nm.

Several modifications to this system have made it more suitable for the measurement of protein-protein interactions in mammalian cells; such as the development of more stable substrates, codon optimised rLuc cDNA and decreasing spectral overlap for donor and acceptor emissions. The major advantage of using BRET over FRET is the reduction of autofluorescence and incidental fluorescence. However, BRET does suffer from low emission from the donor and acceptor fluorophore and therefore has the need for high quality microscopes and powerful photomultiplier detection units, which can be prohibitively expensive. In practice BRET has been used successfully to measure GPCR dimerisation in mammalian cells (Angers *et al.*, 2000) and has undergone vast

improvements which allow it to measure many more, previously invisible protein-protein interactions (Xu *et al.*, 2007).

1.5 Aims and Hypothesis

The studies outlined in this thesis represent a planned body of research directed at developing a robust assay to elucidate the protein-protein interactions involved in CCR5 mediated heterotrimeric G-protein activation. Prior to commencing this research, existing knowledge supported the notion that CCR5 may interact with more than one family or permutation of heterotrimeric G-proteins. It was hypothesised that it may activate different heterotrimers dependent upon the ligand and cell specific environment the receptor is located in. Typical assay methods employed to investigate these interactions in living cells, in real time, rely on inferring interactions from indirect assays that measured downstream effectors. Resonance energy transfer approaches allow a novel approach to identifying protein-protein interactions

To investigate this hypothesis this research was designed to approach the problem addressing three main aims;

- i. The creation and characterisation of suitable cell lines suitable for use in high throughput, real time FRET or BRET assays.
- ii. The development and implementation of a high throughput FRET or BRET assay system to measure protein-protein interactions.
- iii. To explore the molecular interactions of CCR5 activated G-proteins, using existing technologies.

Chapter Two

Materials and Methods

2.1 Cell Culture

All cell lines were grown at 37°C, 5% CO₂. Human Embryonic Kidney cells stably transfected with CCR5 (HEK.CCR5) were a kind gift from British Biotech (Oxford, UK) and were cultured in complete DMEM (Invitrogen) (DMEM, 2mM L-glutamine, 10% foetal calf serum (Invitrogen), 100 U/mL penicillin 100 µg/mL streptomycin (Invitrogen), 1mM sodium pyruvate (Invitrogen), 100µm nonessential amino acids (Invitrogen)) and supplemented with 100µg/ml hygromycin B in order to maintain selection pressure for CCR5. Chinese Hamster Ovary cells stably transfected with CCR5 (CHO.CCR5), as described (Mueller *et al.*, 2002b), were cultured with complete DMEM supplemented with 400µg/mL G418, to maintain selection pressure. HeLa RC-49 cells stably expressing CCR5 were obtained from D.Kabat (Platt *et al.*, 1998) and cultured in complete DMEM. Materials for cell culture and buffer composition were bought from Fisher Scientific, unless otherwise stated. Gallein was bought from Tocris and dissolved in DMSO at a stock concentration of 75 mM.

2.1.1 Routine Conditions

Cells were grown in polystyrene 75 cm² vented cap flasks (Nunc) in a humidified cell culture incubator (Thermo Scientific) with CO₂ levels maintained at 5%, cell culture was performed in a HEPA filtered vertical laminar airflow cabinet (Heraeus). Upon reaching approximately 80% confluency, cells were washed in PBS (Invitrogen) (1.5 mM potassium phosphate monobasic, 3mM potassium phosphate dibasic, 150 mM NaCl; pH 7.2) and resuspended by soaking in PBS supplemented with 1 mM EDTA for 10 minutes at 37°C. The majority of cells

lifted from the cell culture surface within 10 minutes, the remaining were resuspended by gentle agitation of the culture apparatus. Aliquots of cell suspension were centrifuged for 5 minutes at 800 x g and the supernatant was removed. Cells were resuspended in complete DMEM supplemented with selection antibiotics and plated at the appropriate density into cell culture flasks. Cells for cryopreservation underwent the same resuspension procedure, but were resuspended in FCS supplemented with 10% DMSO (Sigma-Aldrich) (v/v) and gently pipetted into vials suitable for cryogenic preservation of mammalian cells. Vials were wrapped in tissue and placed in a cell freezing container at -80°C overnight. This allowed for the critical cooling rate (1°C/min) required for successful cryopreservation of cells. Long term storage of samples was achieved by transferring vials to liquid nitrogen. Batches of stable transfectants were typically preserved between passage 3 and 6.

2.2 Calcium Flux Measurements

2.2.1 Fura-2 loading

Detachment of cells was achieved by removal of the media and incubation with EDTA/PBS (1mM EDTA). Cells were pelleted by centrifugation at 1000 x g for 3 minutes and washed twice in calcium flux buffer (CAF) (137 mM NaCl, 5 mM KCl, 2 mM MgCl₂, 1.5 mM CaCl₂, 10mM HEPES pH 7.4, 25mM D-Glucose) to remove residual EDTA and lysed cells. Cells were resuspended to concentration of 2×10^6 /ml in CAF and loaded with the membrane permeable acetoxymethylester (AM) form of fura-2 (Sigma-Aldrich) at a concentration of 2 μ M. The AM moiety facilitates membrane permeability of fura-2 by masking negative charges of its carboxyl groups, creating an uncharged and hydrophobic compound capable of diffusing across the cell membrane. Once inside the cell, the AM group is cleaved by cellular esterases, resulting in trapping fura-2 in the cytosol. A stock solution of fura-2 AM was made in DMSO to a final concentration of 1 mM and stored at -20°C in the dark. All cells were loaded with Fura-2 for 40 minutes at 37°C in the dark.

2.2.2 Ratiometric Measurement of Calcium Release

Following the loading of cells with Fura-2, cells were pelleted by centrifugation at 1000 x g for 3 minutes and washed twice in CAF before being resuspended to a concentration of 2×10^6 /ml in CAF. Cells were gently pipetted into black, solid bottomed, 96 well plates (Fisher Scientific, UK) and placed in a plate reader. Ratiometric measurements were achieved using a BMG fluorostar spectrofluorometer (BMG Labtech, Germany) set to excite cells sequentially at 340 nm and 380 nm and measure the resulting emission intensities alternately at 510 nm. In order to ensure a standard light path, 100 μ l of loaded cells were pipetted into each well. Data were recorded by Fluorostar control software (BMG Labtech, Germany).

2.3 Spectrophotomic and Statistical Data Analysis

All spectrophotomic data pertaining to calcium flux measurements, FRET, BRET and qualitative cAMP measurements was measured using a BMG fluorostar optima fitted with relevant excitation/emission filters (Table 2.1). Relative emissions were recorded by BMG Optima Evaluation software in conjunction with Microsoft Windows. Data was further transferred to Microsoft Excel 2007 for statistical analysis. Significance between recorded means was calculated in Excel by performing unpaired, two-tailed t-test on samples. Real time traces, area under curves and sigmoidal curve fitting was performed in GraphPad Prism 4. Likewise, $\log EC_{50}$ and efficacy values were calculated in GraphPad Prism 4.

2.3.1 Calcium Flux Analysis

Wells containing Fura2 loaded cells were alternately excited at 340 nm and 380 nm and resulting emission intensities were measured at 510 nm. Fluorostar control software was programmed to excite samples at 340 and 380 nm with an interval of 1.1 seconds between light pulses, allowing real-time ratiometric measurement of calcium mobilisation following stimulation. Respective fluorescent emissions were recorded and a ratiometric trace produced by calculating the ratio of 340 nm emission over 380 nm emission in Microsoft Excel 2007. The pre-stimulation baseline was averaged and subtracted from the maximal ratiometric measurement recorded following stimulation. This value was then divided by the average pre-stimulation value to provide the standard calcium flux value. This method of analysis allows for comparison between experiments where cell number differs.

2.3.2 FRET and BRET Analysis

FRET measurements were performed in solid bottom, black, 96 well plates (Costar) using a BMG Fluorostar plate reader. Filters were set to excite ECFP at 435 nm and EYFP at 510 nm and resulting emissions recorded at 485 nm and 530 nm, respectively. Filters were programmed to alternately switch between excitation and emission filters with an interval of 1.1 seconds between light pulses. The amount of flashes per measurement was set to ten per well in order to avoid photobleaching. Subsequent emissions were recorded, allowing the real time ratiometric measurement of the FRET signal. As no external light source is used for BRET experiments, filters were set to record emission at 530 nm and overall luminescence. Ratiometric FRET data was produced by dividing fluorescent emission 485 nm by fluorescent emission 530 nm. Traces for real time FRET measurements were created in GraphPad Prism 4 by plotting points on a xy scatter graph. A curve was fitted to data points by plotting the weighted average of each point's nine neighbours. To easily

compare changes in the FRET ratio, the area under the post-stimulation curve (AUC) was calculated. This was performed in GraphPad Prism 4. To ensure comparative readings were accurate, the baseline for measuring the AUC was set to 1 and the area under all peaks above the baseline was calculate and graph dimensions were equalised.

BRET experiments were performed in solid bottomed, white, 96 well (Costar) plates using a BMG Fluorostar platereader. Fluorescent emission was recorded at 530 nm and luminescence by selecting emissions to be recorded at 485 nm. Traces and graphs were created using the same process as for FRET.

Assay	Excitation (nm)	Emission (nm)
Ca Flux	340-10	510-12
Ca Flux	380-10	510-12
ECFP	435-p	485-p
FRET	435-p	530-12
EYFP	510-12	530-12
BRET	None	485-p
BRET	None	530-12
cAMP	None	Lens

Table 2.1. Combinations of filters used for different experimental procedures.

2.3.3 Concentration Response Curve Fitting and Analysis.

Concentration response graphs were plotted and analysed with GraphPad Prism 4. Cells were stimulated with varying concentrations of CCL3 and calcium mobilisation was monitored. Calcium flux values were recorded and plotted on a xy scatter graph against the corresponding CCL3 concentration. Collated data points were fitted to a nonlinear regression curve using a sigmoidal dose-response equation which assumes a hill co-efficient of 1. In-built data analysis software calculated logEC₅₀ values and bottom and top values.

2.4 Fluorescence Microscopy

2.4.1 Slide Preparation for CCR5 and Fusion Protein Visualisation

Cells were resuspended by incubation with 1 mM EDTA/PBS, washed in PBS three times and resuspended in complete growth media containing appropriate selection antibiotic to a density of 2×10^6 /ml. Glass coverslips were meanwhile rinsed in 70% ethanol and allowed to dry in sterile conditions. Coverslips were placed in 35 mm cell culture dishes with 2 ml of complete DMEM containing appropriate selection antibiotics. A final concentration of 2×10^5 cells were added to each dish and left to incubate at 37°C overnight. The following day, glass coverslips were removed from cell culture dishes and gently washed three times in PBS. Cells were fixed in 4% paraformaldehyde solution for 10 minutes at 4°C and washed following incubation. Cells to be stained for CCR5 expression were incubated for 35 minutes at 4°C with anti-CCR5 antibody HEK/1/85a/7a, an antibody raised against intact CHO.CCR5 cells and the CCR5 N-terminal peptide (Mueller *et al.*, 2002a), washed three times with PBS, and incubated for 35 minutes at 4°C with TRITC or FITC labelled anti-rat IgG (see Table 2.2 for a full list of antibodies). Cells were washed three times with PBS and mounted with glycerol onto a glass slide. CCR5 localisation and expression of G-protein fusion proteins linked to ECFP or EYFP was visualised using a Zeiss fluorescent microscope in combination with Axiovision imaging software (Zeiss, Germany).

Antibody	Manufacturer	Dilution
Anti CCR5 HEK/1/85a/7a	Gift from J. A. Mackeating, Reading (Mueller <i>et al.</i> , 2002b)	Undiluted
Anti Rat TRITc conjugated IgG	Sigma- Aldrich	1:200
Anti Rat FITC Conjugated IgG	Sigma-Aldrich	1:1000

Table 2.2 Antibodies used for CCR5 immunofluorescent staining of CCR5

2.4.2 siRNA Transfection Visualisation

AllStars™ negative control siRNA (Qiagen) modified to contain a rhodamine moiety was used to determine transfection rates of siRNA. Cells were transfected in clear bottomed, black, 96 well plates and, after 72 hours, washed with PBS and viewed on a Leica DM IL fluorescence microscope fitted with a CY3 filter cube (excitation λ 546 nm) (Leica, Germany). Cells were counter stained with DAPI (Sigma-Aldrich) in order to visualise the nucleus. DAPI was dissolved in PBS to a final concentration of 100 ng/ml and incubated with cells grown in a clear bottomed, black, 96 well plate at 37°C, 5% CO₂. Following incubation cells were washed three times in PBS and viewed under the microscope.

2.5. Cloning and Molecular Biology Techniques

2.5.1 Plasmids

The pcDNA3.1 vector was used for amplification of all inserts in *E.coli*. pcDNA3.1 with insert were either used for transfection or inserts were excised and ligated into pcDNA6 v5-His or pZEO SV2 ready for transfection. The specific cloning practice utilised for different experimental procedures is outlined where relevant.

2.5.2 Primers

All primers were purchased from Invitrogen and resuspended in PCR quality water to a final concentration of 250 μ M.

Gai2-ECFP		
5' Primer	5' TCG GAT CCA TGG GCT GCA CCG TG 3'	BAM HI introduced
3' Primer	5' TTG GAT CCA AGA GGC CGC AGT CCTT CAG 3'	BAM HI introduced
EYFP-Gβ₁		
5' Primer	5' TTA AGC TTC TTC CAG ATC TTG AGG AAG C 3'	HIND III introduced
3' Primer	5' CGA AGC TTA TGG TGA GCA AGG GCG AGG 3'	HIND III introduced
hrLuc-Gai2		
5' Primer	5' TTA AGC TTC TTC CAG ATC TTG AGG AAG C 3'	HIND III introduced
3' Primer	5' CGA AGC TTA TGG TGA GCA AGG GCG AGG 3'	KPN I introduced

Table 2.3 A list of primers used and the cut sites introduced to inserts used.

2.5.3 Transformation of DH5 α

E.coli DH5 α (Invitrogen) was transformed with various plasmid constructs for amplification of plasmids. 35 μ l of *E.coli DH5 α* were thawed on wet ice and gently mixed by stirring with a pipette tip. 1-5 μ g of plasmid construct was added to *E.coli* that had been left to thaw on ice and incubated on ice for a further 30 minutes. Cells were heat shocked at 42°C for 90 seconds and placed on ice for 2 minutes. 965 μ l of pre-warmed LB broth was added to heat shocked cells and incubated in a rotary shaker at 37°C, 225 rpm for 2 hours. 200 μ l of bacterial broth was spread on LB agar plates containing ampicillin (20 μ g/ ml) and grown overnight at 37°C. Colonies were picked the following day and incubated overnight in 2 ml cultures containing ampicillin (20 μ g/ ml).

2.5.4 Plasmid Isolation (analytical)

Transformed bacterial cultures were centrifuged at 3900g for 5 minutes. The supernatant was discarded and the pellet resuspended in 200 μ l STET-L buffer (Sucrose 8% (v/v), Tris/HCl pH8 50 mM, EDTA 50mM, Triton X-100 0.1% (v/v), and lysozyme 10 mg/mL). The mixture was then placed in a heat block for 60 seconds at 100°C. After heating, the mixture was immediately transferred to ice and then centrifuged at 9000 RCF for 15 mins. The pellet (cell lysate) was removed from the supernatant and 200 μ l of isopropanol was added. Samples were then centrifuged at 9000 RCF for 40 mins. The supernatant was removed and 200 μ l of 70% ethanol was added to the pellet, which was then centrifuged at 9000 RCF for five minutes. The supernatant was carefully pipetted out and the pellet was air dried. Plasmids were then resuspended in 20 μ l of P1 + RNase buffer (Invitrogen).

2.5.4.1 Plasmid isolation (amplification)

Transformed *E.coli DH5α* was picked from an ampicillin resistant agar plate with a sterile pipette tip and grown in 2 ml of LB media supplemented with ampicillin (25µg/mL) at 37°C, 225 RPM. The culture was then transferred into 100ml of LB/Ampicillin media and grown over night at 37°C, 225 RPM in a conical flask. The following morning the bacterial culture was decanted into a 50 ml plastic centrifuge tube and centrifuged at 15000 x g at 4°C for 15 minutes. Reagents for plasmid isolation were purchased as part of a commercially available midiprep kit and used in accordance to the manufacturer's instructions. Briefly, the supernatant was discarded and cells resuspended in 5 ml of resuspension buffer P1 (50mM Tris-Cl, pH 8.0, 10mM EDTA, 100ug/mL RNase A) by careful agitation. 5ml of lysis buffer P2 (200mM NaOH, 1% SDS) was immediately added following resuspension and the sample mixed by carefully inverting the tube 10 times followed by incubation for 5 minutes at ambient temperature. Following incubation, 5 ml of neutralisation buffer P3 (3 M potassium acetate, pH 5.5) was added and mixed by careful inversion of the tube. The sample was centrifuged at 15000 x g for 10 minutes at 4°C to remove cellular debris. Meanwhile a DNA affinity column was equilibrated in equilibration buffer (750mM NaCl, 50mM MOPS, pH7, 15% isopropanol, 0.15% Triton X-100). The supernatant was added to the column and allowed to flow through by gravity. The loaded column was washed twice with wash buffer (1M NaCl, 50mM MOPS, pH 7.0, 15% isopropanol), the flow-through discarded and 5 ml of elution buffer (1.25M NaCl, 50mM Tris-Cl, pH 8.5, 15% isopropanol) added to the column. The flow-through was collected and 3.5 ml of isopropanol added, before centrifuging the sample for 60 minutes at 15000 x g, 4°C. The supernatant was carefully removed and gently rinsed with 3 ml of 70 % ethanol. The sample was centrifuged for 5 minutes at 15000 rcf, 4°C and the supernatant removed. The pellet was allowed to air dry for 5 minutes and resuspended in 200 µl of TE buffer (10mM Tris-Cl, pH 8.0, 1mM EDTA). Plasmid concentration was determined by U.V. spectrophotometry.

2.5.5 Plasmid Digestion

Analytical digests were performed to confirm the correct insertion of inserts into plasmids. Plasmid digestions were also performed to isolate inserts for further processing. For analytical digests, 1 µl of isolated plasmid was mixed with x10 buffer (NEB) and 20U of the relevant restriction enzyme in a total reaction volume of 10 µl, made to volume by the addition of nuclease free ddH₂O (Promega). The mixtures were incubated at 37°C for 2 hrs and analysed by agarose electrophoresis. For digests involved in further processing, 16 µl plasmid, 2 µl x10 buffer and 200U of relevant restriction enzyme were used in a total reaction volume of 20 µl, made up to volume by the addition of nuclease free ddH₂O.

2.5.6 Agarose Gel Electrophoresis DNA Separation and Purification

Digested plasmids were separated on 1% agarose gel (w/v), made by mixing agarose powder in TAE buffer (500 mM TRIS, 50 mM Acetate, 7 mM EDTA, pH 7.1) and boiling the mixture in the microwave until the agarose dissolved. The mixture was left to cool to approximately 60°C then 10 µl ethidium bromide (10mg/mL) was added. The mixture was swirled and poured into a cast to set for one hour, with a well casting comb in order to create wells for samples. The set gel slab was placed in an electrophoresis tank (Bio-Rad), covered with TAE buffer. Digested plasmids were mixed in a 1:4 ratio with X4 sample loading buffer (50 mM TRIS, 5 mM EDTA, 25% Sucrose, 2 mg/mL bromophenol blue). 20 µl of the resulting mixture was loaded to each well. Electrophoresis was performed for 45 minutes at 110 volts. Ethidium bromide intercalates double stranded DNA, allowing for fluorescence visualisation of fragments by excitation with UV light. During brief visualisation, in order to prevent denaturation of DNA, excised fragments were cut from the gel and placed in plastic tubes. Agarose was solubilised and DNA isolated using a commercially available purification kit (Qiagen).

2.5.7 Polymerase Chain Reaction

For PCR, 10µL of X10 *Taq* reaction buffer (Bio-Rad), 1 µL of forward primer, 1µL of reverse primer, 5 µL of 2 mM dNTP (NEB), 8 µL of 25 mM MgCl₂, 500 ng of template DNA were added to a PCR compatible microfuge tube and the volume made to 100 µl by the addition of PCR quality water (Bio-Rad). 0.5 µL of *Taq* polymerase was added to the reaction mixture and the microfuge tube placed in a thermal cycler. The reaction mixture was heated to 94°C for 40 seconds, followed by cooling to 55°C for 90 seconds and heating to 72°C for 60 seconds. This cycle was repeated 30 times, with the 30th cycle holding the 72°C extension for five minutes before cooling the reaction mixture to 4°C. A control containing no DNA template was run to ensure no contamination. Amplification of the desired sequence was confirmed by running samples on an agarose electrophoresis gel loaded. Amplified sequences were purified with a commercially available purification kit.

2.5.8 Phosphatase Treatment of Sequences

Cut vectors were treated with calf intestinal phosphatase (CIP) (NEB) to prevent re-annealing of cut ends. Samples were resuspended in TEbuffer (NEB) to a concentration of 0.5 µg/10 µL, CIP was added to a final concentration of 0.5 U/µg DNA. The reaction was incubated at 37°C for 60 minutes and resulting DNA purified using a commercially available plasmid purification kit (Qiagen).

2.5.9 Purification of DNA after Enzymatic reactions

Enzymes and other impurities were removed from DNA containing solutions by passing the reaction mixture through a Qiaquick DNA clean up kit (Qiagen). Buffer PN was added to the DNA mixture and pipetted to spin column containing a silica membrane and centrifuged for 1 minute at 8000 x g. Nucleic acids in the mixture adsorb to the silica membrane in the high-salt conditions provided by buffer PN, while other impurities are collected in a disposable tube and discarded. 30µL of PCR quality water (p.H. 7-8.5) was added directly to the silica membrane and left to stand for 1 minute before centrifuging for 1 minute at 17,000 x g. DNA concentration was determined by absorbance at 260 nm.

2.5.10 Ligation

For ligation 100-250 µg of DNA was added to ligation buffer (660 mM TRIS-HCl, 50 mM MgCl, 10 mM ATP, pH 7.6) and 1 µL (1U) of T4 DNA Ligase (NEB) was added to the mixture and incubated at room temperature for 3 hours. Ligated constructs were confirmed by digestion and analytical agarose electrophoresis.

2.6 Transfection

2.6.1 Transfection of DNA

Transfection of plasmid constructs into HEK.CCR5, CHO.CCR5 and HeLa RC-49 were performed using GeneJuice (Novagen), Lipofectamine (Invitrogen), or FuGene(Roche), following the manufacturers procedure for transfection of adherent cells in a 35 mm cell culture dish. Cells were seeded one day prior to transfection and were always between 50-80% confluent when transfected. Exact amounts of GeneJuice and plasmid were optimised for each cell type and plasmid (Table 2.4).

2.6.2 Transfection of siRNA

siRNA sequences were resuspended in siRNA resuspension buffer (Qiagen) to a final concentration of 20 μ M. HeLa RC-49 were resuspended by incubation with EDTA/PBS for 10 minutes at 37°C, washed and resuspended to a final concentration 5×10^4 /ml in complete DMEM. Cells were seeded immediately before transfection into a 24 well plate, 500 μ l of cell suspension was added to each well and the plate incubated at 37°C 5%CO₂. For each well to be transfected 100 μ l of plain DMEM and between 7.5 ng – 15 ng of siRNA was added to the media in an RNase free plastic vial and immediately vortexed for 10 seconds. 1.5 μ l of INTERFERin (Polyplus, France) was then added to the mixture, mixed by agitation with the pipette and incubated in sterile conditions at room temperature for 15 minutes. Following incubation, which allows transfection reagent – siRNA complexes to form, 100 μ l of mixture was added to each well. The cell culture dish was mixed by swirling the plate gently then subsequently incubated for 72hrs at 37°C, 5% CO₂ before harvesting for experiments. Final siRNA amounts used during transfection were optimised for each sequence (Table 2.5).

2.6.3 Transfection Reagents and Volumes

Reagent	Manufacturer	Ratio to Plasmid DNA (μ L: μ g)
GeneJuice	Novagen	10:5
FuGene	Roche	10:5
Lipofectamine	Invitrogen	10:4

Table 2.4 Reagents and Ratios for Plasmid DNA transfections in 35mm dishes

Reagent	Manufacturer	Ratio to siRNA (μ L:ng)
INTERFERin	Polyplus	1.5:7.5-15

Table 2.5 Reagent and Ratios for siRNA transfections in 24-well plates per well

2.7 Western Blotting

Western blot analysis enables the qualitative detection of a specific protein from a mixture of proteins by utilising antibodies directed against the protein of interest. Not only does it provide information about the level of protein expression but also the size of the protein.

2.7.1 Protein Extraction and Preparation

Protein was extracted from cells cultured in a 35 mm cell culture dish using a combination of cell lysis buffer (Tris-HCl 0.1 M, 20% glycerol, 10% SDS, pH 7.6) and sonication of cellular material. Cultured cells were resuspended with EDTA/PBS and centrifuged at 4000g for five minutes. The pellet was resuspended by vigorous pipetting in lysis buffer followed by approximately 10 pulses with a sonicating probe for 2 s at 80% amplitude and 0.8 pulse. Samples were spun for 5 minutes at 14000 g, the pellet discarded and x4 sample buffer (4% SDS, 0.02% bromophenol blue, 20% glycerol, 10% mercaptoethanol, 80 mM Tris pH 6.8) added to the supernatant to ensure all proteins are denatured and to facilitate loading to the gel. Samples were then heated to 95°C for 5 minutes and placed on ice to cool during the assembly of apparatus.

2.7.2 SDS-PAGE Gel Electrophoresis and Protein Transfer

Samples were run on a 13% acrylamide resolving gel (0.67155g Tris/SDS 2% pH 8.8, 13% acrylamide v/v, 0.1% ammonium persulphate w/v, 0.01% TEMED v/v) and loaded onto a 4.5% acrylamide stacking gel (0.1089g Tris/SDS 2% pH 8.8, 4.5% acrylamide v/v, 0.1% ammonium persulphate w/v, 0.01% TEMED v/v). Protein samples were loaded to the gel together with broad range protein marker (NEB). Samples were run at room temperature

at a constant voltage of 200V, until the dye front reached the bottom of the gel, which typically took 45 minutes.

Protein transfer was achieved using a Bio-Rad semi-dry electroblotter. Sponges, filter paper (Whatman) and nitrocellulose membranes (Whatman) were soaked in transfer buffer (pH8.3, 25 mM Tris, 192 mM glycine, 10% methanol) at room temperature for 15 minutes prior to assembly. The SDS-Page gel was placed together with the nitrocellulose membrane in a sandwich of thick filter papers and sponges, and a voltage of 15V was passed through the stack for 45 minutes to ensure complete transfer.

2.7.3 Immunoblotting and Development

To avoid unspecific binding of antibodies to transferred proteins, membranes were incubated in a blocking solution of 0.5% Tween-20 in PBS (PBS-T) with 5% fat-reduced milk powder (Marvel) for one hour at room temperature with gentle shaking. Membranes were then washed for 10 minutes in PBS-T three times before being incubated with primary antibody diluted in 5% PBS-T overnight at 4°C in a rotary wheel. Dilution factors for primary antibodies were 1:100 for HEK/1/85a/7a and 1:500 for all probed G α subunits (Table 2.6). Membranes were then washed for 10 minutes in PBS-T three times before being incubated with secondary antibody for one hour at room temperature on a shaking plate. Secondary antibodies were diluted in blocking buffer by a dilution factor of 1:10000 (Table 2.7). Membranes were then washed for 10 minutes, three times in PBS-T. Proteins were detected using Novax Chemiluminescence reagents (Pierce) according to the manufacturer's instructions. The light reaction produced was detected with an X-ray film (GE-Healthcare Life Sciences) and developed using an automatic X-ograph developing machine (Kodak) according to the manufacturer's guidelines. Developed films were then photographed using a digital camera (Samsung) and transferred to computer file.

2.7.4 Antibodies for Immunoblotting

Antibody	Manufacturer	Dilution
Anti CCR5 HEK/1/85a/7a (Rat)	A kind gift from J. A. Mckeating, Reading	1:100
Anti-G α_{i2} (Rabbit)	Santa-Cruz	1:500
Anti-G α_q (Rabbit)	Santa-Cruz	1:500
Anti-G $\alpha_{i1/3}$ (Rabbit)	Santa-Cruz	1:500

Table 2.6 Primary Antibody Details

Antibody	Manufacturer	Dilution
Anti-Rat IgG Horseradish Peroxidase	Sigma-Aldrich	1:10000
Anti-Rabbit IgG Horseradish Peroxidase	Sigma-Aldrich	1:10000

Table 2.7 Secondary Antibody Details

2.8 cAMP Measurement

cAMP levels were determined using the bioluminescent cAMP-Glo™ assay developed by Promega. The assay allows for the measurement of cAMP without the use of radioactive compounds or the need for prohibitively expensive antibody ELISA assays. The assay is based on the activation of protein kinase A by cAMP, resulting in decreased ATP levels in homogenised cell lysate. In this assay, bioluminescence produced is proportional to levels of ATP, and therefore reversely proportional to cAMP levels.

HeLa RC-49 cells were grown to approximately 80% confluency in 35 mm cell culture dishes. Cells were resuspended in EDTA/PBS, centrifuged at 1000 g for five minutes and resuspended in induction buffer (PBS containing 1 mM Isobutylmethylxanthine (IBMX)), to prevent phosphodiesterase activity, to a density of 1.5×10^5 /ml and incubated for 30 minutes at 37°C 5% CO₂. Cells were then incubated in induction buffer containing 10 μM forskolin (Tocris), an activator of adenylyl cyclase, and treated with Gallein or a DMSO control and incubated for a further 20 minutes. Following treatment, cells were centrifuged and resuspended to 1.5×10^5 /ml in induction buffer. For dose response curves, cells were treated with varying concentrations of CCL3 for 3 minutes, before the addition of lysis buffer (Promega, proprietary formula). The qualitative amounts of cAMP under different conditions were determined using the cAMP-Glo assay according to the manufacturer's instructions (Promega).

Chapter Three

Creation and Characterisation of Cells Stably Expressing Tagged G-Proteins

3.1 Introduction

The task of measuring protein-protein interactions in living cells is fraught with difficulty, with no single method able to simply and adequately detect the vast variety of interactions within living cells. FRET has, in recent years, become a relatively popular method to disseminate the interactions of a protein couple in model single cell systems. Transient transfection of DNA coding for the protein(s) of interest linked to a fluorescent protein is a well defined method of monitoring interactions. Although there are advantages to this methodology, there are several drawbacks and limitations associated with single cell work. Over-expression of tagged protein is often required in order to create a system capable of being monitored by FRET, this can result in the loss of normal physiological function of the cell. Transient transfection required to create this system can result in inconsistent expression between cells. Measurement of FRET in single cell systems often relies upon a laboratory being equipped with a high quality live cell imaging confocal microscope. Development of a stable expression system would circumnavigate these issues and allow for rapid high throughput screening of ligand specific protein-protein interactions.

At present there are no cell lines that possess all the characteristics required for the measurement of protein-protein interaction by FRET. However, several cell lines are suitable to use for creating stable cell lines due to their ease of transfection and simplicity of cell culture. Human Embryonic Kidney 293 (HEK) cells and Chinese Hamster Ovary (CHO) cells are well established and well characterised cell lines to carry out transfections in, and have previously been described to stably over express CCR5 with no physiological perturbation (Mueller *et al.*, 2002b; Mueller *et al.*, 2004a). The ease of transfection and culture will aid the clonal selection of cells exhibiting qualities required for the creation of a cell line capable of being used to measure G-protein activation by FRET.

3.2 Results

A prerequisite to the creation of stable cell lines is the creation of plasmids containing the coding sequence for the protein of interest. Plasmids containing full length, sequence verified, and expression verified cDNA sequences for human $G\alpha_{i2}$ and human $G\beta_1$ were bought from Missouri S&T cDNA Resource Center. These sequences were free of extraneous 3' and 5' untranslated regions and were propagated in pcDNA3.1+.

During the course of this project several plasmids containing G-protein fusion constructs were created. pcDNA3.1: $G\alpha_{i2}$ -ECFP and pcDNA6/V5-His:EYFP- $G\beta_1$ were initially created alongside pcDNA3.1:EYFP- $G\beta_1$ and pcDNA6/V5-His: $G\alpha_{i2}$ -ECFP for transfection into HEK.CCR5, which stably expresses CCR5 concomitantly with a hygromycin resistance gene. pcDNA3.1 contains a geneticin resistance gene and pcDNA6v5-His contains a blasticidin resistance gene, therefore allowing selection of multiple transfectants. The stable expression of CCR5 in CHO.CCR5 cells was selected by the concomitant expression of a geneticin resistance gene, consequently additional vectors for transfection of constructs were created to allow multiple selection in CHO.CCR5. pZeo SV2:EYFP- $G\beta_1$ containing a zeocin resistance gene was created to circumnavigate the problem of identical resistance genes in plasmids and facilitate selection of stable cell lines in CHO.CCR5. pcDNA6/V5-His: $G\alpha_{i2}$ -ECFP was used in CHO.CCR5 as well as HEK.CCR5. For a full list of plasmids used in the creation of stable cell lines see Table 3.1.

Cell line	1 st plasmid	Expression	2 nd plasmid	Expression	3 rd plasmid	Expression
HEK.CCR5 Parental	pIRES:CCR5 (Hygromycin B)	CCR5				
HEK.CCR5 EYFP	pIRES:CCR5 (Hygromycin B)	CCR5	PcDNA6 V5-HIS (Blasticidin)	EYFP-G β_1		
HEK.CCR5 ECFP	pIRES:CCR5 (Hygromycin B)	CCR5	PcDNA6 V5-HIS (Blasticidin)	G α_{i2} -ECFP		
HEK.CCR5 EYFP-ECFP	pIRES:CCR5 (Hygromycin B)	CCR5	PcDNA6 V5-HIS (Blasticidin)	EYFP-G β_1	PcDNA3.1 (G418)	G α_{i2} -ECFP
CHO.CCR5 Parental	PcDNA3:CCR5 (G418)	CCR5				
CHO.CCR5 EYFP	PcDNA3:CCR5 (G418)	CCR5	pZeo SV2 (Zeocin)	EYFP-G β_1		
CHO.CCR5 ECFP	PcDNA3:CCR5 (G418)	CCR5	PcDNA6 V5-HIS (Blasticidin)	G α_{i2} -ECFP		
CHO.CCR5 ECFP-EYFP	PcDNA3:CCR5 (G418)	CCR5	PcDNA6 V5-HIS (Blasticidin)	G α_{i2} -ECFP	pZeo SV2 (Zeocin)	EYFP-G β_1

Table 3.1. A complete list of stable cell lines produced during this project. Plasmid and cDNA inserts used for stable cell line production are listed; the antibiotic resistance gene used for selection of the stable cell line is in brackets.

3.2.1 Creation of Plasmids for HEK.CCR5 Stable Expression

$G\alpha_{i2}$ cDNA was amplified by PCR introducing Xma1 cut sites at the 5' and 3' regions, and ligated into pAC409. Guided by previous studies showing fusion of ECFP does not perturb the normal activity of the G alpha subunit (Janetopoulos *et al.*, 2001). ECFP was obtained by PCR amplification of the ECFP cDNA sequence located in pECFP-C1, purchased from Clontech, with primers coding for N and C terminus Pst1 cut sites. The amplified cDNA was purified by agarose gel electrophoresis solubilisation and inserted into pAC409: $G\alpha_{i2}$ at the naturally occurring Pst1 cut site (5' CTGCAG 3') 304 bases into the $G\alpha_{i2}$ cDNA sequence. Correctly expressed $G\alpha_{i2}$ -ECFP has ECFP inserted between a leucine and glycine residue which form the turn between the 1st and 2nd alpha helix of the G-protein. The pAC409: $G\alpha_{i2}$ -ECFP construct was amplified by PCR with primers that introduced BamH1 sites at the 5' and 3' regions. ($G\alpha$ BamHI 5', 5' TCG GAT CCA TGG GCT GCA CCG TG 3', $G\alpha$ BamHI 3', 5' TTG GAT CCA AGA GGC CGC AGT CCTT CAG 3'). The $G\alpha_{i2}$ -ECFP construct ligated into pGEM, amplified, excised, and was purified by agarose gel electrophoresis solubilisation then ligated into pcDNA3.1(+) creating a plasmid construct that allows for selection in transfected mammalian cells with G418 (Figure 3.1A).

The cDNA sequence for $G\beta_1$ was amplified by PCR introducing a 5' EcoR1 cut site and a 3' BamH1 cut site, purified by agarose gel electrophoresis solubilisation and ligated into pVL1392. EYFP was obtained by PCR amplification of the EYFP cDNA located in pEYFP-N1, purchased from Clontech, with primers coding for 5' and 3' EcoR1 cut sites. Isolated EYFP was then ligated into pGEM, transformed into *E.coli* and amplified, the plasmid was purified by midiprep and EYFP was excised with EcoR1 and purified by agarose gel electrophoresis solubilisation. The resulting fragment was then ligated to the N-terminus of pVL1392: $G\beta_1$. The EYFP- $G\beta_1$ construct was amplified by PCR with primers containing HindIII

cut sites to the 5' and 3' regions ($G\beta_1$ HindIII 5', 5'TTA AGC TTC TTC CAG ATC TTG AGG AAG C3', $G\beta_1$ HindIII 3', 5'CGA AGC TTA TGG TGA GCA AGG GCG AGG3') and then ligated into pcDNA6/V5-His allowing selection in mammalian cells with blasticidin (Figure 3.1B). The EYFP- $G\beta_1$ construct was removed from the pcDNA6/V5-His vector by restriction nuclease digest with Hind III and ligated into pcDNA3.1(+) to form an additional vector for transfection.

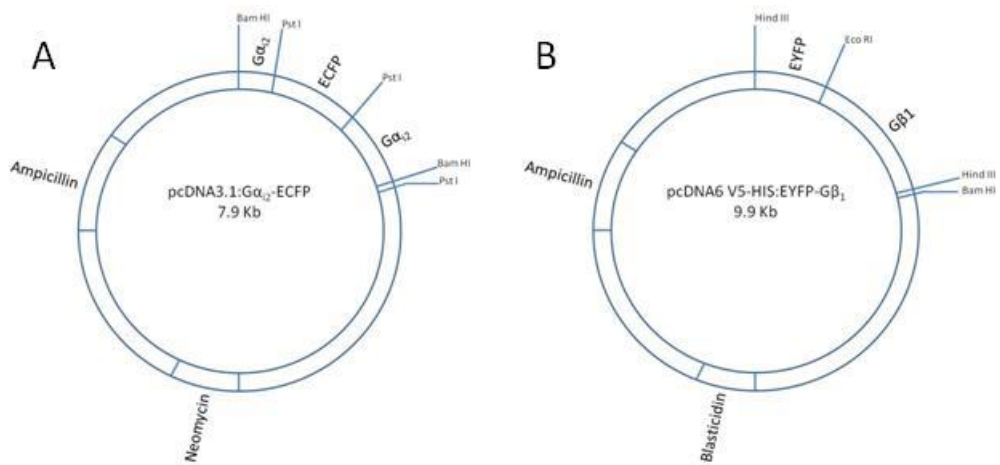


Figure 3.1 Schematic representations of the plasmids produced and transfected to create stable HEK.CCR5 expressing G-proteins tagged with fluorescent proteins. Both plasmids contain ampicillin resistance genes for selection in bacteria. (A) ECFP is approximately 700 bp in length and $G\alpha_{12}$ is approximately 1100 bp in length. However, Insertion of ECFP at the Pst1 site in the $G\alpha_{12}$ cDNA gives rise to two coding regions of approximately 300 bp and 800 bp. pcDNA3.1 contains a neomycin resistance gene allowing selection using G418 in mammalian cells. (B) EYFP is approximately 700 bp in length and $G\beta_1$ is approximately 1000 bp in length. The blasticidin resistance gene in pcDNA6/V5-His allows selection in mammalian cells using blasticidin.

3.2.2 Selection of Stable Single Expression HEK.CCR5

Following transfection, with either pcDNA6/V5-His:EYFP-G β_1 or pcDNA3.1:G α_{i2} -ECFP, cells were left to grow for 72 hours and then harvested and seeded out at low density in a 96 well plate in appropriate selection media. Proliferation and morphology of transfected cells was monitored by periodic viewing with a light microscope, proliferation in both transfectants was noted to be slightly slower than in the parental cell line. There was no noticeable effect upon cell morphology following transfection.

Several cell lines that had a similar proliferation rate to the parental cell line were scaled up. Cell morphology was observed not to be different to parental cells and expression of fluorescent construct appeared to be relatively high and uniform in the selected cell lines. The cell lines chosen for further studies displayed excellent expression of tagged G-protein (Figure 3.2).

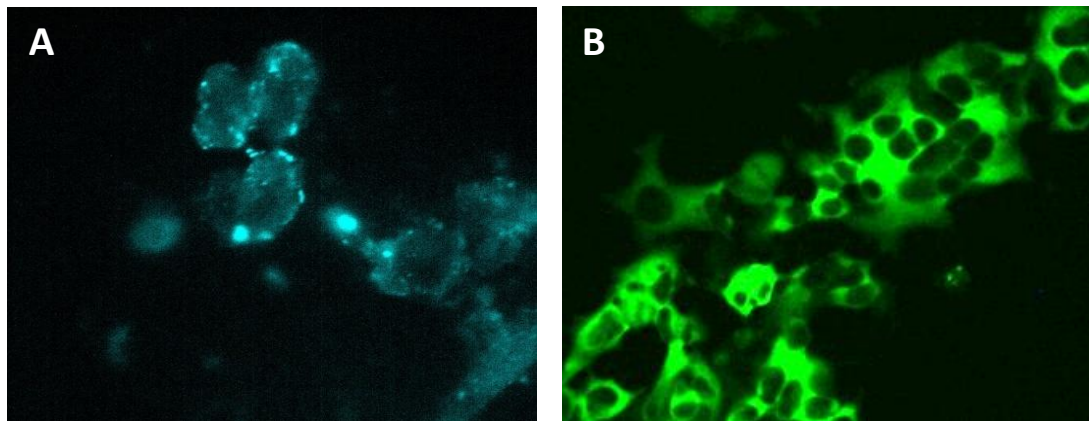


Figure 3.2 (A) HEK.CCR5 G α_{i2} -ECFP showing population wide expression of G α_{i2} ECFP. (B) HEK.CCR5 EYFP-G β_1 stable cell line, showing population wide expression of EYFP-G β_1 . These pictures are representative of the stable cell lines cultured in further experiments.

3.2.3 Characterisation of Stable HEK.CCR5 Single Transfectants

Stable single expression cell lines were characterised by measuring response to CCL3 stimulation compared to the parental cell line. Expression of constructs had no significant effect on potency of CCL3 activating CCR5 mediated calcium release. Log EC_{50} values of stable HEK.CCR5 $G\alpha_{i2}$ -ECFP and HEK.CCR5 EYFP- $G\beta_1$ closely matched parental value of -7.451M (± 0.1107 M, n=6) being -7.472 M (± 0.1376 M, n=6) and -7.554 M (± 0.1482 M, n=3), respectively (Figure 3.3). This clearly indicates that the stable expression of either construct does not perturb the normal signalling mechanisms of CCR5.

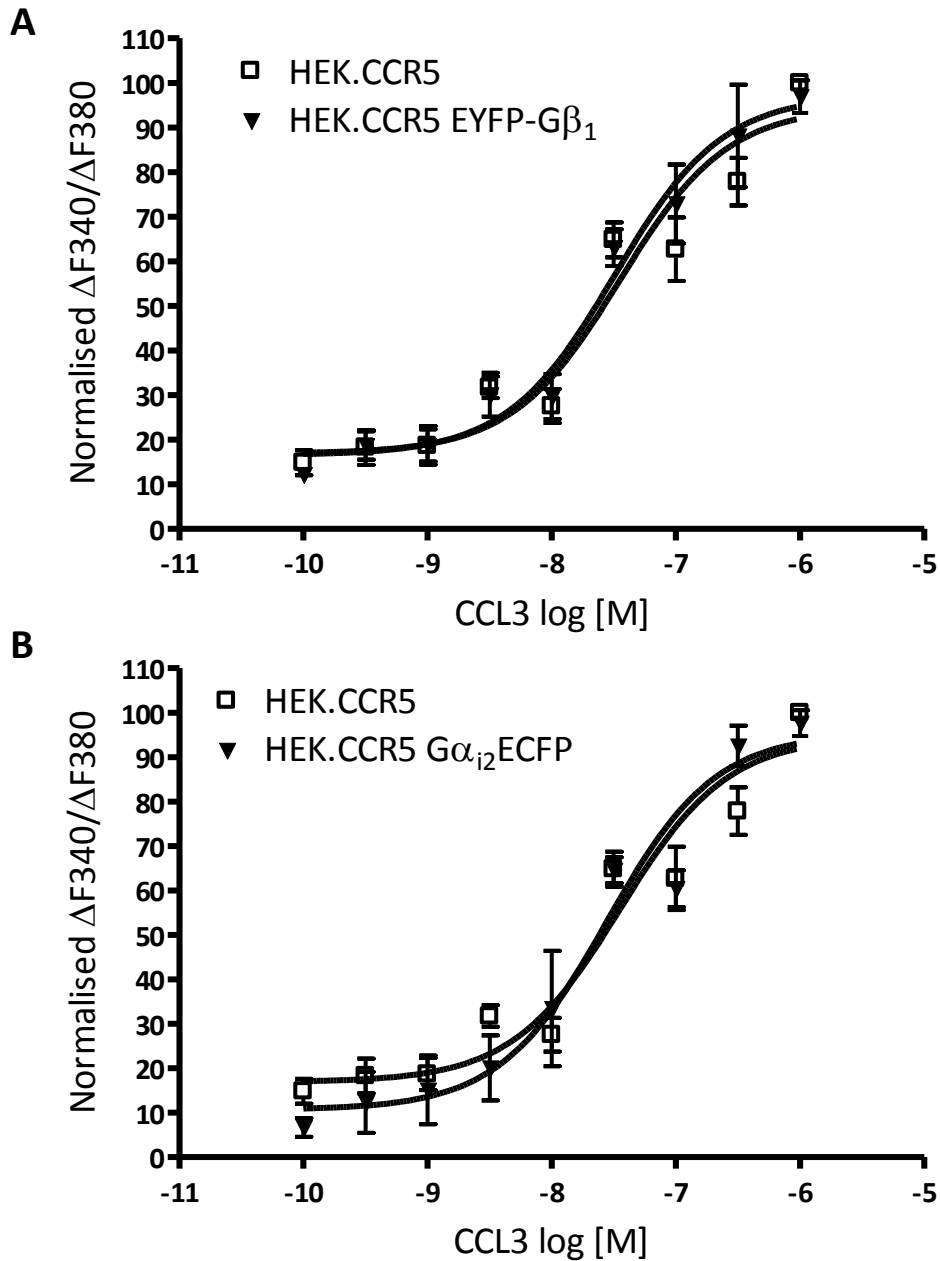


Figure 3.3 Dose response curves of single stable transfected cell lines. (A) HEK.CCR5 EYFP-G β_1 shows no decrease in efficacy or potency for CCL3 following transfection and selection. Log EC₅₀ HEK.CCR5 -7.451 M, HEK.CCR5 EYFP-G β_1 -7.554. (B) HEK.CCR5 G α_{12} -ECFP shows no decrease in efficacy or potency for CCL3 following transfection and selection. Log EC₅₀ HEK.CCR5 -7.451 M, HEK.CCR5 G α_{12} -ECFP -7.472 M. Plotted points were normalised to the maximal HEK.CCR5 calcium flux. Each point represents three or more individual experiments.

3.2.4 Creation of HEK.CCR5 EYFP-G β_1 G α_{i2} -ECFP

HEK.CCR5 EYFP-G β_1 was favoured for transfection with pcDNA3.1:G α_{i2} -ECFP to create a stable cell line capable of FRET, due to its quicker proliferation rates. Following transfection, stable cell lines were selected using a dual selection media containing blasticidin, G418, and hygromycin. Cells that survived were harvested and seeded into a 96 well plate at low density. Cell proliferation and morphology was monitored by observation with light microscope. Proliferation was markedly impaired in the stable HEK.CCR5 EYFP-G β_1 /G α_{i2} -ECFP and cells noticeably clumped together. A result of which was the inability to form a consistent adherent monolayer. When cells reached approximately 80% confluence they were scaled up into a 24 well dish. Wells with slow proliferating and non adherent cell lines were discarded. Once cells reached approximately 80% confluence they were seeded onto coverslips and expression was observed by fluorescent microscopy. Several cell lines expressed very low amounts of recombinant protein and were discarded. Eight dual expression cell lines expressed both constructs with relative constancy across the cell population and were scaled up for further characterisation.

3.2.5 Characterisation of Dual Fluorescence HEK.CCR5

Scaled up stable HEK.CCR5 EYFP-G β_1 /G α_{i2} -ECFP were assigned identification initials. Measurement of Log EC₅₀ values by dose response calcium flux measurements indicated that signalling had been perturbed in some cell lines, these cell lines were discarded. Cell lines 3, 5, B1, B2, and C1 were not significantly perturbed by stable expression of G α_{i2} -ECFP and EYFP-G β_1 (Table 3.2). However, cell line 3 was discarded due to observed unusual morphology. Cell lines 5 and C1 were discarded due to a significant decrease in CCL3 efficacy. Cell lines B1 and B2 displayed signalling responses and proliferation rates closest to that of the parental cell line and therefore were selected for FRET experiments. However, there was a substantial loss in the adherence of these cells to cell culture surfaces, consequently making the culture of these stable cell lines difficult.

The Fate of HEK.CCR5 EYFP-G β_1 , G α_{i2} -ECFP Sub-Clones

Cell line	Log EC ₅₀ [M]	n	Notes
Parental	-7.746	3	
2	-5.979	2	Discarded
3	-8.034	2	Unusual Morphology
4	N/A	0	Discarded, slow proliferation
5	-7.876	2	Low efficacy
A5	-6.810	3	Discarded
B1	-7.140	3	Further studies
B2	-7.863	3	Further studies
C1	-7.489	2	Low efficacy

Table 3.2 Log EC₅₀ values for HEK.CCR5.Y/C selected stable cell lines. Log EC₅₀ values were determined by plotting dose response curves using CCL3 as the ligand. It was not possible to get an n=3 result for all created stable cell lines due to difficulties with cell culture.

Stable cell line B2, here on in referred to as HEK.CC5.Y/C, was selected for further studies over cell line B1 as it was found to adhere with greater resolve to microscopy coverslips during washing, albeit with greatly reduced adherence compared to parental cell lines. Log EC₅₀ values for HEK.CC5 Y/C closely resembled those of the parental cell lines, however there was a difference in maximal response when stimulated with CCL3 (Figure 3.4A). HEK.CCR5.Y/C on average signalled at 77.68% ($\pm 10.26\%$, n3) of the parental maximal response following treatment with 1 μ M CCL3, suggesting expression of both constructs together interferes with CCR5 regulated calcium release. Analysis by Student's t-test showed there to be no significant difference for any of the plotted points.

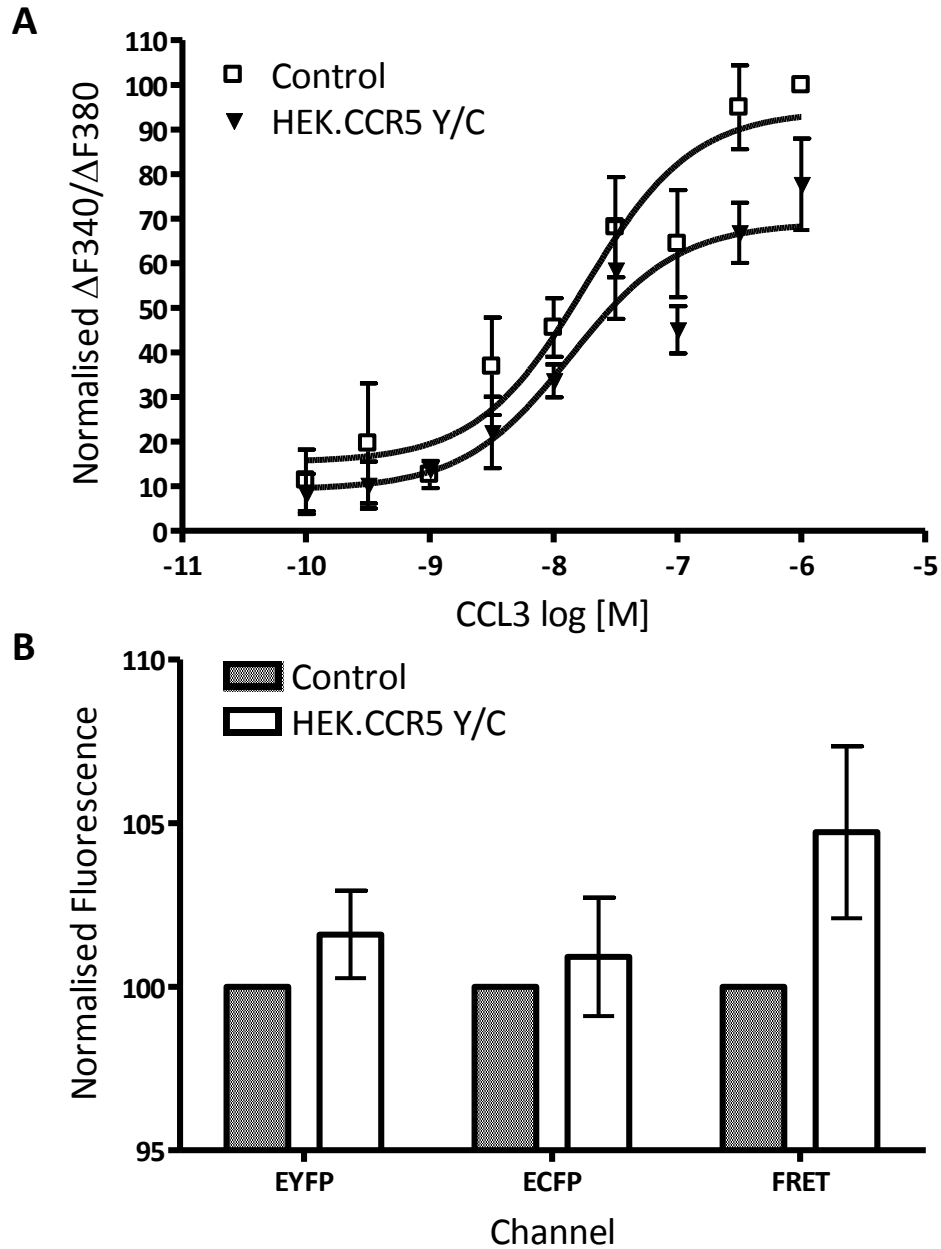


Figure 3.4. Characterisation of HEK.CCR5.Y/C. (A). Dose response curve of HEK.CCR5.Y/C and HEK.CCR5 (control). Log $E_{c_{50}}$ values; Control-7.746 M, HEK.CCR5.Y/C -7.863 M. Curves are the result of three independent experiments. No significant difference was observed between points. (B). Relative fluorescence levels of HEK.CCR5.Y/C. EYFP fluorescence is measured at 530 nm after excitation at 510 nm. ECFP fluorescence is measured at 485 nm following excitation at 410 nm. FRET is the emission at 530 nm following excitation at 410 nm.

Fluorescence was measured for three channels to confirm and quantify expression of fluorescent protein in transfected cell lines. In HEK Y/C cells there is a trend towards increased FRET coupling as well as enhanced ECFP and EYFP fluorescence (Figure 3.4B). HEK.Y/C exhibited a 4.7% ($\pm 2.63\%$, n=3) increase in FRET emission. Cells also fluoresced at a 0.91% ($\pm 1.33\%$, n=3) and 1.59% ($\pm 1.81\%$, n=3) greater intensity for ECFP and EYFP. However, variance in expression levels over time lead to inconsistent results and difficulty with reproducibility. Data show a trend that constructs are being expressed in HEK cells and forming donor-acceptor complexes in conjunction with typical G-protein heterotrimers. Fluorescence images of HEK Y/C further confirmed the likelihood of formation of donor acceptor complexes, showing co-localisation of $G\alpha_{i2}$ -ECFP and EYFP- $G\beta_1$ at the plasma membrane (Figure 3.5).

Microscopy of HEK.CCR5.Y/C was difficult due to issues with adherence. Cells grown on coverslips would come loose, even with gentle washing in PBS. Fluorescent images show expression of fluorescent constructs and an altered morphology to that of cells grown in a cell culture flask

Due to difficulties in imaging and culture of HEK.CCR5.Y/C studies with this cell line were not pursued beyond preliminary measurements of resting FRET levels. Instead a new series of stable double fluorescent cell lines were created in CHO cells stably expressing CCR5. CHO.CCR5 had been previously created for other studies (Mueller *et al.*, 2002a).

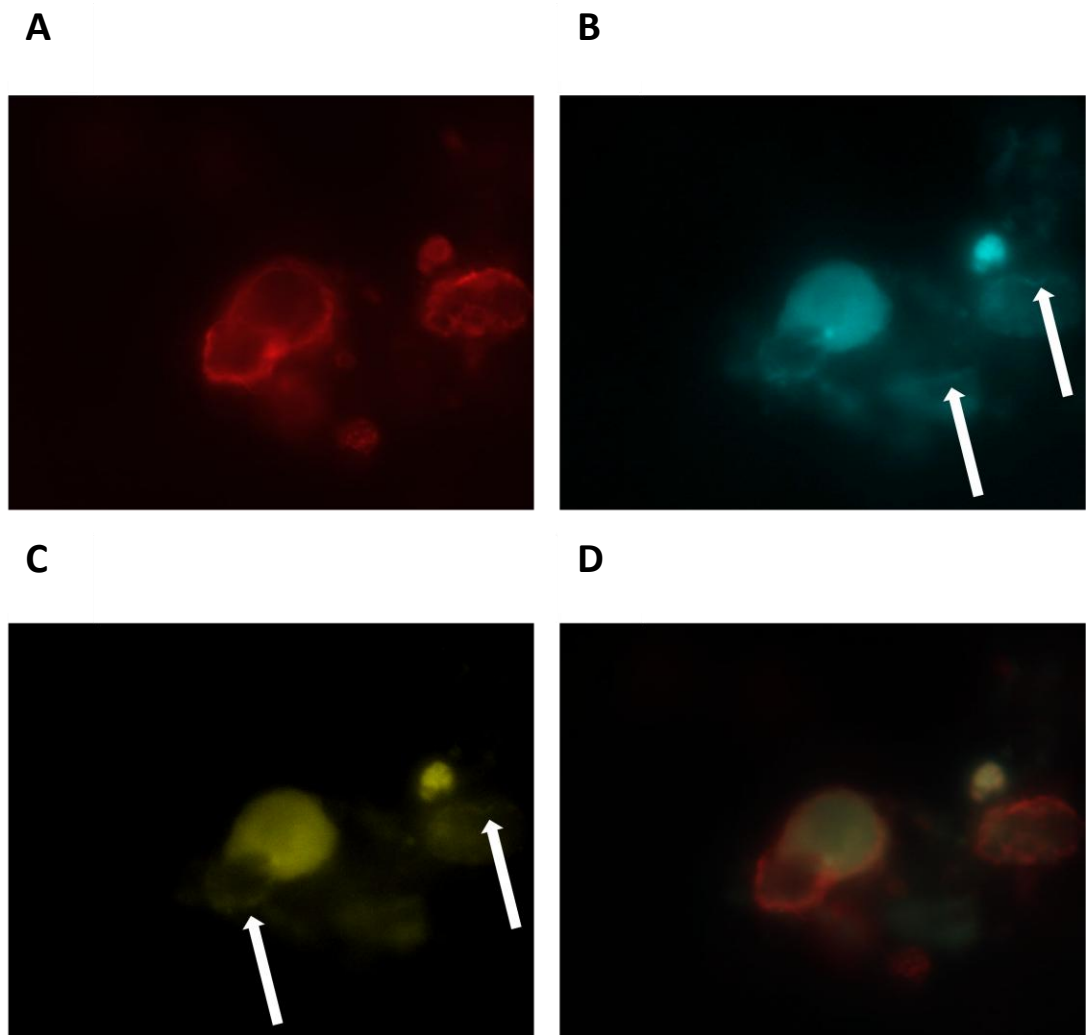


Figure 3.5 Fluorescent microscopy images of HEK.CCR5.Y/C. (A) Immunofluorescence of CCR5 expression in HEK.CCR5.Y/C. Cells were labelled with the anti CCR5 IgG HEK/1/85a/7a and stained with TRITC conjugated anti rat IgG. Images show functional CCR5 is adequately expressed and co-localised at the plasma membrane. (B) Stable expression of $G\alpha_{i2}$ -ECFP. Arrows indicate tagged G-protein is expressed and co-localised at the plasma membrane. (C) Stable expression of EYFP- $G\beta_1$. Good examples of plasma membrane localisation are indicated with arrows. (D) Overlay, image clearly shows CCR5 and tagged G-proteins co-localise at the plasma membrane.

3.3.1 Creation of Plasmids for Stable Expression in CHO.CCR5

CHO cells, like HEK cells, are well characterised cell lines used commonly in the expression of recombinant proteins and the pharmacological study of G-protein signalling. Similarly, they also have the advantage of being cells that transfect readily, express relatively high yields of the transfected protein and have simple cell culture requirements (Geisse *et al.*, 1996). In addition, they are renowned for their resilience in *in vitro* cell culture (Puck *et al.*, 1958). Although origin of the cells is not human, sufficient studies have shown expression of recombinant human protein in CHO does not affect protein folding or post translational modifications. As such, CHO.CCR5 provides a perfect model for proof of concept and can be considered analogous to a human derived cell line.

CCR5 expression is maintained in CHO.CCR5 by the expression of a G418 resistance gene, therefore ruling out the use of the already created, G418 resistance gene containing, pcDNA3.1:G α_{i2} -ECFP construct used previously. Additional plasmid constructs were created for expression of fluorescently tagged G-proteins in CHO.CCR5 cells and to allow the selection of stable cell lines. Fusion protein constructs made for expression in HEK.CCR5 were removed from their vectors by restriction endonuclease digestion. EYFP-G β_1 was excised with HindIII, HEK.CCR5.Y/C, purified by agarose gel electrophoresis and ligated into pZeo SV2, G α_{i2} -ECFP was excised with BamHI and ligated into pcDNA6/V5-His (Figure 3.6). Restriction digests were carried out to ensure the correct orientation of constructs into new vectors (Figure 3.7).

Both constructs are approximately 1.7 kb in length. Correct orientation of EYFP-G β_1 was determined with HindIII and EcoRI digestion, yielding a 700 base pair EYFP fragment and a 1 kb G β_1 fragment (Figure 3.7). Correct orientation of G α_{i2} was determined PstI digestion, which yields two fragments of approximately 700 bp and 800 bp corresponding to ECFP and part of G α_{i2} , respectively (Figure 3.8 B). Incorrect insertion of G α_{i2} is characterised by the appearance of a 300 base pair fragment (Figure 3.8 A)

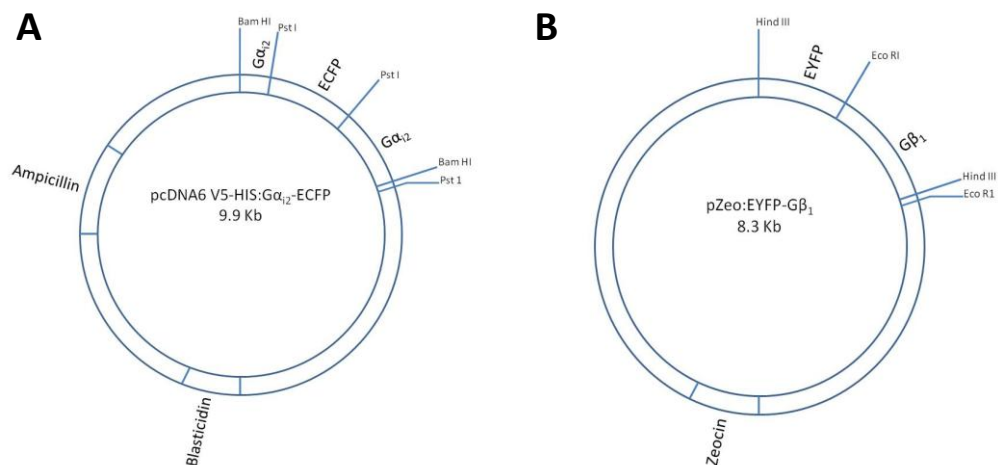


Figure 3.6 Schematic representations of the plasmids produced and transfected to create stable CHO.CCR5 expressing G-proteins tagged with fluorescent proteins. (A) ECFP is approximately 700 bp in length and G α_{i2} is approximately 1100 bp in length. However, Insertion of ECFP at the Pst1 site in the G α_{i2} cDNA gives rise to two coding regions of approximately 300 bp and 700 bp. pcDNA6/V5-His allows selection in mammalian cells using blastidicin and selection in bacteria using ampicillin. (B) EYFP is approximately 700 bp in length and G β_1 is approximately 1000 bp in length. The zeocin resistance gene in pZeo SV2 allows selection in bacterial and mammalian cells using zeocin.

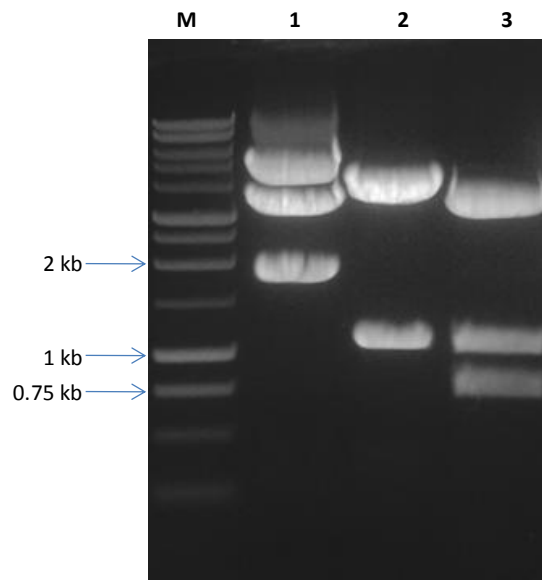


Figure 3.7. Analytical digests of pZeo SV2:EYFP-G β_1 . (M) 1 kb Marker. (1) HindIII digest, showing excised construct of approximately 1.7 kb running below the 2 kb marker. (2) EcoRI digest, showing excised G β_1 . (3) Hind III and Eco RI digest, showing excised G β_1 and EYFP.

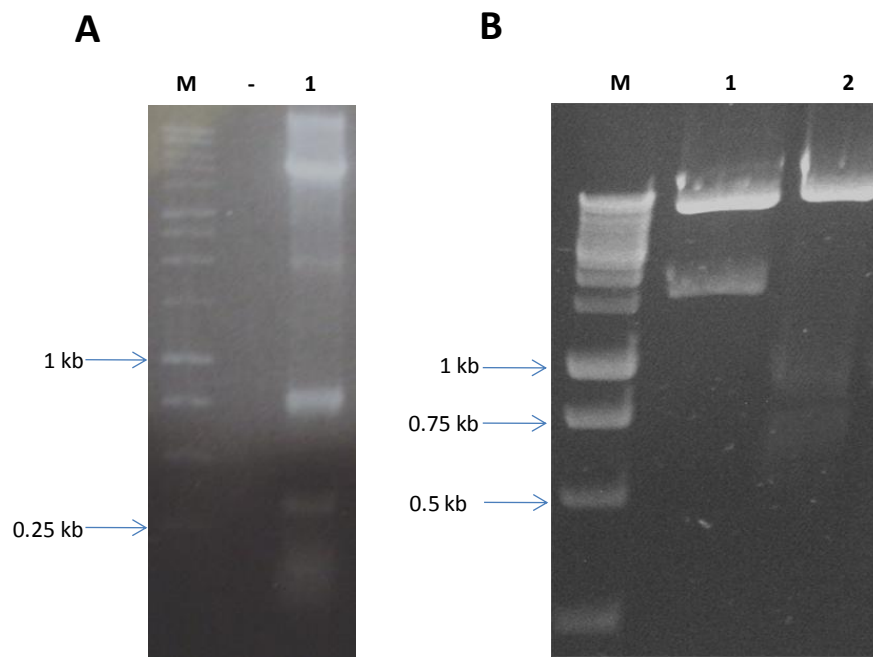


Figure 3.8. Analytical digests of pcDNA6/V5-His:G α_{12} -ECFP (A) Incorrect construct insertion. (M) 1 kb Marker. (1) PstI digest, giving rise to 800 bp and 300 bp fragments. (B) Correct construct insertion (M) 1 kb marker. (1) BamHI, showing excised construct just below the 2 kb marker. (2) PstI digest showing excised ECFP at approximately 700 bp and an excised fragment of G α_{12} at approximately 800 bp

3.3.2. Selection of Stable Single Expression Cell Lines

Following transfection with either pcDNA6/V5-His:G α_{i2} -ECFP or pZeo SV2:EYFP-G β_1 cells were cultured to approximately 80% confluency. Cells were harvested and seeded into a 96 well plate at very low density and cultured in relevant selection media. Once stable cell lines reached 80% confluency relative expression of fluorescent construct was quantified using a plate reader. Cells with higher fluorescence readouts were harvested and seeded into 24 well plates, non-proliferating or slow proliferating cell lines were discarded. In total 23 ECFP clones were initially scaled up. Stable cell lines were examined for expression by fluorescent microscopy. Only one CHO.CCR5 G α_{i2} -ECFP clone was found to have uniform expression, this cell line underwent subcloning to produce a stable cell line with good expression and proliferation rates (Figure 3.9A). This cell line was used for all further studies. For creation of CHO.CCR5 EYFP-G β_1 the same process was followed. In total, 17 EYFP clones were scaled up, all of which displayed normal morphology and proliferation rates. Several of these clones were found to have relatively high expression rates and uniform expression, one clone was selected for further study (Figure 3.9B).

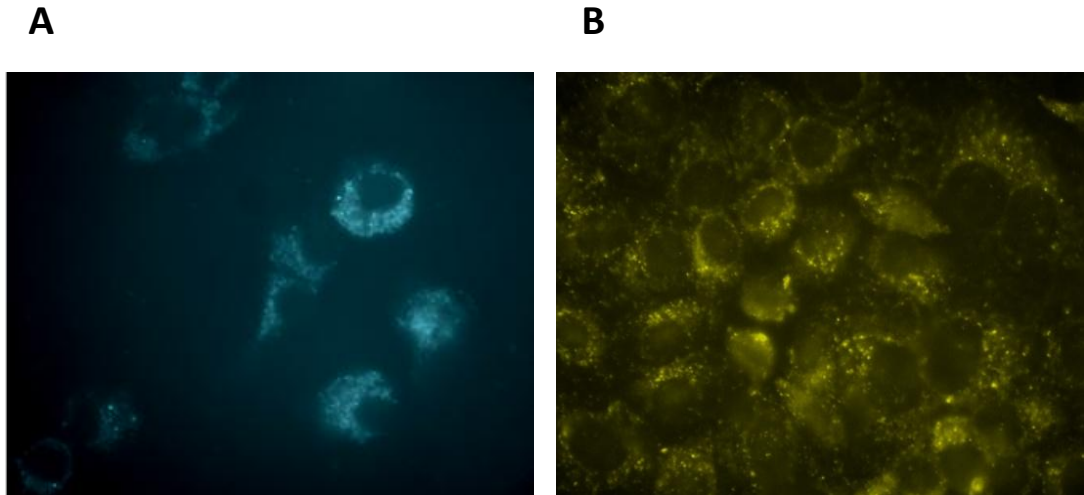


Figure 3.9 Fluorescent microscope images of single stable transfectants (A) CHO.CCR5 stably expressing pcDNA6/V5-His:Gα₁₂-ECFP, there is clear localisation to the plasma membrane of Gα₁₂-ECFP. High levels of Gα₁₂-ECFP can also be seen located in discrete punctations within the cell. (B) CHO.CCR5 stably expressing pZeoSV2:EYFP-Gβ₁. EYFP Gβ₁ is found at the plasma membrane as well as in punctations within the cell. These images are representative of typical cell population expression of pcDNA6/V5-His:Gα₁₂-ECFP or pZeo SV2:EYFP-Gβ₁ used throughout the project.

3.3.3 Characterisation of CHO.CCR5 Stable Single Transfectants

Characterisation of single expression stable cell lines was performed by comparing the intracellular release of calcium following CCR5 activation with CCL3 to that of the parental cell line. Both stable cells lines responded normally to CCL3 activation. Log EC₅₀ values of CHO.CCR5 Gα_{i2}-ECFP and CHO.CCR5 EYFP-Gβ₁ closely matched the Log EC₅₀ value of CHO.CCR5 of -7.146 M (±0.1577 M, n=3), being -6.950 M (±0.139 M, n=3) and -7.247 M (±0.1557 M, n=3), respectively. Efficacy of CCL3 was not affected by expression of either construct (Figure 3.10).

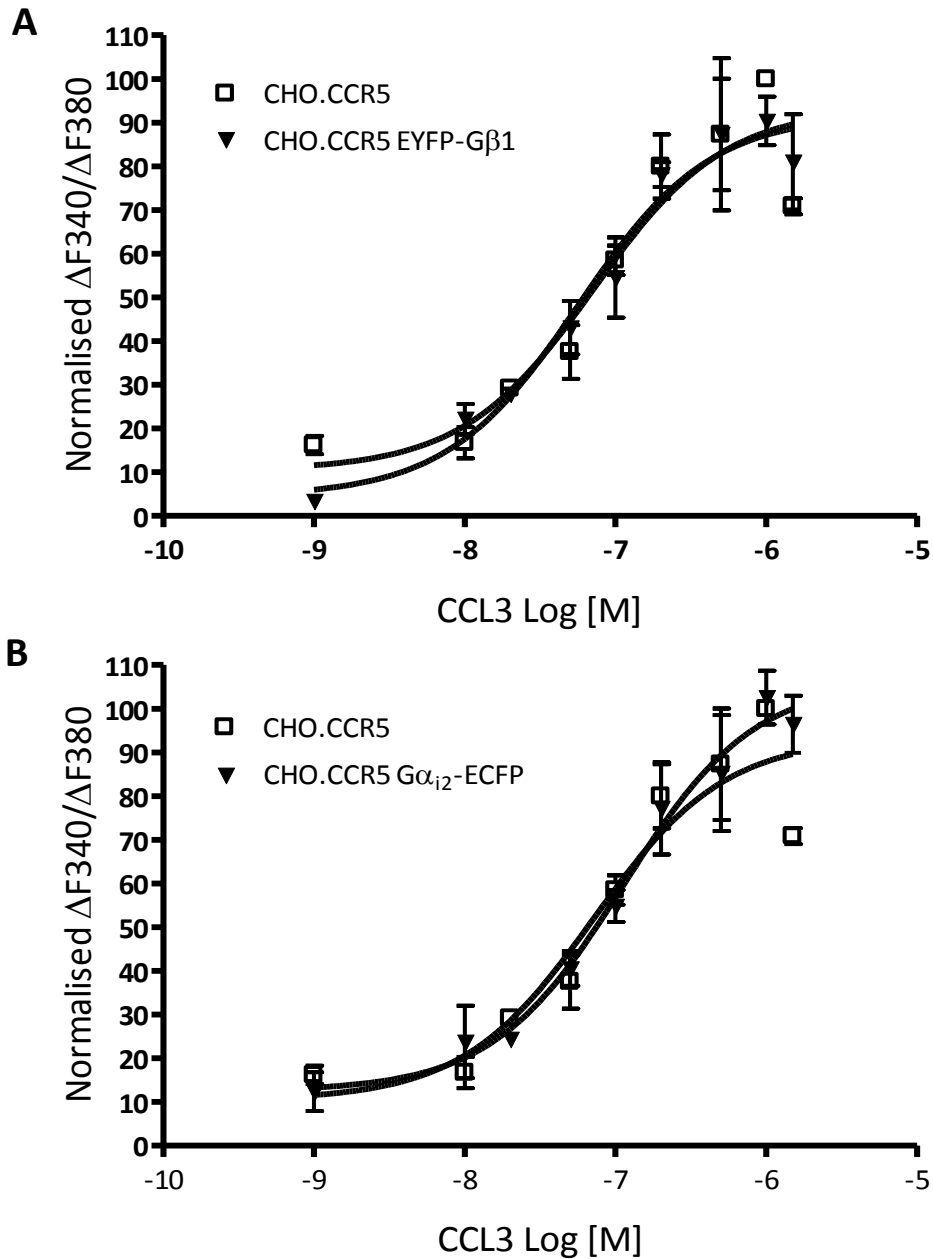


Figure 3.10 Dose response curves for CHO.CCR5 single transfectants (A) CHO.CCR5 EYFP-G β ₁ shows no decrease in efficacy or potency for CCL3 following transfection and selection. Log EC₅₀ CHO.CCR5 -7.146 M, CHO.CCR5 EYFP-G β ₁ -7.247 M. (B) CHO.CCR5 G α ₁₂-ECFP shows no decrease in efficacy or potency for CCL3 following transfection and selection. Log EC₅₀ CHO.CCR5 -7.146 M, CHO.CCR5 EYFP-G β ₁ -6.950 M. Plotted points were normalised to CHO.CCR5 calcium flux following 1 μ M stimulation with CCL3. Each plotted point represents three individual experiments.

3.3.4 Creation and Characterisation of CHO.CCR5 Stably expressing pcDNA6/V5-His:G α_{i2} -ECFP/pZeo SV2:EYFP-G β_1

CHO.CCR5 G α_{i2} -ECFP was selected for transfection with pZeo SV2:EYFP-G β_1 following characterisation. Creation of the single expression ECFP cell line had required the creation of several subclones in order to ensure uniform and high expression of G α_{i2} -ECFP without influencing cell morphology, it was therefore reasoned that similar problems could be encountered if transfection of pcDNA6/V5-His:G α_{i2} -ECFP into a stable CHO.CCR5 EYFP-G β_1 cell line was attempted. Following transfection, cells were cultured in selection media containing blasticidin and zeocin (Invitrogen) and upon reaching 80% confluence were harvested and seeded into a 96 well plate at very low density. Cells with favourable proliferation characteristics were sub cloned by harvesting and seeding into a new 96 well plate. On reaching 80% confluency cells were scanned for fluorescence of both ECFP and EYFP in a plate reader, one subclone was selected for further studies.

The concomitant stable expression of pcDNA6/V5-His:G α_{i2} -ECFP and pZeo SV2:EYFP-G β_1 had no significant effect CCL3 potency at CCR5. Log EC₅₀ values for CHO.CCR5 and CHO.CCR5.Y/C were closely matched at -6.948 M (± 0.123 M, n=3) and -6.871 M (± 0.1853 M, n=3), respectively. However, CCL3 efficacy was affected by concomitant expression. Maximal CHO.CCR5.Y/C response to CCL3 being only 70.03 % ($\pm 7.12\%$, n=3) that of the parental (Figure 3.11A). This suggests that expression is interfering with signalling via the CCR5 receptor. Analysis by student's t test shows this difference is not significant at any concentration, although nears significance at 1 μ M CCL3 (p=0.07963). Interestingly these data are very similar to those gained from HEK.CCR5.Y/C.

Fluorescence was measured for three channels to confirm and quantify expression of fluorescent protein in transfected cell lines. In CHO.CCR5.Y/C cells there is significant FRET coupling ($p=0.01674$) as well as enhanced EYFP and ECFP fluorescence (Figure 3.11B). CHO.CCR5.Y/C exhibited a 2.63% ($\pm 0.345\%$, $n=3$) increase in FRET emission. EYFP and ECFP emission increased by 5.79% ($\pm 3.42\%$, $n=3$) and 3.86% ($\pm 2.634\%$, $n=3$), respectively. Data show a trend that constructs are being expressed in CHO.CCR5.Y/C and forming donor-acceptor complexes akin to typical G-protein heterotrimers. Fluorescence images of CHO.CCR5.Y/C further confirmed the likelihood of formation of donor acceptor complexes, showing co-localisation of $G\alpha_{i2}$ -ECFP and EYFP- $G\beta_1$ to the plasma membrane (Figure 3.12). CHO.CCR5 Y/C, like HEK.CCR5, had a reduced propensity to adhere to cell culture surfaces, however, comparatively, they adhered with greater resilience. Proliferation rates for CHO.CCR5 Y/C were also slower to that of the parental cell line, but displayed comparable morphology to CHO.CCR5. Expression of both constructs was uniform and of a reasonable level (Figure 3.12).

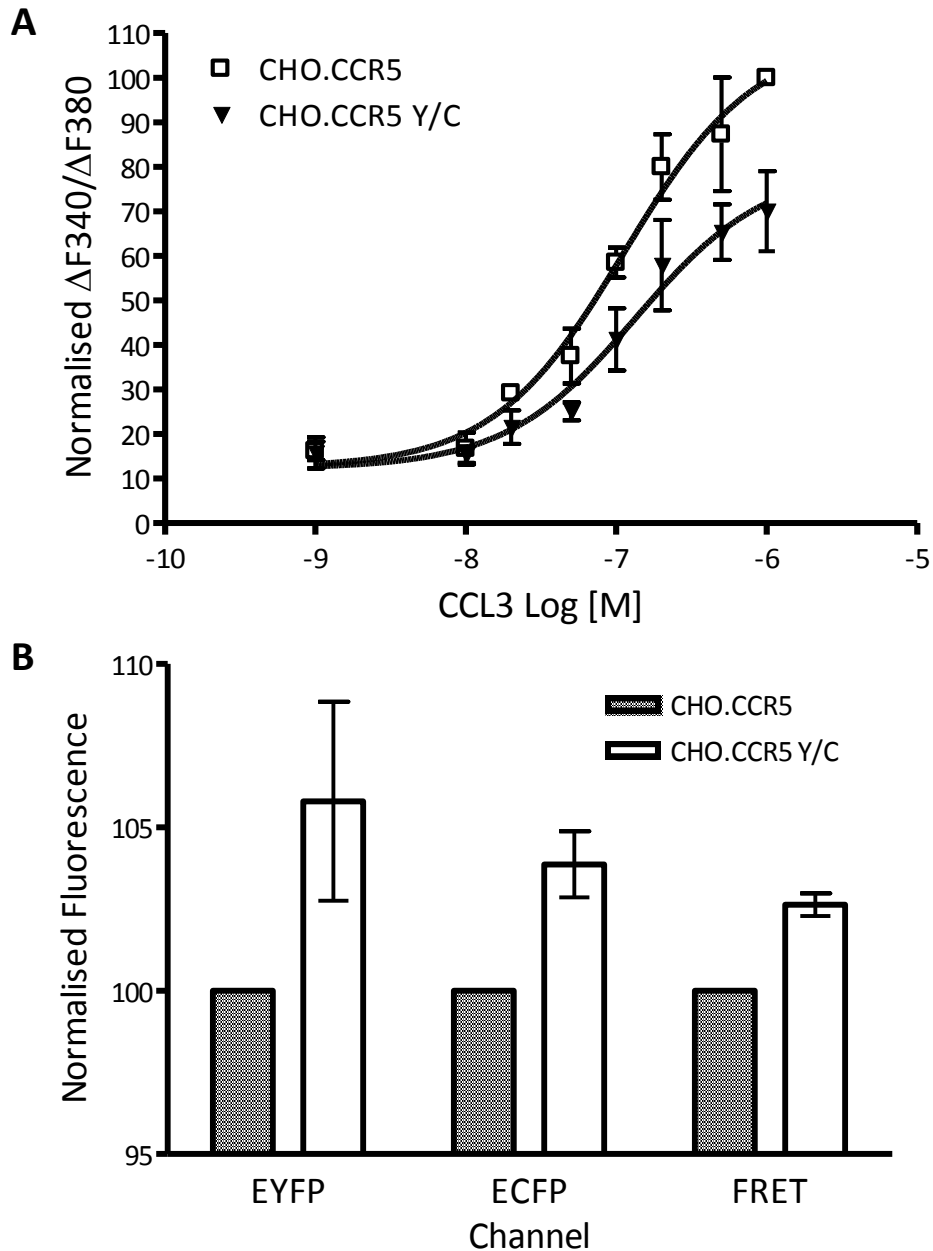


Figure 3.11 Characterisation of CHO.CCR5 Y/C (A) Dose response curve of CHO.CCR5 Y/C and CHO.CCR5, values were normalised to CHO.CCR5 $\Delta 340/\Delta 380$ at 1 μ M CCL3 stimulation. Log E_{c50} values; Control-6.948 M, CHO.CCR5 Y/C -6.871 M. Curves are the result of three independent experiments. No significant difference was observed between any CHO.CCR5 and CHO.CCR5 Y/C points. (B) Relative fluorescence levels of CHO.CCR5 Y/C. EYFP fluorescence is measured at 530 nm after excitation at 510 nm. ECFP fluorescence is measured at 485 nm following excitation at 410 nm. FRET is the emission at 530 nm following excitation at 410 nm. FRET measurements were significantly higher in CHO.CCR5 Y/C than in CHO.CCR5 ($p=0.01674$, $n3$), EYFP and ECFP readings were higher but did not reach significance.

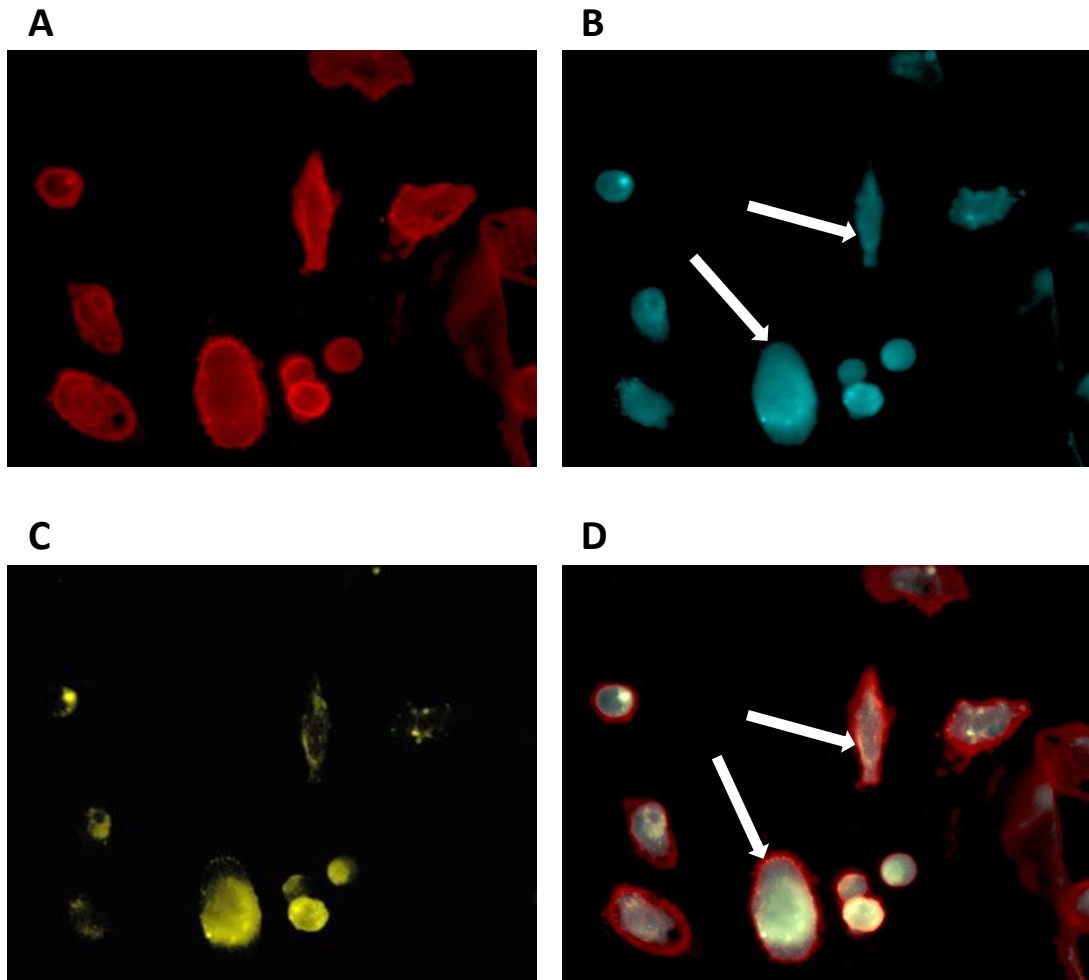


Figure 3.12 Fluorescent microscopy images of CHO.CCR5 Y/C. (A) Immunofluorescence of CCR5 expression in CHO.CCR5 Y/C. Cells were labelled with the anti CCR5 IgG CHO/1/85a/7a and stained with TRITC conjugated anti rat IgG. Functional CCR5 is adequately expressed and targeted to the plasma membrane. (B) Stable expression of $G\alpha_{12}$ -ECFP. Arrows indicate tagged G-protein is expressed and targeted to the plasma membrane. (C) Stable expression of EYFP- $G\beta_1$. (D) Overlay, CCR5 and tagged G-proteins co-localise at the plasma membrane, arrows indicate regions where there is substantial co-localisation.

3.4 Discussion

The aims of this chapter were threefold; to create a stable cell line expressing both $G\alpha_{i2}$ and $G\beta_1$ fused to either EYFP or ECFP forming a FRET donor acceptor pair, to characterise effects the expression of these fusion G-proteins may have on signalling through isolated CCR5, and to measure interaction of fusion G-proteins by FRET in a population of live mammalian cells. The development of a robust stable expression cell line may have applications in high throughput screening of compounds, allowing the measurement of heterotrimer activation and kinetics following stimulation with different agonists. Other potential advantages of developing a stable cell line to measure G-protein interactions are decreased throughput time; cells would not have to be cultured through two transient transfections, a stable cell line could be continually cultured instead. By removing the need for repeated transient transfections, reproducibility in experimental outcome will be improved. Stable cell lines have a defined expression of constructs, whereas expression in transiently transfected cells can vary.

The measurement of G-protein interactions and their receptor mediated activation with FRET has been demonstrated in living cells previous to this study. Measurements of G-protein interaction and activation were first shown in *Dictyostelium discoideum* (Janetopoulos *et al.*, 2001). Although proving the concept that the measurement of G-protein activation with FRET was possible in this simple eukaryotic system, limitations to the use of this model include the potential absence or reduced number of isoforms of some G-proteins as well as potential differences in the cellular role or binding partners of *Dictyostelium* and mammalian G-proteins (Williams *et al.*, 2006). More recently, G-protein interactions and activation kinetics were measured in HEK cells expressing the α_{2A} -adrenergic receptor. The study used transiently transfected cells and took FRET

measurements from single cells using live confocal microscopy and complex image processing software (Bunemann *et al.*, 2003). The creation of a stable cell line and an assay procedure that can be performed in a plate reader could simplify and streamline the measurement of protein-protein interactions, allowing FRET to become a routine method for the discovery of protein-protein interactions.

Native CCR5 expressing cells, predominantly T cells, macrophages, and dendritic cells, also express other members of the chemokine receptor family and which exhibit overlapping ligand specificity. It was therefore necessary to use transfected cells that do not exhibit overlapping ligand specificity. HEK and CHO cells stably transfected with CCR5 were used to create an analogous system in this study for several reasons. Native HEK and CHO cells do not express chemokine family receptors, so the stable introduction of CCR5 into the cells allows for isolation of the receptor and its signalling pathways. The isolation of a single receptor of interest ensures no unintended activation of downstream signalling through other chemokine receptors. The transfection, cell culture and creation of stable cell lines in HEK or CHO is also comparatively easier than in native CCR5 expressing cells.

Although transient transfection has the advantage of allowing quick expression and analysis of products, one of its major drawbacks is ensuring reproducibility of results. Selection of a stable transfectant ensures defined gene expression, thus promoting greater reproducibility of results. Current methods of measuring protein interactions by FRET employ timely and expensive procedures which typically focus on isolating a single cell from a transiently transfected population, and measuring FRET with a confocal microscope equipped with complex and expensive imaging soft- and hardware (Hein *et al.*, 2005).

While this has yielded some interesting results regarding the dynamics and interaction of G-protein heterotrimers, results may be misleading due to the variable levels of expression of fusion protein. High expression levels have been shown to increase the likelihood of forced spurious interactions occurring (Massotte, 2003). Measurements from a single cell opposed to a cell population may also give rise to misleading results, a single cell may be undergoing unique stresses when it is measured that don't represent those of the entire cell population. A stable cell line may circumnavigate these problems. However, one drawback of creating stable cell lines is the extensive time required culturing, isolating, and characterising clones before any experimental methods can be carried out.

Adequate expression of recombinant protein in stable cell lines relies on several factors. For expression to occur cDNA sequences must reach the nucleus following transfection, for creation of stable cell lines the cDNA sequence must be integrated into the hosts chromosomal DNA. To ensure the constitutive expression of constructs, constructs were located downstream of either a CMV immediate early promoter/enhancer or SV40 early enhancer promoter regions. The mechanisms of plasmid integration into a mammalian host's chromosome are still not well understood and are believed integrate randomly into the hosts DNA following a typical plasmid DNA transfection (Hayata, 2002). The position at which transfected cDNA integrates into the genome can have an effect on transcription levels. Integration into inactive heterochromatin results in little or no construct expression, whereas integration into active euchromatin will result in transcription (Wurm, 2004). The creation of single fusion protein stable cell lines was relatively straightforward. However, proliferation rates for the selected stable cell lines decreased in both CHO.CCR5 and HEK.CCR5 transfectants for all combinations of transfections. For all created cell lines, except CHO.CCR5 $G\alpha_{i2}$ -ECFP, expression of the constructs was evident in a majority of sub

clones. It is a possibility that integration of this $G\alpha_{i2}$ -ECFP was predominantly located in heterochromatins, resulting in lower transcription of the construct. Another factor that may have altered the expression of the fusion construct is methylation of the integrated cDNA. Methylation of chromosomal DNA prevents its transcription (Yoder *et al.*, 1997). Chromosomal and transfected DNA methylation has been widely reported and acknowledged to play a role in regulation of gene expression (Bird *et al.*, 1999), but the mechanisms by which methylation is targeted is not clearly understood. It is also a possibility that the $G\alpha_{i2}$ -ECFP transgene introduced into CHO.CCR5 was methylated following integration, leading to lower transcription levels.

Stable transfection and expression of either EYFP- $G\beta_1$ or $G\alpha_{i2}$ -ECFP had no noticeable effect upon cell morphology, demonstrating that the introduction of single heterotrimeric G-protein subunits fused to a fluorescent protein is not toxic to the cells. Fluorescent images show that fusion proteins are located in the cytoplasm and at the plasma membrane, which suggest that the introduction of EYFP or ECFP does not induce protein mis-folding and aggregation. However, the doubling time of single transfectant stable cell lines was markedly increased. The observed decrease in proliferation may be explained by the extra stresses the cells are under following transfection. The forced expression or over expression of transfected constructs artificially removes energy from the cell ecosystem that would have otherwise been used for cell growth (ATCC, 2007). The result of this is the stable cell line has a slower than normal growth rate.

The addition of a large fluorophore such as ECFP or EYFP, which are approximately 30 kDa, to a heterotrimeric G-protein could prevent normal interactions of the G-Protein

heterotrimer unit with the CCR5 cytosolic tail and/or between the sub units of the heterotrimer by steric hindrance. CCR5 activation is well characterised and has been shown to result in lowering of cAMP levels and the release of intracellular calcium (Mueller *et al.*, 2002b). Measurement of calcium release following stimulation with CCL3 did not show any evidence of canonical $G\alpha_i$ pathways being perturbed by the stable expression of one fluorescently labelled G-protein. Maximal response values were almost identical to stable cell lines as in the parental cell lines. In HEK.CCR5 single stable cell lines Log EC_{50} values were close to that of the parental value of -7.451 M, being -7.452 M in $G\alpha_{i2}$ -ECFP containing clones and -7.554 M in EYFP- $G\beta_1$ clones. In CHO.CCR5 single stable cell lines' signalling through CCR5 was also unaffected, maximal responses were similar and Log EC_{50} values were not significantly different from the parental value of -7.146 M, being -6.950 M in CHO.CCR5 $G\alpha_{i2}$ -ECFP and -7.247 M in CHO.CCR5 EYFP- $G\beta_1$. This demonstrates that the introduction of a single G-protein fusion protein does not interfere with signalling through CCR5.

The creation of stable HEK.CCR5.Y/C encountered various setbacks, following selection of stable cell lines proliferation rates had reduced substantially. Typical parental HEK.CCR5 would reach 80% confluence in approximately 3 days, whereas in HEK.CCR5.Y/C cells it would take approximately 14-18 days. Selection stresses were not very well tolerated in HEK.CCR5 cells, this manifested in morphological changes and cells becoming detached from cell culture surfaces with very gentle agitation. Regardless of these difficulties, the expression of constructs was measured by fluorescence, CCR5 signalling characterised, and FRET interactions were detected in stable cell lines. HEK.CCR5.Y/C expressed higher fluorescence in all measured channels than HEK.CCR5 and FRET was measured to be 4.72% ($p=0.2139$, $n3$) higher than wild type, confirming interaction of EYFP- $G\beta_1$ and $G\alpha_{i2}$ -ECFP

with one another. The introduction of a second fluorescently labelled G-protein interfered with CCL3 stimulated signalling through CCR5. There was an overall trend for reduced calcium release following CCL3 stimulation in HEK.CCR5.Y/C. This was most evident at higher CCL3 concentrations with HEK.CCR5.Y/C only responding at 77% ($p=0.1902$, $n3$) of parental values following treatment with $1\mu\text{M}$ CCL3 and 70% ($p=0.2230$, $n3$) following treatment with 300 nM CCL3. However, these differences were not significant when assessed by students two tailed t-test. The $\text{Log } E_{c_{50}}$ value was not significantly altered in HEK.CCR Y/C compared to parental being recorded as -7.863 M and -7.746 M , respectively. These results indicate CCR5 signalling is moderately but not significantly ablated in stable cell lines and that the constructs orientate to permit FRET. However, the introduction and expression of two new antibiotic resistance genes as well as two fusion proteins put extreme stress upon the cells. The difficulties associated with culturing and performing experiments with these cells made them unsuitable for further experimentation.

Different plasmids were selected for the creation of a stable CHO.CCR5.Y/C cell line, due to CHO.CCR5 using a blasticidin resistance gene to select for CCR5 expression. CHO.CCR5.Y/C also proliferated at a slower rate than the parental cell line taking approximately 12-14 days to reach 80% confluence, slightly quicker than HEK.CCR5.Y/C. The CHO.CCR5.Y/C cell line was more resilient to the stresses encountered during selection, and although proliferation was slow, adherence to the cell culture surfaces was not significantly diminished, nor was typical morphology noticeably disrupted. EYFP- β_1 and $G\alpha_{i2}$ -ECFP localised in the cytosol and at the plasma membrane and gave rise to a small but significant FRET reading in resting cells 2.63% above parental ($p=0.0167$, $n3$) which demonstrates the stable interaction of tagged subunits in the cell. CHO.CCR5.Y/C also had higher fluorescence emission readings for EYFP, 5.79% above parental ($p=0.1968$, $n3$), and ECFP, 3.86% above

parental ($p=0.06217$, $n3$). Although these values seem small they correspond well to values published for the FRET interactions between GPCR and G-proteins (Hein *et al.*, 2005; Lohse *et al.*, 2008). There was, as with HEK.CCR5.Y/C, an overall trend for reduced calcium release in stable CHO.CCR5.Y/C following CCL3 stimulation. This was most evident at higher CCL3 concentrations with HEK.CCR5.Y/C only responding at 70% ($p=0.1515$, $n3$) of parental values following treatment with 1 μM CCL3. The Log $E_{c_{50}}$ value was not significantly altered in CHO.CCR5.Y/C compared to parental being recorded as -6.948 M and -6.871 M, respectively.

These results provide evidence that although fluorescent proteins are bulky, fusion to G-proteins still allows for formation of the G-protein heterotrimer and their close proximity to one each other and the GPCR. However, there was a noticeable trend for a decrease in functionality when measuring calcium release following CCL3 stimulation. Bunemann and colleagues hypothesise that the $G\alpha_i$ heterotrimer family undergo subunit rearrangement rather than dissociation (Bunemann *et al.*, 2003). I speculate that the addition of ECFP and EYFP may affect the heterotrimers ability to bind to downstream effectors. The β subunit is known to bind and activate its' targets by binding to them using the same face that binds to the α subunit (Davis *et al.*, 2005), increasing steric hindrance at on a heterotrimer that potentially doesn't dissociate may prevent activation following association of the β subunit with its downstream targets, thus resulting in a decrease in calcium released following stimulation. It should be stressed that the measurement of calcium release acts as an indirect method of measuring G-protein activation, only providing information about downstream effects.

The creation and characterisation of CHO.CCR5.Y/C in this study demonstrates a system capable of measuring G-protein heterotrimer interactions in resting cell populations and represents a system with the potential to measure G-protein dynamics in live cell populations. High homology exists between members of the $G\alpha_i/o$ family making it a possibility that the measurement of interactions between different constellations of heterotrimer is a reality.

Chapter Four

Monitoring Heterotrimer Activation by CCR5 with FRET

4.1 Introduction

Fluorescent resonance energy transfer (FRET) is a phenomenon where energy is passed from a donor chromophore that is in close proximity to an acceptor chromophore in a nonradiative manner. The donor/acceptor pair must exhibit overlapping spectral properties, that is to say the emission wavelength of the donor must overlap with the absorbance properties of the acceptor for energy transfer to occur. The most commonly used donor-acceptor pair used in biological systems is ECFP and EYFP. Both ECFP and EYFP are mutant variants of GFP. Mutations were made in a region of the protein that forms an imidazolidinone ring, resulting in skewed absorption and emission wavelengths of GFP (Kretsinger, 2005). The absorption wavelength of EYFP overlaps with the emission wavelength of ECFP allowing FRET to occur (Gryczynski, 2005).

It is important to note that the efficiency of FRET energy transfer is inversely proportional to the sixth power of the distance between donor and acceptor fluorophores (Stryer *et al.*, 1967). This means the ability to transfer energy rapidly decreases over distance. The effective range for FRET to occur over is 1-10nm dependent on experimental conditions (dos Remedios *et al.*, 1995). Interestingly, this distance is within the extent of conventional protein dimensions and similar to those of multimeric protein complexes observed in biological systems (Sheng *et al.*, 2007). Therefore donor acceptor fluorophores will undergo FRET if tagged to proteins that closely interact.

G-protein heterotrimers have been shown to precouple to relevant receptors in a targeted manner, and are known to closely interact with each other in their inactive state (Nobles *et al.*, 2005). In this inactive state the heterotrimer is formed of G α subunit bound to GDP, associated to the G $\beta\gamma$ dimer. The close association of the heterotrimer prevents the active faces of the G α and G $\beta\gamma$ subunits from interacting with downstream effectors. The binding of a ligand to CCR5 results in a conformational change in the receptor resulting in the movement of the membrane spanning helices and intracellular loops that are connected to the precoupled heterotrimeric G-proteins. This shift in the receptors shape allows previously masked regions of the G α subunit to be exposed and catalyzes the release of GDP for exchange with GTP (Farrens *et al.*, 1996). The binding of GTP to the G α subunit results in the destabilisation of the heterotrimer allowing their interaction with downstream effectors. There is some uncertainty as to whether the heterotrimer undergoes full dissociation or a large structural rearrangement that allows the active faces of the subunits to become exposed. Currently both ideas are being courted by different groups. The G α_{i2} subunit has been shown to fully dissociate (Digby *et al.*, 2006) and remain bound to the G $\beta\gamma$ subunit (Bunemann *et al.*, 2003) using FRET to measure interactions.

This chapter does not aim to address the contentious issue of heterotrimer dissociation versus structural rearrangement, but rather develop a high throughput FRET assay as a method to scan the ligand G-protein specificity conferred on a GPCR by the ligand it interacts with. Successful development of such an assay may expedite the understanding of GPCR - G-protein signalling specificity. As such, a heterotrimeric G-protein complex that has been shown to interact with CCR5 and can be activated by CCL3 was chosen to provide proof of concept for this assay system.

4.2 Results

Following the creation and characterisation of CHO.CCR5.Y/C, an assay was developed with the aim of measuring the CCL3 stimulated activation and kinetics of $G\alpha_{i2}$ and $G\beta_1$ through CCR5. A problem common to plate reader based FRET assay is interference with readings from high cellular autofluorescence. Early in assay development CHO.CCR5 were identified as highly autofluorescent cells. High autofluorescence masks signals from transfected fusion proteins, thus increasing the noise to signal ratio. Cellular autofluorescence was particularly noticed through ECFP (ex 435 nm, em 485nm) and FRET (ex 435 nm, em 530) channels when measured in the plate reader. Therefore cells were diluted in several different buffers, CAF, PBS, Hanks balanced salt solution (HBSS), and HEPES, and autofluorescence was measured through ECFP and FRET channels for CHO.CCR5 in order to assess the effect of buffers had on autofluorescence. Cells were diluted to 2×10^6 /mL and results were normalised to readings from CHO.CCR5 diluted in CAF for each experiment. There was little difference in readings and PBS was found to perform satisfactorily. As such cells were resuspended in PBS for all experiments (Table 4.1).

Buffer	ECFP%	EYFP%	N
CAF pH7.4	100 (± 0)	100 (± 0)	4
PBS pH7.4	98.62 (± 1.34)	99.95 (± 0.84)	4
HBSS pH7.4	101.79 (± 2.71)	101.68 (± 2.23)	4
HEPES pH7.4	101.23 (± 1.79)	101.78 (± 3.78)	4

Table 4.1. The effect of varied buffer composition on measured autofluorescence for CHO.CCR5. All readings were normalised to readings for CHO.CCR5 diluted in CAF at a concentration of 2×10^6 /ml

4.2.1 Sodium Butyrate Treatment of CHO.CCR5.Y/C

The relatively high autofluorescence resulted in substantial noise in FRET traces. Initially there was concern that the levels of donor and acceptor expression in CHO.CCR5.Y/C would be too low for the measurement of subtle changes in cell fluorescence in an entire cell population. In an attempt to increase signal to noise ratios, CHO.CCR5.Y/C were treated with 5 mM sodium butyrate (NaBu), a histone deacetylase inhibitor (Candido *et al.*, 1978), for 24 hours to increase levels of transcription in CHO.CCR5.Y/C, therefore increasing expression of G-protein fusion proteins.

Three excitation channels were measured, ECFP (ex 430 nm, em 485 nm), EYFP (ex 510 nm, em 530 nm), and FRET (ex 430 nm, em 530 nm), and normalised to fluorescence readings from untreated CHO.CCR5. Incubation of CHO.CCR5 with 5 mM NaBu for 24 hours resulted in no significant change in ECFP (101.15%, $\pm 4.82\%$, n=8) or EYFP (100.13%, $\pm 5.81\%$, n=8) emissions, however FRET emission was significantly decreased (93.39%, $\pm 7.37\%$, n=8, p=0.0389) (Figure 4.1, Table 4.2).

Untreated CHO.CCR5.Y/C consistently exhibited significantly higher levels of fluorescence for ECFP (103.73%, $\pm 3.82\%$, n=8, p=0.0282), EYFP (105.09%, $\pm 4.77\%$, n=8, p=0.0194) and higher levels of FRET emission (103.22%, ± 3.89 , n=8 p=0.0517) than untreated CHO.CCR5, corresponding well to previous results gathered during creation of CHO.CCR5.Y/C. NaBu treatment of CHO.CCR5.Y/C did not lead to any increase in average fluorescence, but did increase the variability of fluorescence readings (Figure 4.1, Table 4.2).

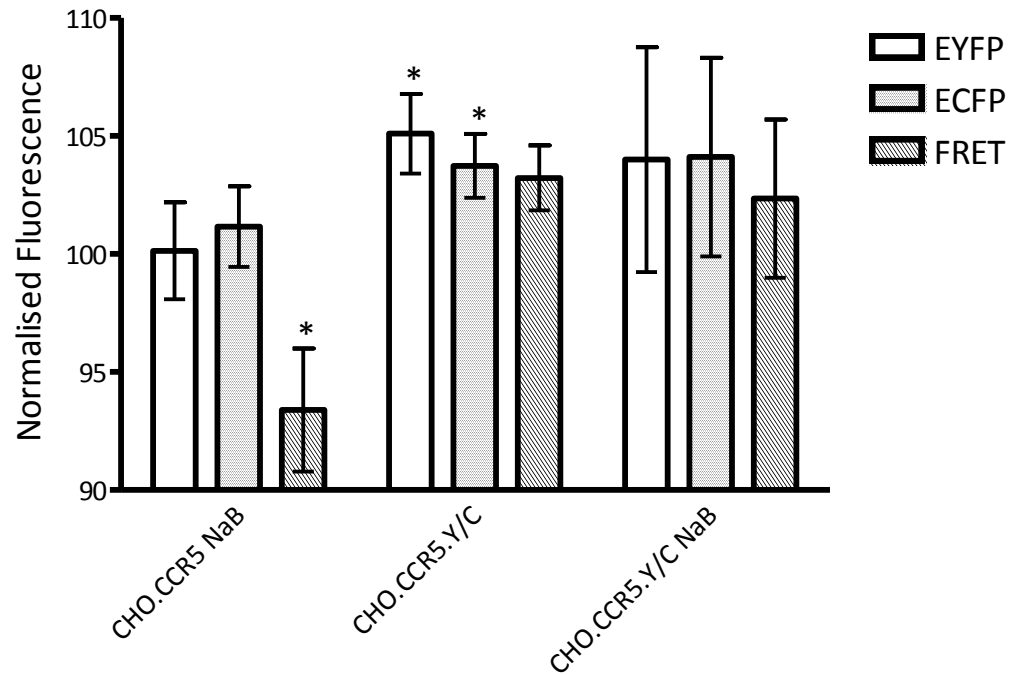


Figure 4.1. Fluorescence measurement for cell populations following 24 hr 5 mM sodium butyrate treatment

CHO.CCR5 NaBu	EYFP	ECFP	FRET
Mean	100.1323	101.1549	93.39244
SEM	±2.054	±1.706	±2.606
P Value	P>0.05	P>0.05	P=0.0389
CHO.CCR5.Y/C	EYFP	ECFP	FRET
Mean	105.0952	103.7311	103.222
SEM	±1.688	±1.353	±1.376
P Value	P=0.0194	P=0.0282	P>0.05
CHO.CCR.Y/C NaBu	EYFP	ECFP	FRET
Mean	104.0036	104.1082	102.3467
SEM	±4.762	±4.207	±3.353
P Value	P>0.05	P>0.05	P>0.05
n	8	8	8

Table 4.2. Fluorescence values for CHO.CCR5 and CHO.CCR5.Y/C with 5 mM NaBu treatment, all values were normalised to untreated CHO.CCR5 fluorescence measurements for each repeat.

4.2.2 Fluorescent Emission in Following CCL3 Stimulation

The conformational change of the G-protein heterotrimer can be measured directly by measuring the ratio of emissions at 485 nm and 530 nm when excited at 430 nm. A larger gap between the $G\alpha$ and $G\beta\gamma$ unit would result in a reduction in emission at 530 nm and an increase at 485 nm. Fluorescence levels were measured for a 30 second period prior to activation, by addition of 500 nM CCL3, in order to calculate a resting base line for samples. Following activation with CCL3 there was a rapid increase in the ECFP fluorescence in CHO.CCR5.Y/C and CHO.CCR5 of roughly 2.5% (Figure 4.2A). Increases in the control could partly be the result of cellular disturbance caused by the volume of CCL3 injected into the well, and changes in autofluorescence as a result of cellular activation. A concomitant decrease in emissions measured in the FRET channel was also recorded following CCL3 stimulation (Figure 4.2B).

Measurement of two emission wavelengths is achieved by rapid alternation between filters, a consequence of which is an increase in the time between points measured. Emission at one wavelength can be measured every 1.1 seconds, for two discrete emissions measurements can be taken every 2 seconds. Although this system is not appropriate for measurement of extremely rapid kinetic interactions, it allows monitoring of dissociation and reassociation of the $G\alpha_{12}$ heterotrimer.

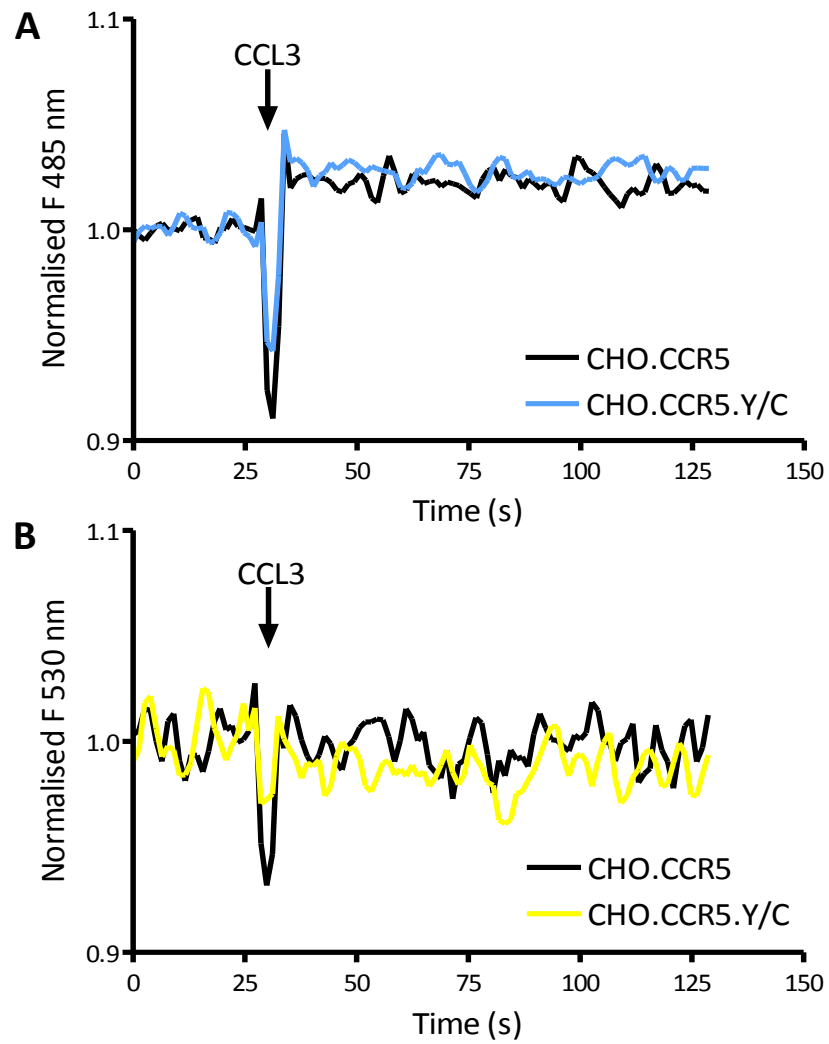


Figure 4.2. Emission traces for CHO.CCR5.Y/C. (A) ECFP emission, measured at 485 nm, increased following stimulation with 500nM CCL3 at 30 seconds. (B) FRET emission measured at 530 nm decreases following stimulation with 500 nM CCL3 at 30 seconds. These traces are a representative trace from three independent experiments.

4.2.3 CHO.CCR5.Y/C Exhibit variation in their FRET Ratio

FRET ratio measurement of the activation and dissociation of the G-protein heterotrimers was very variable between repeats during an assay (Figure 4.3), this led to extreme variation for measured points and therefore large standard deviation. For clarity, all data points were normalised to the average prestimulation FRET ratio and the curve was smoothed by plotting the weighted average for each data point and its five neighbouring values according to the Savitsky and Golay smoothing filter (Savitzky *et al.*, 1964). Following CCL3 stimulation there was an overall trend for the normalised FRET ratio to be higher in CHO.CCR5.Y/C than CHO.CCR5. However, readings suffered from high noise to signal ratio, therefore differences between CHO.CCR5.Y/C and CHO.CCR5 seem comparatively small. Quantification of the change in FRET ratio can conveniently be compared by measuring the area under the curve (AUC) following stimulation that is above that of the baseline. For comparison the FRET ratio in Figure 4.3A peaks at 7% above baseline and has a total curve area of 1.944 units whereas Figure 4.3B peaks at 2.81% above baseline and has a total curve area to 0.4676 units, approximately a quarter of the value seen in Figure 4.3A. This highlights the considerable variation between assay runs and difficulties when measuring FRET in whole cell populations.

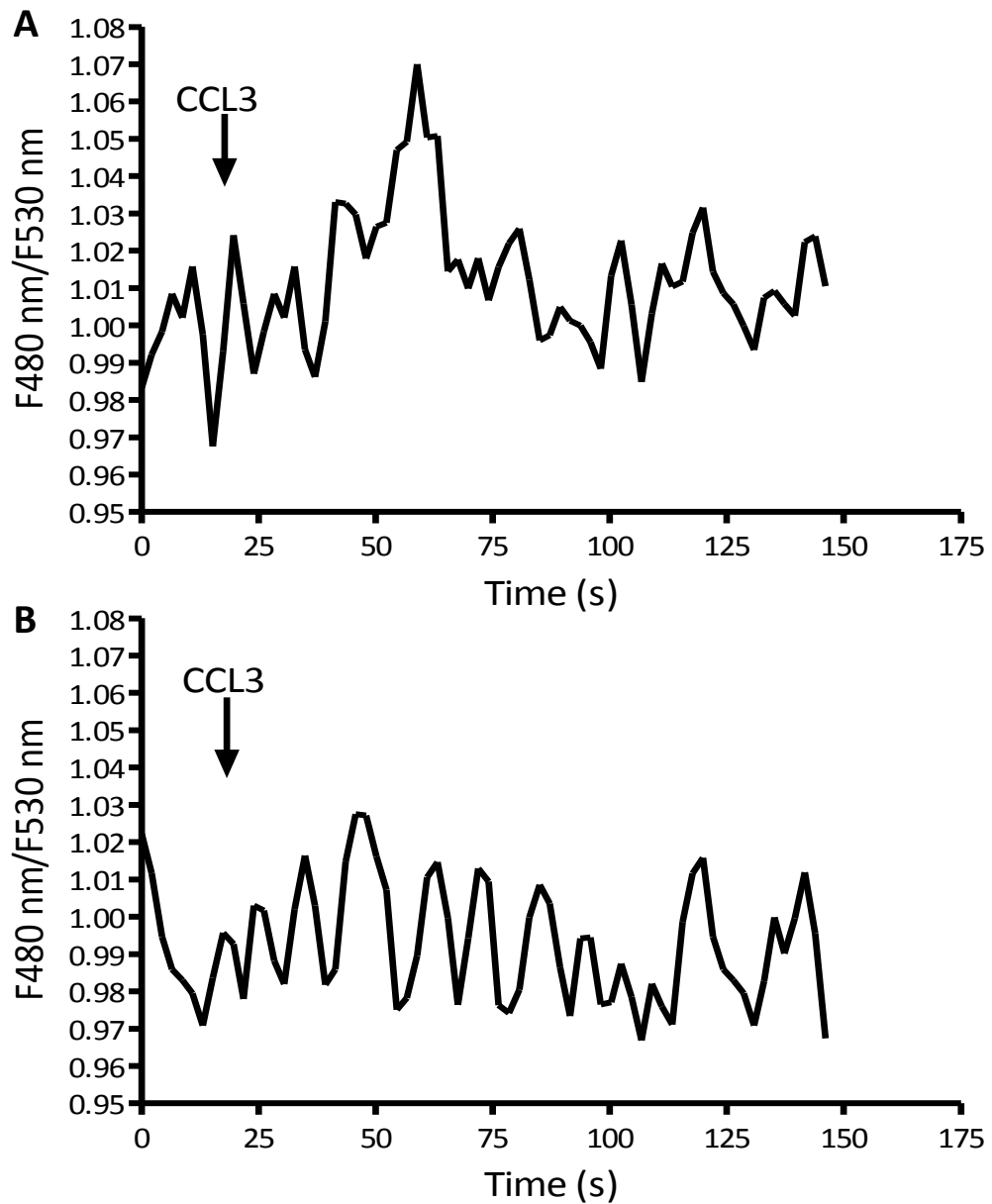


Figure 4.3. FRET ratio varies between repeats in the same sample. Addition of 500 nM CCL3 indicated by arrow (A) FRET ratio for CHO.CCR5.Y/C, showing rapid dissociation of the $G\alpha_{i2}$ heterotrimer and reassociation approximately 60 seconds. (B) FRET ratio for repeat of A measured immediately after. High noise and variability of FRET ratio masks the dissociation kinetics of the heterotrimer. The Figure represents the maximum variation seen in duplicate runs from one experiment and is a single representative of fourteen independent experiments.

4.2.4 Kinetics of $G\alpha_{i2}$ Activation by CCR5

The activation of the $G\alpha_{i2}$ $G\beta_1\gamma$ heterotrimer was successfully monitored by measuring the FRET ratio in stable cell lines. In total, six independent experiments measuring activation of the heterotrimer by FRET were performed. Activation and conformational change of $G\alpha_{i2}$ $\beta_1\gamma$ occurs rapidly after CCL3 addition to the well, unfortunately limitations with instrumentation didn't allow for the measurement of the millisecond kinetics of this activation. However, results demonstrate that there is substantial dissociation of subunits within six seconds of CCL3 being added. Following activation, reassociation of the heterotrimer can be observed by monitoring the decrease in the FRET ratio. Following dissociation, reassociation of the heterotrimer occurs over the next 70-100 seconds, which is comparable with the slow GTPase activity of the alpha subunit (Figure 4.4). Following stimulation with 500 nM CCL3 the FRET ratio for CHO.CCR5.Y/C peaked at 3.66% over baseline ($\pm 3.51\%$, $n=6$) and the area under the curve, above baseline, was 2.270. The FRET ratio for CHO.CCR5 peaks immediately after injection 1.75% ($\pm 4.29\%$, $n=6$) over base line, which could be an artefact from disturbance caused by the injection of chemokine to the well. The FRET ratio undulates with an almost consistent frequency, peaking several times well after stimulation. For comparison the total peak area above baseline is 0.951.

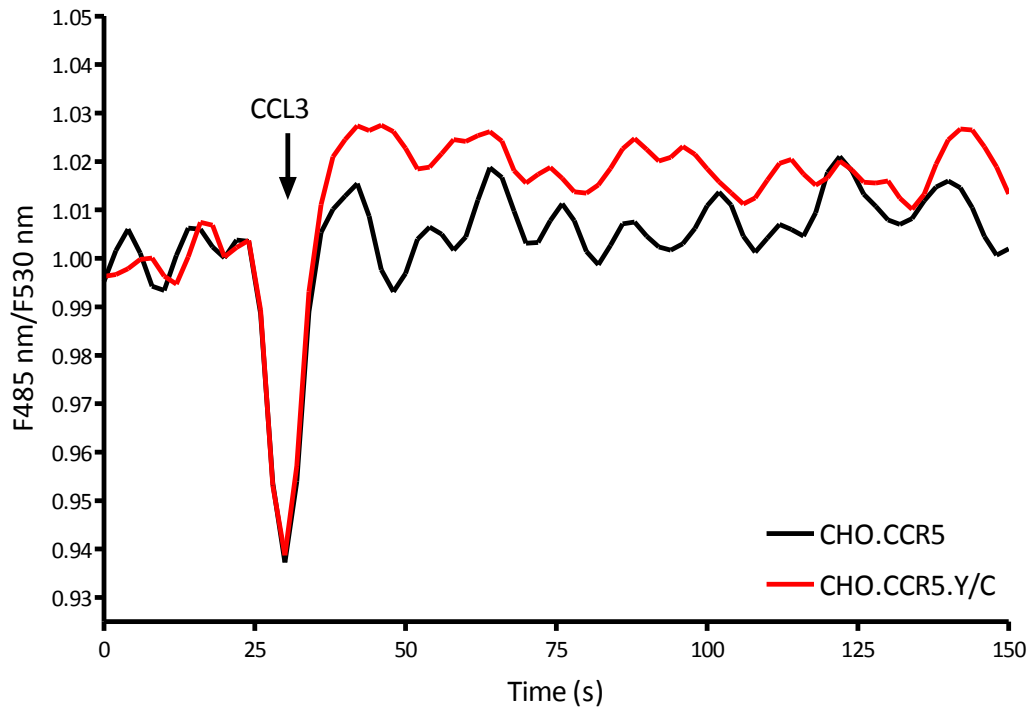


Figure 4.4 Dissociation of the $\alpha_{i2} \beta_1 \gamma$ heterotrimer can be measured using the FRET ratio between the sub units. 500 nM CCL3 was added at 30 seconds, the FRET ratio rapidly increases in CHO.CCR5.Y/C, peaking at 3.66% ($\pm 3.51\%$, n6) more than resting levels and at most 3.30% higher than post stimulation levels in CHO.CCR5. (Peak AUC, CHO.CCR5 0.951, CHO.CCR5.Y/C 2.270) The substantial increase in FRET ratio indicates that dissociation has taken place. Data are the results of six independent experiments.

To ensure observed changes in the FRET ratio were evoked by CCL3 stimulated dissociation of $G\alpha_{i2}$ and $\beta_1\gamma$ subunits, CHO.CCR5.Y/C were incubated with 100 ng/ml pertussis toxin (PTX). Pertussis toxin catalyses the irreversible ADP-ribosylation of the $G\alpha_i$ family preventing its activation and dissociation (Neer *et al.*, 1984), for 24hrs to prevent $G\alpha_{i2}$ activation. Upon stimulation with 500 nM CCL3 no overall change in the FRET ratio was observed in PTX treated CHO.CCR5.Y/C. PTX treated cells peaked 2.42% over base line ($\pm 3.06\%$, n4), but probably as an artefact of injection. CHO.CCR5.Y/C peaked 4.13% ($\pm 3.03\%$, n4) over baseline, although this peak was measured 30 seconds after stimulation (Figure 4.5). The most robust indication of PTX abrogation of FRET ratio is the difference between the peak area under curve over baseline. PTX treated cells had a peak AUC of 0.801, which is comparable to that of CHO.CCR5, whereas CHO.CCR5.Y/C have an AUC of 2.315.

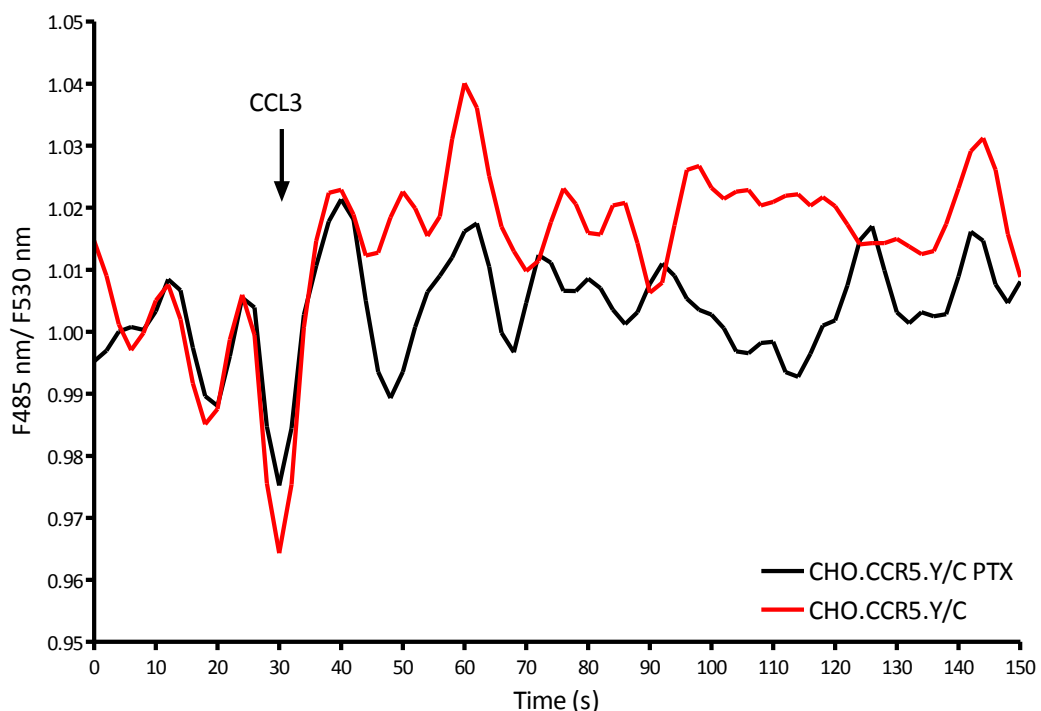


Figure 4.5 Inactivation of $G\alpha_{i2}$ by treatment with 100 ng/ml pertussis toxin prevents an increase in FRET ratio following stimulation with 500 nM CCL3 at 30 seconds. CHO.CCR.Y/C PTX (peak AUC 0.801, peak 2.42% $\pm 3.06\%$, n=4) CHO.CCR5.Y/C (Peak AUC 2.315, peak 4.13%, $\pm 3.03\%$, n=4) Traces represent data from four independent experiments.

The addition and incubation of NaBu decreased levels of autofluorescence in CHO.CCR5, particularly for measurements on the FRET channel. In an attempt to maximise the signal to noise ratio cells were treated with 5mM sodium butyrate for 24 hours prior to activation. FRET ratios were normalised to their pre-stimulatory base line. Lower FRET channel measurements led to higher pre-stimulation CHO.CCR5 FRET ratios. Normalising the CHO.CCR5 trace to the base line led to a proportional reduction in noise amplification, allowing differences in FRET ratios to be clearly inspected. It did not affect the CHO.CCR5.Y/C trace, which peaked at 4.37% ($\pm 3.99\%$, n4) higher than base line; comparatively CHO.CCR5 peaked at 1.75% ($\pm 1.66\%$, n4) above baseline in the first 120 seconds following stimulation. Peak AUC was much lower for CHO.CCR5 following treatment with NaBu at 0.146, CHO.CCR5.Y/C peak AUC was slightly higher to previous observations at 2.677, due to the increase in the length of the signal. Incubation with NaBu prior to measurement lead to a decrease in the signal to noise ratio, but affected the duration of the increase in FRET ratio by approximately 75 seconds (Figure 4.6).

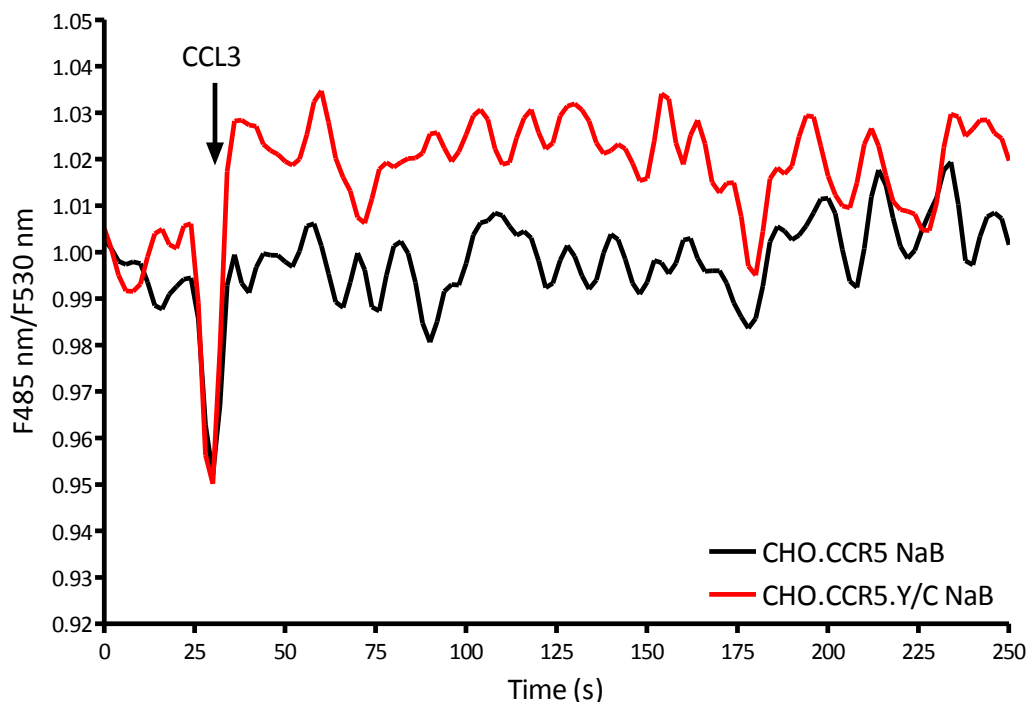


Figure 4.6 The effect of 5 mM NaBu treatment on FRET ratios in CHO.CCR5.Y/C and CHO.CCR5. There is a clearer difference between CHO.CCR5 (Peak AUC 0.146, Peak 1.75%, \pm 1.66%, n=4) and CHO.CCR5.Y/C (Peak AUC 2.677, peak 4.37%, \pm 3.66%, n=4) following NaBu treatment, duration of the FRET ratio signal is prolonged in CHO.CCR5.Y/C. Traces represent data from four independent experiments.

As an alternative way to confirm changes in FRET ratio were due to the activation of the fluorescently tagged heterotrimer 10 μ M mastoparan, an activator of PTX sensitive G-proteins (Higashijima *et al.*, 1988), was added to cells directly before the assay began. Activation of G-proteins by mastoparan could not be measured due to technical limitations, but the FRET ratio was measured in comparison to that of CHO.CCR5 before and after CCL3 stimulation. Accordingly, there was no discernable increase in the normalised FRET ratio of mastoparan treated CHO.CCR5.Y/C, which peaked at 2.56% (\pm 2.66%, n=4) over basal and had a peak AUC of 1.240 compared to that of CHO.CCR5, which peaked at 1.56% (\pm 2.35%, n=4) and had a AUC of 1.362 cells following CCL3 addition (Figure 4.7).

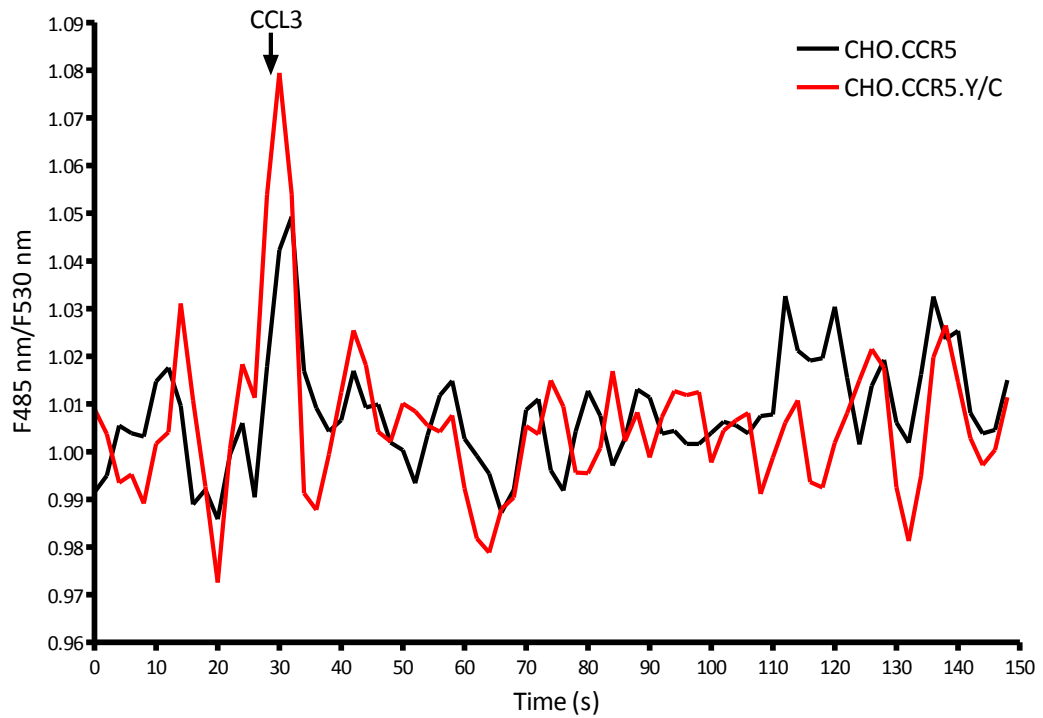


Figure 4.7 Mastoparan activation of the heterotrimer prior to CCL3 addition, led to no change in FRET ratio following stimulation with CCL3. CHO.CCR5 (peak AUC 1.362, peak 1.56%, $\pm 2.35\%$, n=4), CHO.CCR5.Y/C (Peak AUC 1.240, Peak 2.56%, $\pm 2.35\%$, n=4). Traces represent data from four independent experiments.

The lack of increase in the FRET ratio suggests that all $G\alpha_{i2}$ and $\beta_1\gamma$ heterotrimers had dissociated before reading took place. This hypothesis is backed up by measuring FRET ratios in prestimulated cell populations that have not been normalised (Figure 4.8). CHO.CCR5 cells treated with mastoparan displayed no variation to untreated control cells. CHO.CCR5.Y/C cells tended to display a marginally higher, although not significant, FRET ratio than control. This is most likely a consequence of donor acceptor pairs not associating in a 1:1 ratio, therefore leading to an increased emission at 485 nm. Pretreatment of cells with mastoparan resulted in an increase in prestimulation FRET ratios of 2.25% ($\pm 4.66\%$, $n=4$), calculated by measuring 30 the FRET ratio for 30 seconds and taking the mean average. This suggests that 10 μ M mastoparan treatment activates all PTX sensitive G-protein heterotrimers rapidly after treatment. This supports previous studies performed in vesicles showing rapid activation of G_o following mastoparan treatment(Higashijima *et al.*, 1988).

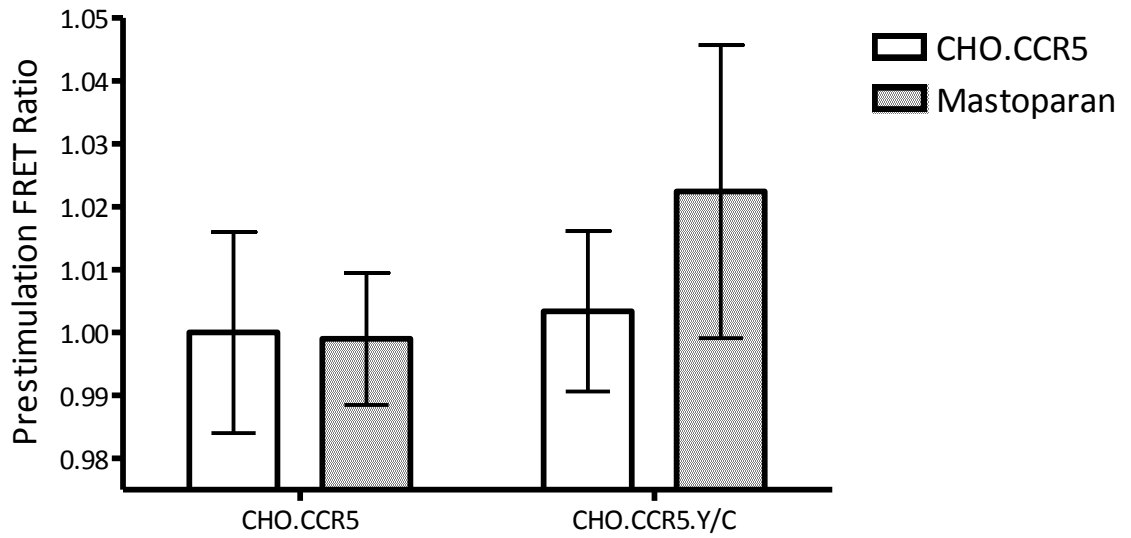


Figure 4.8 Treatment of CHO.CCR.Y/C with 10 μ M mastoparan before addition of 500 nM CCL3 resulted in higher prestimulation FRET ratios. (CHO.CCR5) 1.0000 ± 0.0319 , (+mastoparan) 0.9989 ± 0.0209 . (CHO.CCR5.Y/C) 1.0033 ± 0.0255 (+mastoparan) 1.0225 ± 0.0466 . All data has been normalised to the average prestimulation ratio obtained for untreated CHO.CCR5 cells. Bar chart represents the mean and SEM of four independent experiments.

4.3 Discussion

The aim of this chapter was to characterise the interaction and activation kinetics of the $G\alpha_{12}$ heterotrimer when activated by CCR5 following CCL3 stimulation. A further aim of this chapter was to develop an assay capable of measuring this interaction in whole cell populations in real time. Experimental data from this chapter provides proof of concept supporting the notion that FRET measurements can be performed in a live whole cell population to measure protein-protein interactions and their activation kinetics, in a high throughput system. However, during development of this assay numerous drawbacks to the experimental approach undertaken were discovered, which render this assay, in its current condition, unfeasible.

As discussed in the previous chapter, creation of a stably transfected cell line was a prerequisite for the development of a whole cell population assay. Aside from already discussed cell culture issues relating to multiple stable transfections, there are other issues that limit the further development of this assay system. The majority of successful live cell FRET work has been performed on small regions of interest in transiently transfected cells, with the use of confocal microscopy (Nikolaev *et al.*, 2007; Nobles *et al.*, 2005). This approach to measuring the FRET ratio has technical advantages over the whole cell population approach trialled by me in this research. Isolation of a region of interest in an individual cell allows for selection of areas that are robustly expressing fluorescent constructs of interest, as well as minimising autofluorescence signals that naturally occur from incidental excitation of cytosolic compounds. Most autofluorescence originates from mitochondria and lysosomes (Monici, 2005); structures which are easily excluded from readings with a confocal microscope (Sangmi *et al.*, 2009), but impossible to exclude from

whole cell readings on a plate reader. Several of the most commonly expressed cellular compounds, NADPH, FAD and lipofuscin, have overlapping excitation and emission spectra with both ECFP and EYFP. The abundance of these compounds is increased during times of cellular stress and protein misfolding (Herr *et al.*, 2001).

Each of these compounds interferes with fluorescence readings. Lipofuscin is a highly oxidised crosslinked protein aggregate, typically associated with the postmitotic aging. Lipofuscin structures absorb light between 364 nm and 633 nm (Marmorstein *et al.*, 2002) with fluorescent emissions peaking at 450 nm and 530 nm following excitation at lower wavelengths (Benson *et al.*, 1979). Although relatively little is known about the processes surrounding accumulation of lipofuscin, recent work has indicated that oxidative stress as a consequence of protein misfolding increases its accumulation (Bader *et al.*, 2006). Although the levels of protein misfolding were not investigated in CHO.CCR5.Y/C, there is an increased likelihood of misfolding incidences in stably transfected cells that overexpress constructs (Friguet, 2006). The over expression of transfected constructs could potentially raise oxidative stress in cells, due to compensatory degradation of over expressed G-protein subunits.

During cellular oxidative stress events reactive oxygen species (ROS) is generated. A countermeasure employed by cells to minimise damage caused by ROS is an increase in the production of NADH/NADPH (Ying, 2008) and FAD for use in flavoproteins (Massey, 2002). NADH and NADPH absorb light at 340 nm and 260 nm with broad peaks and are responsible for fluorescence peaking at 450 nm (De Ruyck *et al.*, 2007) in cells examined by fluorescent microscopy. The lenses used to excite cells in order to record FRET ratios from

CHO.CCR5.Y/C prevent wavelengths below 410 nm exciting cells, therefore autofluorescence from NADH/NADPH will be minimised when using the plate reader, however, this is not the case when analysing cells by fluorescent microscopy. FAD complexed proteins are also upregulated as a consequence of increased cellular stress from enhanced protein production (Pahl, 1999). FAD complexed enzymes have long been known to interfere with cellular fluorescent readings and have a broad excitation peak at 450 nm and a broad emission peak at 535 nm (Benson *et al.*, 1979). This, coupled with lipofuscins emission, could account for the highly variable emission at 535 nm seen in CHO.CCR5.Y/C when measured with the EYFP channel. It is also likely that Lipofuscin emission at 450 nm interfered with ECFP readings, recorded from the FRET channel. Direct measurements of the FRET channel may have been enhanced by lipofuscin emission, although as the fluorescent signal from lipofuscin is relatively constant and is not photosensitive, emissions would just add to the noise in recordings. However FAD is extremely photosensitive and degrades quickly on exposure to light which could possibly have resulted in perturbation of the FRET ratio by decreasing EYFP emission seen over long periods of exposure to excitatory wavelengths (Scheideler *et al.*, 1988).

There are two straightforward methods that could potentially help minimise problems with the signal to noise ratio in a plate reader FRET system. The first method utilises differences in the properties of light emitted at the same wavelength but by different fluorophores. Fluorescence polarisation spectroscopy is a technique used to differentiate emission from large and small fluorophores. It exploits the anisotropy of a molecule, i.e. the ability of a molecule to produce a different result if measured from a different direction. Small molecules rotate quickly, whereas large molecules rotate slowly. Illumination of large fluorophore, such as ECFP, with plane polarised light will result in a large proportion of

emitted light remaining polarised with respect to the excitation source, due to its slow rotation. Whereas illumination of small fluorophores results in less light remaining polarised (Knight *et al.*, 2002).

Another approach that can be considered in order to increase the signal to noise ratio is to use a brighter donor acceptor pair. Although, the ECFP-EYFP donor acceptor pair is well characterised and has been extensively utilised in many successful FRET studies, there are drawbacks to their use in a live cell system. Some problems with employing fluorescent proteins for FRET are that they exhibit relatively broad emission and small stokes shift, ECFP and EYFP emission is contaminated with cellular autofluorescence, reduced quantum yield compared to GFP, and ECFP photobleaches rapidly (Marc *et al.*, 2006). In response to the growing interest in FRET based method to investigate protein-protein interactions numerous improvements to the basic CFP/YFP acceptor donor pair have been made. Several mutations have been made to both proteins in order to create fluorescent proteins with higher quantum yields. The Cerulean CFP Mutant and MiCy protein, derived from stony coral, display less complex, and slower decay kinetics and enhanced quantum yield compared to ECFP (Karasawa *et al.*, 2004; Rizzo *et al.*, 2004). Mutations made to EYFP resulted in the development of Venus and Citrine EYFP, which both displayed higher quantum yield, quicker recovery times, lower photosensitivity and higher resistance to acidic conditions (Griesbeck *et al.*, 2001; Nagai *et al.*, 2002). Although there is not a great improvement in the spectral overlap or stokes shift of these variants; they are brighter and when used in tandem and result in an enhanced FRET signal, and therefore a higher signal to noise ratio. More recently the FRET optimised ECFP and EYFP derivatives, YPet and CyPet have been developed that exhibit a sevenfold increase in FRET signal compared to an ECFP-VenusEYFP pair (Nguyen *et al.*, 2005). However, these constructs suffer from an increase propensity to dimerise, resulting in perturbation of the FRET signal. Selective mutation to

the proteins can reduce the propensity for them to dimerise making the YPet CyPet FRET pair a superior alternative to the ECFP-EYFP pair used in this study (Ohashi *et al.*, 2007).

An interesting development in the development of donor acceptor pairs is the use of a 'dark' acceptor, i.e. an acceptor that doesn't fluoresce. Resonance Energy-Accepting Chromoprotein (REACH) is a mutant form of YFP that fluoresces at 2% that of YFP emission. The use of REACH as an acceptor in a FRET pair allows for the use of EGFP, which is photophysically superior to all other fluorescent proteins in terms of emission, and allows the removal of spectral filtering from assay apparatus (Ganesan *et al.*, 2006).

Obtaining and culturing a stable triple transfected cell line is often unsuccessful using traditional plasmid transfection technologies (Kingsbury *et al.*, 2000). More recently, with the development of lentiviral transfection techniques the generation and use of a triple transfected stable cell lines has been reported in HTS studies (Yamanaka *et al.*, 2007). The data gathered in this project indicate that a high through put method of measuring protein-protein interactions by FRET could become a reality if the difficulties with cell culture can be overcome. A lentiviral approach to generating the stable cell lines, the use of a brighter FRET pair, and improved spectroscopic techniques may provide methods to overcome the pitfalls encountered during the development of this assay.

Regardless of the circumstantial limitations placed on this research, these data represent the first cell based high throughout protein-protein interaction assay capable of measuring the kinetics of activation in G protein heterotrimers. The cornerstone of this assay was the development of a triple transfected stable cell line expressing consistent levels of donor

acceptor FRET pairs. To my knowledge the development of a stably transfected cell line expressing a fluorescent protein FRET pair to measure protein interactions, in a high throughput system, represents a completely unique approach to solving the problem of mapping protein-protein interactions. Results from this chapter may not provide a robust assay system for the systematic identification of G-protein heterotrimer interactions and kinetics, but they do recapitulate G-protein heterotrimer characteristics. Monitoring of the FRET ratio in CHO.CCR5.Y/C cells revealed that following stimulation with CCL3 $G\alpha_{i2}$ and $G\beta_1$ undergo a conformational change brought about by the CCR5 receptor. This conclusion was confirmed by treatment of the cells with PTX, which prevented an increase in the FRET ratio following stimulation, or by mastoparan treatment which also prevented an increase in the FRET ratio, but resulted in an increased FRET ratio prior to stimulation. Limitations with the temporal spacing of measurements meant very rapid interactions could not be monitored. However, data obtained show that G-protein heterotrimers are activated in less than 4 seconds following CCL3 addition and reassociation occurs over a period of 2 minutes.

Several studies have suggested that heterotrimers from the $G\alpha_i$ family do not undergo dissociation following activation (Lohse *et al.*, 2008), but rather a conformational change, which allows the active face of the protein to interact with downstream effectors. Unfortunately this is not a question that can be addressed with this assay system. The FRET ratio in performed assays never returns to basal levels, which could suggest that following activation and dissociation of the heterotrimer $G\alpha$ and $G\beta\gamma$ subunits reassociate with non tagged subunits, however without massive reduction in background noise it is impossible to ascertain whether long term changes in the FRET ratio are due to this or the relative photobleaching of autofluorescent compounds. However, with the continued development

of plate reader technology and brighter fluorescent proteins a FRET based whole cell population assay to measure protein-protein interactions in real time could become a reality in the near future.

Chapter Five

Development of a BRET Assay to Measure $G\alpha_{i2}$ $G\beta_1$ Interaction

5.1 Introduction

Studies of G-protein association and activation using a FRET based system assay, although partially successful, were not as successful as anticipated. Low proliferation rates, the potential for photobleaching of fluorescent fusion constructs, and a high signal to noise ratio owing to autofluorescence contributed to inconclusive results. Consequently, a bioluminescence resonance energy transfer (BRET) based assay was developed in order to circumnavigate some of these problems. To expedite the development of this assay a transient transfection approach was used as an alternative to the creation of stable cell lines. In a BRET system, resonance energy transfer is accomplished by utilising light produced by the conversion of coelenterazine into coelenteramide by renilla luciferase. Photons are emitted at approximately 480 nm, comparable to ECFP's emission of 485 nm and, as with FRET, will non-radiatively transfer energy to an acceptor protein if within adequate proximity. As there is no external light source involved in BRET, it results in very low cellular autofluorescence.

BRET incorporates the attractive advantages of FRET while avoiding the difficulties associated with fluorescence excitation. Additionally, BRET has been shown to be workable in transiently transfected cells examined in a plate reader (Angers *et al.*, 2000) and has recently been utilised to investigate the functional selectivity of the GPCR EP4 (Leduc *et al.*, 2009). With this in mind, it was decided to run a preliminary investigation to see if BRET assays in transiently transfected cells could provide an alternative method for the measurement of G protein heterotrimer protein-protein interactions.

5.2 Results

5.2.1 Creation of pcDNA3.1:hrLuc-G α_{i2}

cDNA for humanised renilla luciferase, a kind gift from Dr. M. Bouvier, was amplified by PCR to introduce HINDIII and KPNI cut sites at the 5' and 3' prime ends respectively (hrLuc HIND 5', 5'GAA GCT TAT GAC CAG CAA GCT GTA CGA CC 3') (hrLuc KPN I 3', 5' CGG TAC CGA GCC GAT CCC CCT GCT CGT TCT TCA 3'). PCR products were purified by gel electrophoresis purification, ligated in pGEM, and transformed into DH5 α competent *E.coli* for amplification. The plasmid was purified by a commercially available plasmid purification kit, hrLuc was then excised from the plasmid by digestion with KPNI and HIND III and purified by gel electrophoresis solubilisation. The excised fragment was ligated to the C terminus of G α_{i2} in pcDNA3.1:G α_{i2} linearised with KPNI. The construct was then transformed into *E.coli*, scaled up and purified with a commercially available plasmid purification kit.

5.2.2 Optimisation of hrLuc Transient Transfection

CHO.CCR5 were seeded into a 35mm dish at a density of 2×10^5 per dish. Cells were transiently transfected the following day at varying concentrations of pcDNA:hrLuc-G α_{i2} and transfection reagent (Genejuice, Novagen). 72 hours after transfection the relative levels of expression of hrLuc-G α_{i2} was examined by measuring luminescence at 485 nm following addition of, and 30 minute incubation with, EnduRen (Promega). Expression of transfected rLuc-G α_{i2} was plasmid concentration and transfection reagent concentration dependent. The optimal concentration of plasmid and transfection reagent was selected for its high luminescence and low variability and was determined to be 2 μ g plasmid and 6 μ l transfection reagent (Figure 5.1). Transfection of pZeoSV2:EYFP-G β_1 into CHO.CCR5, under these conditions, had previously been determined to be 2 μ g plasmid and 4 μ l transfection reagent.

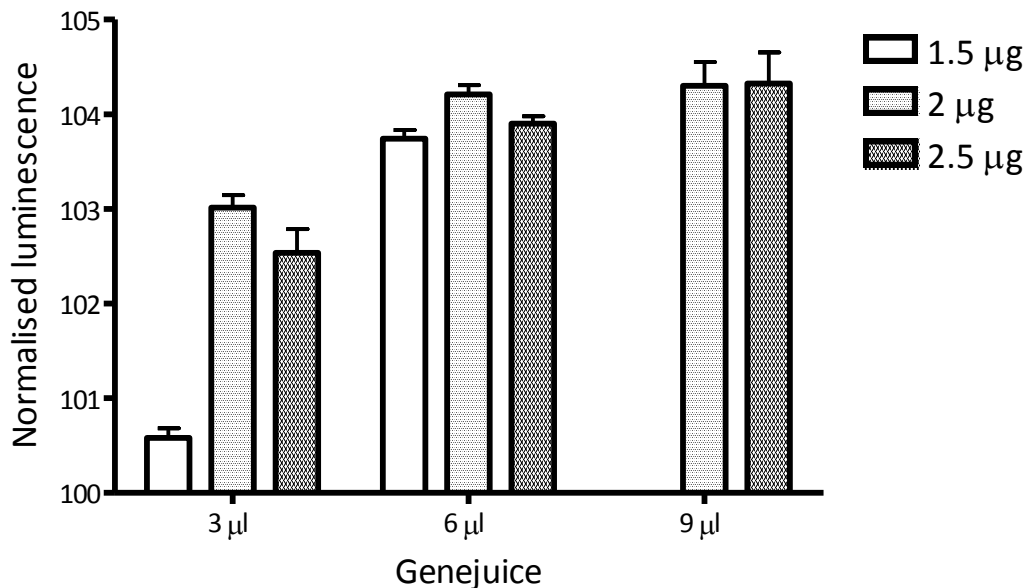


Figure 5.1 Varying expression of rLuc-G α_{i2} in CHO.CCR5 under different transfection conditions. Total luminescence at 485 nm was normalised to background levels in CHO.CCR5 not expressing rLuc-G α_{i2} but in the presence of rLuc substrate, EnduRen. Measurements were performed on a BMG Fluorostar optima FL platereader, the data represent the mean \pm SEM of three independent experiments.

5.2.3 Dual Transient Transfection

Transfection of either plasmid singularly resulted in robust expression of the construct. However, transfection of more than one plasmid construct resulted in a decrease in EYFP and rLuc expression, as examined by luminescence and fluorescence readings (Figure 5.2). Various transfection conditions were tried, including transfection of the second construct one day after the first. However, no significant increase in the expression of both constructs was seen through varying the protocol. Nevertheless, increases in fluorescence and luminescence were significantly above that of control cells for dual transfected cells.

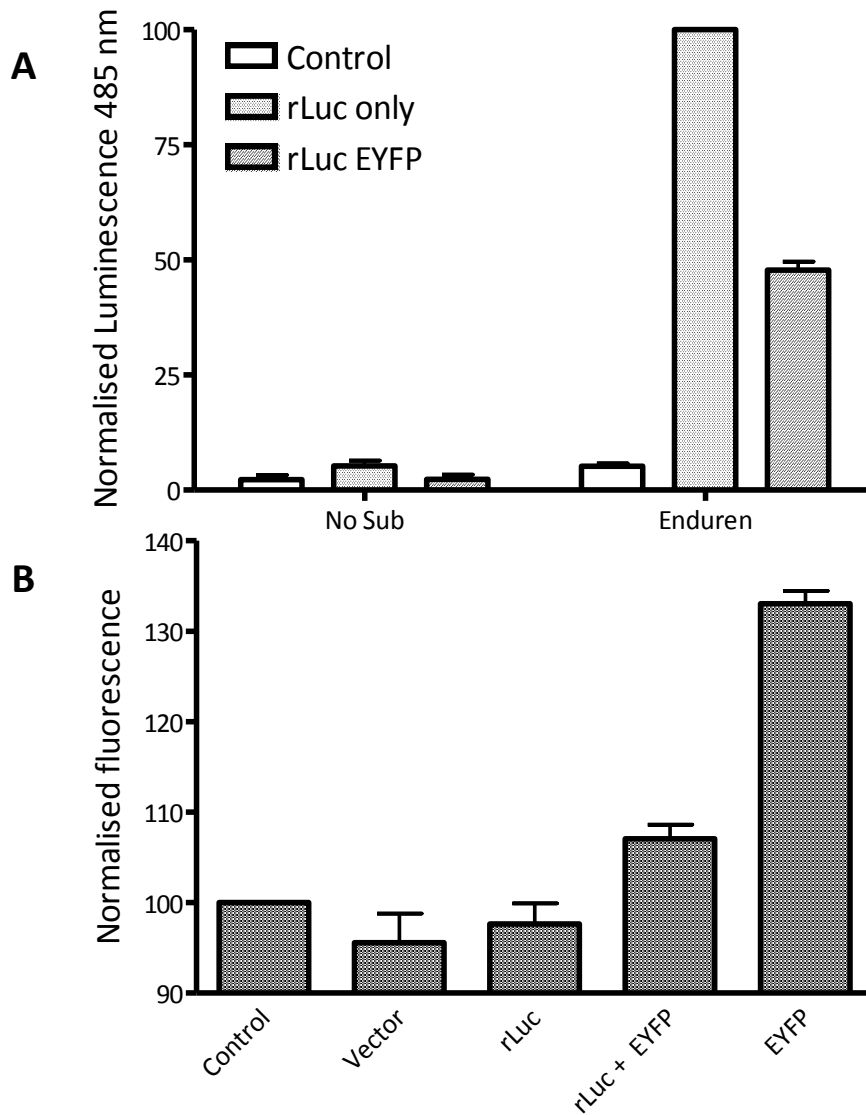


Figure 5.2. Relative expression levels of transient transfection of rLuc and EYFP in CHO.CCR5 assay system determined spectroscopically. (A) rLuc expression is altered by concomitant transfection of EYFP-G β_1 . CHO.CCR5 transiently transfected with renillia luciferase in the absence of EnduRen, have a background luminescence of 5.23%, ± 1.116 ($p=0.000151$) maximal luminescence in the presence of EnduRen. CHO.CCR5 transfected concomitantly with rLuc and EYFP, in the presence of EnduRen, show luminescence of 47.76%, ± 1.8055 ($p=0.00129$) maximal luminescence. (B) EYFP-G β_1 expression is effected by concomitant transfection of rLuc. Single transfection resulted in EYFP fluorescence 133.04%, ± 2.476 ($p=0.00004$) that of control, whereas concomitant transfection with rLuc resulted in EYFP fluorescence decreasing to 107.01%, ± 2.674 ($p=0.0192$) that of control. The data represent the mean and SEM of three independent experiments.

5.2.4 Substrate Kinetics and BRET

The kinetics of EnduRen turnover by rLuc in transiently transfected cells was investigated following EnduRen addition at a final concentration of 60 μM . Luminescence increased rapidly after addition of EnduRen and peaked after approximately 2000 seconds. This peak in luminescence signal plateaued and remained relatively stable for approximately a further 4000 seconds. After 7000 seconds the signal slowly decreases. Emission at 520 nm was concomitantly measured (Figure 5.3).

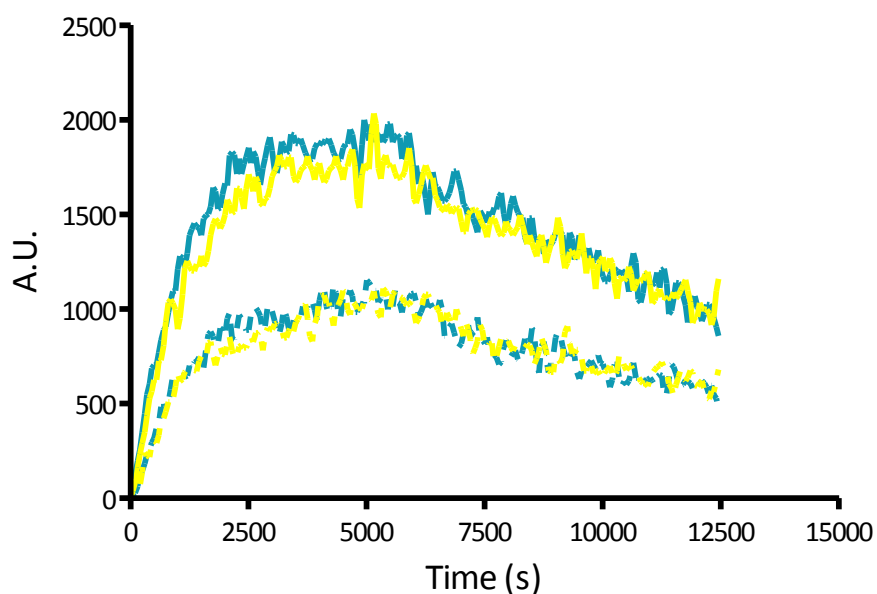


Figure 5.3 Luminescence and fluorescence levels following EnduRen addition in transiently transfected CHO.CCR5. Solid lines CHO.CCR5 rLuc emission; Blue 485 nm, yellow 520 nm. Dashed lines CHO.CCR5 rLuc EYFP; Blue 485 nm Yellow 520 nm. These are representative traces from a single experiment.

Surprisingly, there was not a great deal of difference between normalised emission at 520 nm for cells transfected only with rLuc and those with both rLuc and EYFP. This observation was quantified by calculating the proportional emission (PE) at 520 nm compared to that at 485 nm. For Figure 5.3 the proportional emission for CHO.CCR5 transfected with rLuc was 94.77 and for CHO.CCR5 transfected with rLuc and EYFP was 98.52. When this method is applied to all kinetic traces undertaken there is a trend for rLuc and EYFP transfected cells to have a higher PE. (Table 1). Raw PE values are variable between runs due to the variance in the levels of luminescence and fluorescence and the photo detection electrode's dependence upon those levels during calibration. Therefore, raw values have been normalised to the raw PE of rLuc transfectants. Normalised PE for rLuc and EYFP transfected CHO.CCR5 was on average 1.14% (± 1.571 , n6) higher than that of CHO.CCR5 transfected only with rLuc, suggesting interaction of the $G\alpha_{i2}$ -rLuc and EYFP- $G\beta_1$ constructs to form a functioning BRET pair.

Run #	rLuc PE	rLuc+EYFP PE	Normalised rLuc+EYFP PE
1	87.58	88.41	1.0094
2	87.61	88.43	1.0093
3	97.5	96.61	0.9908
4	86.76	87.74	1.0112
5	94.77	98.52	1.0395
6	94.19	94.94	1.0079

Table 5.1. Proportional emission of transiently transfected CHO.CCR5. PE values are calculated from all data points from entire traces by representing emission at 520 nm as a percentage of 485 nm emission. Normalised values indicate there is a non significant trend for cells with rLuc and EYFP to have a higher PE. rLuc+EYFP PE, 1.0114, ± 0.0157 (p=0.1351)

There are several published methods for calculating the BRET ratio. Data recorded throughout these investigations were analysed using equations published by Angers et al (Angers *et al.*, 2000) and BMG Labtech. The real time BRET ratio traces determined using these equations revealed no usable data regarding protein-protein interactions, there was too little resolution between values recorded for control cells and dual transfectants. This was most likely due to the very high emission recorded from rLuc only transfected cells in the 520 nm channel. There was also large variation in emission values recorded on a point by point basis, which, when analysed using BRET ratio calculations, amplified these variations. Analysis of the proportional emission shows very low distinction between ratiometric measurements for rLuc only and rLuc and EYFP transfected cells (Figure 5.4)

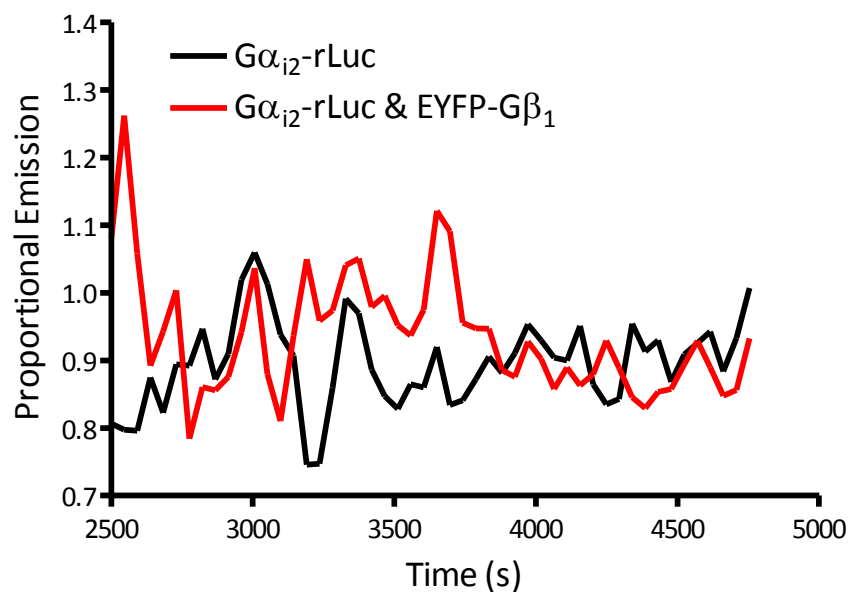


Figure 5.4 Proportional emission of CHO.CCR expressing Gα_{i2}-rLuc and Gα_{i2}-rLuc & EYFP-Gβ₁. Proportional emission was very variable and showed little resolution between control and BRET capable CHO.CCR5, making it difficult to draw conclusions about protein-protein interactions in a real time trace. These are representative traces from a single experiment.

5.3 Discussion

The aim of this chapter was to characterise the interaction and activation kinetics of the $G\alpha_{i2}$ heterotrimer when activated by CCR5 following CCL3 stimulation. A BRET based assay was constructed as an alternative to earlier FRET based protein-protein interactions. Luminescence at 485 nm and fluorescence at 520 nm were measured concomitantly in order to calculate interactions of $G\alpha_{i2}$ and $G\beta_1$ fusion proteins capable of undergoing BRET. Transient transfection into CHO.CCR5 of single constructs resulted in robust expression. However, co-transfection of both constructs into CHO.CCR5 resulted in a reduced transfection efficiency and/or expression.

Reduction in expression of transfected plasmids has previously been reported in several studies. Suppression of a plasmid containing a reporter gene when co-transfected with another plasmid was first reported for β -galactosidase (Farr *et al.*, 1992). Expression of β -galactosidase was shown to be modulated by the type of promoter on the other plasmid and the cell type that the co-transfection was taking place in. Interestingly, renilla luciferase expression has been shown to be suppressed by co-transfection with plasmids containing different promoter regions, in MCF-7 breast cancer cells. Suppression of renilla luciferase was reported to be between 3 fold to 252 fold, dependent upon the promoter region on the other plasmid (Vesuna *et al.*, 2005). These findings were reiterated, and expression was shown to be transgene and cell line dependent, as well as influenced by GPCRs such as androgen receptors. (Mulholland *et al.*, 2004). These reports combined with experimental data gathered during the development of this assay system suggest that co-transfection of renilla luciferase is more complex than commonly anticipated. Low expression of renilla luciferase and consequentially low luminescence in co-transfected CHO.CCR5 cells ready for BRET analysis represents a huge hurdle to overcome in the

development of this assay. Potentially these issues could be circumnavigated by the use of bi-or poly-cistronic vectors, i.e. vectors capable of expressing two or more proteins of interest from one transcription sequence. The plasmid pIREs has been used in mammalian cells for this purpose, and recent investigations show that repeated insertions downstream of the IRES (internal ribosome entry sites) promoter region are equally transcribed, allowing equal transcription of recombinant proteins (Bouabe *et al.*, 2008). The cloning of two genes into one plasmid requires extra planning, but ultimately could result in more consistent expression levels of tagged constructs.

Nevertheless, there are numerous reports of successful BRET assays being utilised to monitor protein-protein interactions in live cells (Gales *et al.*, 2005; Xu *et al.*, 2007). Early assays utilised the same donor and acceptor couple as used in this investigation. However, potential problems with luminescence levels were reported and the need for extremely sensitive light measuring equipment was also stressed (Xu *et al.*, 1999). The majority of published BRET assays have since been performed with modified donor and/or acceptor proteins as well as with specialised equipment. An example is the use EYFP topaz as the acceptor, EYFP topaz has a 17 fold greater emission over standard EYFP (Angers *et al.*, 2000). Further subsequent improvements to the initial BRET assay system have been made. One such improvement, is the creation of the proprietary BRET2 system (Perkin Elmer, wherever) which results in a substantially higher level of luminescence and a greater spectral resolution between rLuc and acceptor protein emission. BRET2 utilises a mutant form of rLuc, that in conjunction with deepblueC substrate, emits light at 395 nm, and a mutant form of GFP, called GFP2, which emits light at 510 nm. This assay system has been used widely and successfully by many groups (Bertrand *et al.*, 2002; Kocan *et al.*, 2008) and

has the advantage that emission for donor and acceptor are spectrally discrete from one another and mutations to rLuc result in enhanced luminescence signals.

Data acquired using this system showed a small overall increase in emission at 520 nm in cells expressing the EYFP-G β_1 construct over control cells. This trend suggests that there is a diminutive transfer of energy due to the close proximity of the G α_{i2} and G β_1 proteins. However, this result represents the summation of all temporal points measured. The assay system, as it stands, is not robust enough to allow real time monitoring of interactions.

BRET as a technique to measure protein-protein interactions offers some attractive advantages over the use of FRET, namely the removal of an external light source, which removes the risk of photobleaching fluorescent proteins and eradicates cellular autofluorescence; both of which can have significant impacts on the ability of a consistent FRET ratio to be measured. In addition, the use of a luciferase as the primary light source guarantees that light emitted by the fluorophore is a result of resonance energy transfer. However, no technique is perfect and in its current form BRET suffers from some technical limitations. As with FRET, the addition of donor and acceptor proteins to native proteins potentially reduces the ability of proteins to interact through steric hindrance of the native proteins interaction sites. Alternatively the candidate proteins could be interacting without allowing the donor acceptor pair to be in adequate proximity for resonance energy transfer. The latter of these two situations means that means that a BRET assay displaying no BRET does not necessarily prove non-interaction. Therefore it may be prudent to experiment with different combinations of donor acceptor fusion constructs.

Another consideration for the development of a BRET assay to measure the interaction of G-protein interactions is the limitations of the equipment used. The plate reader used in these assays was a fluorostar optima (BMG labtech, Germany) which has only been validated for measurement of basic BRET2 assays by the manufacturer. One concern is that the photo multiplier detector is not sensitive enough to record the low emission signals that were measured in this assay configuration. Data garnered during the development of this assay also indicated that there is considerable overlap in rLuc emission with the EYFP filter used, resulting in false readings for EYFP fluorescence. This observation strongly supports the development of enhanced BRET methods, such as BRET2, that allow a larger spectral window between donor and acceptor emission.

In summary, earlier FRET experiments have recapitulated that $G\alpha_{i2}$ and $G\beta_1$ interact and disassociate upon activation of the CCR5 receptor. The same conclusion cannot be made from data obtained from these BRET studies. However, analyses of data by long temporal integration of BRET signals suggest that the subunits do interact. For a BRET based assay to measure protein-protein interactions of G-protein heterotrimers in real time to become reality, associated instrumentation must continue its technological development, and the use of various donor acceptor proteins must continue to be optimised.

Chapter Six

The Impact of Mutant Forms of $G\alpha$ on CCR5 Signalling

6.1 Introduction

Mutations to different regions of the $G\alpha$ subunit give rise to dominant negative (DNM) and constitutively active (CAM) mutant phenotypes of the subunit. Data gained from these mutant forms, when expressed in a cell, can provide information about signalling cascades through a particular receptor. DNM $G\alpha$, when expressed in cells, competes with wild type $G\alpha$ for binding of other proteins involved in the G-protein cycle and can block or reduce the response caused by wild type $G\alpha$. CAM $G\alpha$ either has a reduced GTPase activity or no GTP binding capability, but is locked in the active conformation. Therefore, CAMs constantly bind downstream effectors, which results in constitutive activation of those effectors, although currently the mechanisms by which they achieve this are not well understood.

The $G\alpha$ subunit has a conserved guanine nucleotide binding region formed of five conserved polypeptide regions or boxes, termed G1-G5 (Tesmer *et al.*, 1997b). DNM $G\alpha_{12}$ has a single point mutation in the G3 box, in which a glycine has been exchanged for a threonine at position 203 (G203T). This mutation results in abrogated ability to bind GTP and an increased rate of dissociation from GDP (Inoue *et al.*, 1995). CAM $G\alpha_{12}$ has a single point mutation in the G3 box, in which a glutamine is exchanged for a leucine at position 205 (Q205L). This results in a markedly reduced GTPase function (Hermouet *et al.*, 1991). CAM $G\alpha_{12}$ has a single point mutation in the third switch region, in which a glutamine has been exchanged for a lysine at position 231 (Q231L), resulting in markedly reduced GTPase function.

CCR5 has been shown to directly induce changes in the actin cytoskeleton, by the activation of rho dependent cytoskeletal pathways (Di Marzio *et al.*, 2005). The $G\alpha_{12}$ subunit was included in these studies as it is a known player in the activation of rho dependent cytoskeletal pathways (Buhl *et al.*, 1995).

The specific mechanism by which DNM $G\alpha_{12}$ blocks G-protein signalling is not known. However, there are general mechanisms described in the literature and further possible theoretical mechanisms are also described. There are two mechanisms that have been experimentally described. The first of which involves DNM $G\alpha$ subunits sequestering all $\beta\gamma$ subunits, therefore preventing WT heterotrimers binding to the GPCR (Clapham *et al.*, 1997). The second described method involves DNM $G\alpha$ sequestering activated GPCR either in combination with $\beta\gamma$ or individually (Natochin *et al.*, 2006; Yu *et al.*, 1998).

DNM and CAM $G\alpha$ subunits will be used to help disseminate the interactions of CCR5 with specific $G\alpha$ subunits and thus provide information on the downstream signalling pathways that are activated by CCR5. In addition to data from studies with DNM and CAM, findings will be backed up by systematic siRNA knockdowns of $G\alpha$ subunits. The use of siRNA provides a means to further investigation into the roles of $G\alpha$ subunits through CCR5.

The development of siRNA as a tool has provided the research community with a method to precisely target genes and knockdown of the expression of the protein. This specificity allows the removal of predicted players involved in CCR5 signal transduction. By monitoring the effects the systematic removal of $G\alpha$ subunits has upon CCR5 signalling we hope to

provide evidence that CCR5 induced calcium mobilisation relies on other G-protein heterotrimers other than the already defined $G\alpha_{i2}$ interaction.

This study was focussed on measuring calcium release following stimulation of the receptor. Chemokine receptor activation patterns can differ between various read-out systems, so therefore, ideally, these experiments should be repeated using chemotaxis or GTP γ S binding assays as well. However, this project will give a first indication as to whether CCR5 interacts with different G-proteins and will illuminate aspects of CCR5 G-protein interactions.

6.2 Results

6.2.1 The Expression of DNM $G\alpha_{i2}$, CAM $G\alpha_{i2}$, and $G\alpha_{12}$ Result in Increased Basal Calcium Levels.

CHO.CCR5 were transiently transfected with DNM $G\alpha_{i2}$, CAM $G\alpha_{i2}$, or $G\alpha_{12}$. Cells were harvested for calcium flux analysis 72 hours after transfection, and intracellular calcium levels were assessed. CHO.CCR5 was transfected with pcDNA3.1, and basal cytosolic calcium levels were compared with CHO.CCR5. There was no significant difference between untransfected and transfected controls, with the transfected control showing an average increase of 1.9% (± 2.2 %, n=3, p=0.49399) CHO.CCR5 was used as control and ratiometric calcium measurements were normalised to control resting levels. All transfected cells displayed increased cytoplasmic calcium levels compared to control (Figure 6.1 A). Baseline levels of calcium were increased by approximately 30-40% of that of control, dependent upon the CAM or DNM transfected. Interestingly, $G\alpha_{i2}$ G203T displayed the highest overall increase in resting calcium levels with an increase of 40.5% (± 10.93 %, n3, p=0.00099), with $G\alpha_{i2}$ Q205L increasing basal calcium by 37.7% (± 4.12 %, n3, p=0.00001) over control and $G\alpha_{12}$ Q231L increasing basal calcium 31.6% (± 3.26 %, n3, p=0.00003) over control (Figure 6.1 B).

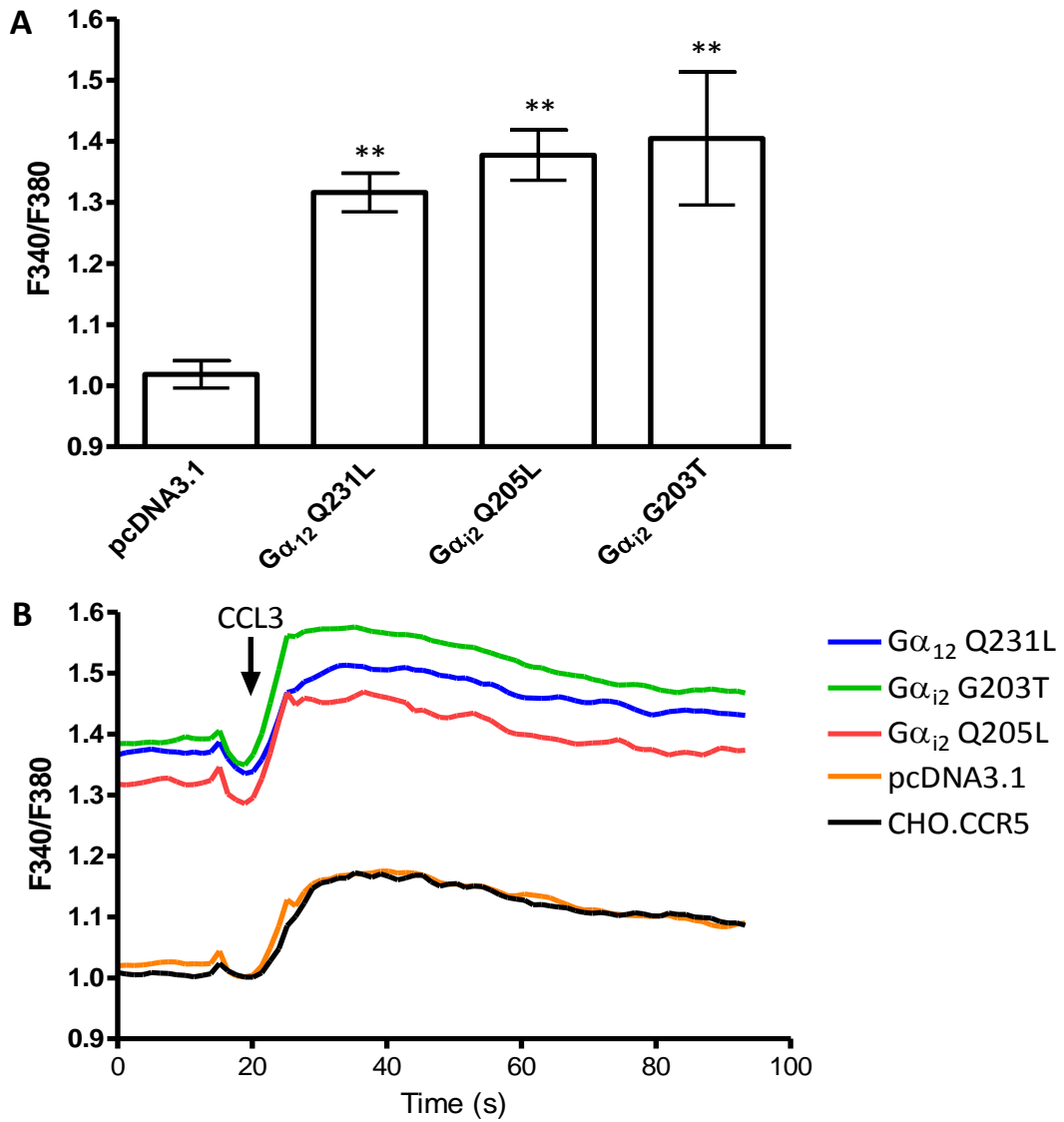


Figure 6.1 Transient transfection of DNM and CAM $G\alpha_{12}$ and CAM $G\alpha_{12}$ result in increased basal cytosolic calcium. (A) Basal levels of calcium in transfected cells (mean \pm SEM) show an increase in cytosolic calcium levels in unstimulated cells. These data represent the average basal levels of calcium normalised to control from three independent experiments. Double asterisks represent $p < 0.001$ (B) Calcium traces showing basal levels of calcium in transfected cells. Cells were stimulated at 20 seconds with 200 nM CCL3. Points plotted represent the mean values weighed to their nine neighbours for three independent experiments.

6.2.1.1 The Expression of DNM $G\alpha_{i2}$, CAM $G\alpha_{i2}$, and $G\alpha_{i2}$ Affect Speed and Quantity of CCL3 Stimulated Calcium Mobilisation

The expression of $G\alpha_{i2}Q231L$ and $G\alpha_{i2}Q205L$ resulted in moderate increases in calcium mobilisation following 200nM CCL3 stimulation, with $G\alpha_{i2}Q231L$ at 1.022 (± 0.0058 , $n=3$, $p=0.625$) and $G\alpha_{i2}Q205L$ at 1.044 (± 0.0109 , $n=3$, $p=0.570$) that of control. Expression of $G\alpha_{i2}G203T$ resulted in a larger significant increase in calcium mobilisation following stimulation being 1.070 (± 0.0112 , $n=3$, $p=0.0248$) of control (Figure 6.2). Interestingly, the expression of $G\alpha_{i2}Q205L$ and $G\alpha_{i2}G203T$, but not $G\alpha_{i2}Q231L$, resulted in an increase in the speed of calcium mobilisation following CCL3 stimulation with calcium flux peaking approximately 7.5 seconds faster than control in these cells (Figure 6.3).

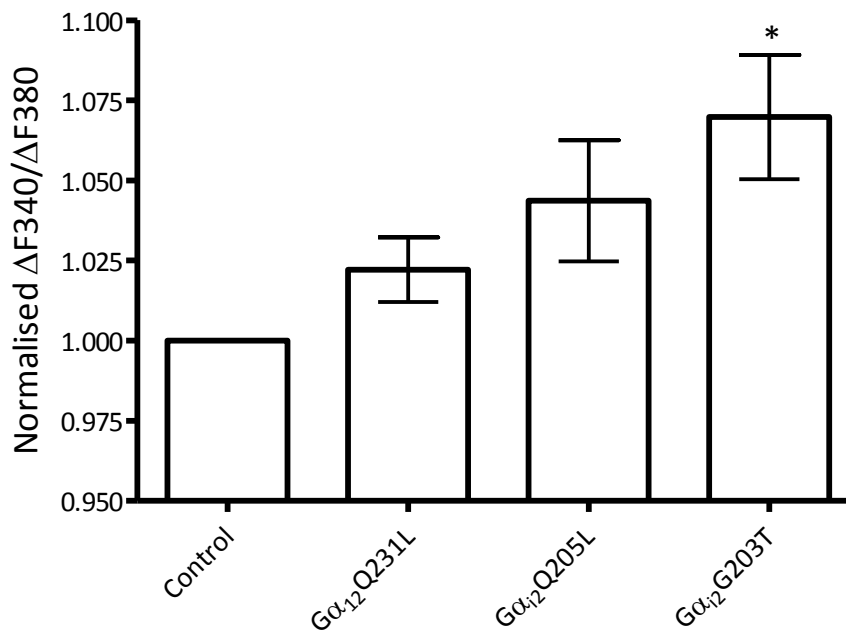


Figure 6.2 Transient transfection of DNM and CAM $G\alpha_{i2}$ result in perturbation of typical CCR5 mediated calcium flux. (A). Calcium flux following 200 nm CCL3 stimulation shows a significant increase in the amount of calcium released in cells expressing $G\alpha_{i2}G203T$ ($p=0.0248$), these data represent the mean and SEM for three independent experiments.

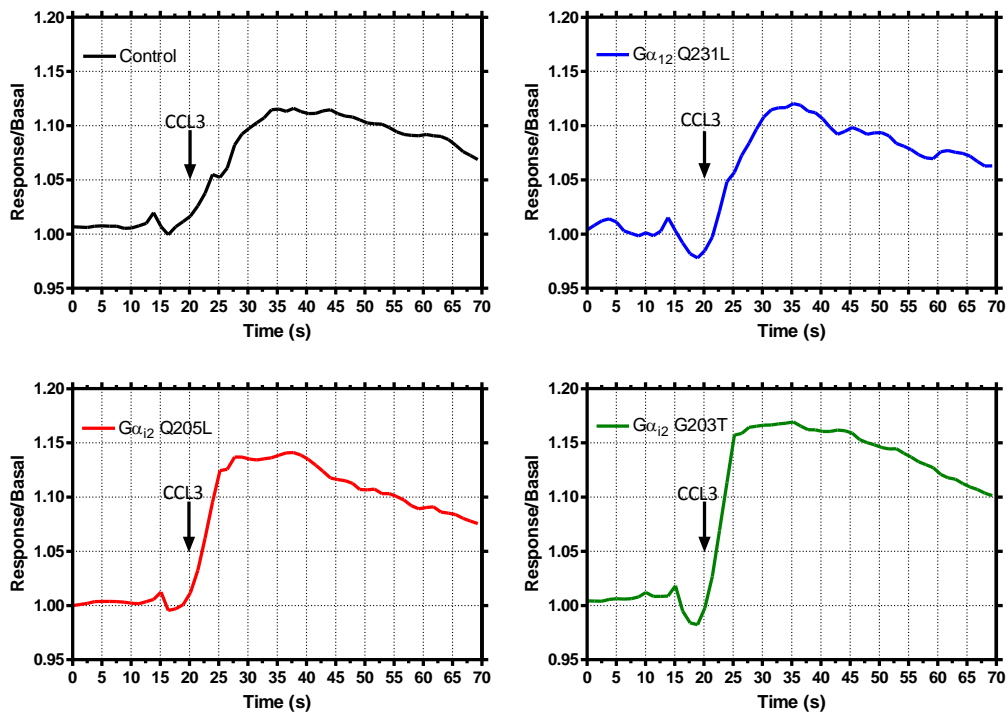
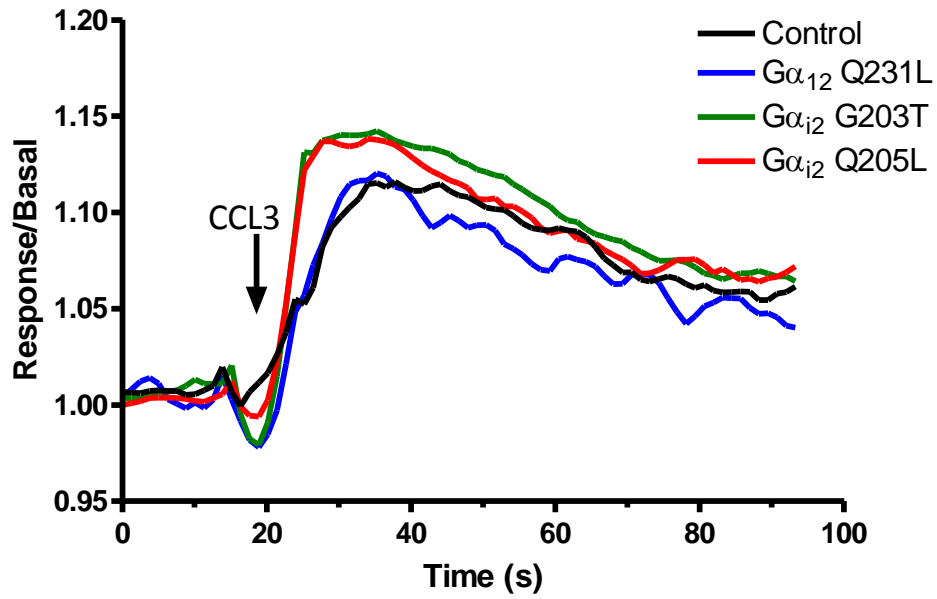


Figure 6.3 Expression of $G\alpha_{i2}G203T$ and $G\alpha_{i2} Q205L$ increase the speed of calcium mobilisation. (A) Combined traces showing calcium flux and speed of mobilisation following stimulation at 20 second with 200 nM CCL3. (B) As figure A, but individual traces. Control and $G\alpha_{i2}Q231L$ transfected cells require approximately 15 seconds for calcium flux to peak. $G\alpha_{i2}Q205L$ and $G\alpha_{i2}G203T$ peak in approximately 7.5 seconds. Traces plotted are a single representative trace of three similar independent experiments.

6.2.2.1 Effects of systematic knockdown of G α subunits.

HeLa RC-49 cells were systematically transfected with validated siRNA capable of knocking down expression of G α_i (1-3) and G α_q , control cells were transfected with validated negative control siRNA (Qiagen). The negative control siRNA has no homology to any known mammalian gene. Cells were transfected and left to grow for 72 hours, in line with the manufacturers guidelines. Transfection procedures were optimised by varying the amounts of transfection reagent and rhodamine tagged negative control siRNA. 72 hours after transfection, cells were observed and compared using a fluorescence microscope. Transfection efficiency was compared by counting a random field in a transfection dish for transfected cells. The optimal transfection volumes were determined to be 1 μ L Interferon (Polyplus) and 9.2 ng siRNA/ (7500 cells/100 μ l).

Individual knockdown of G α_i subunits (1-3) and G α_q , as well as combinations of knockdowns, did not result in increased basal levels of calcium, as seen in DNM and CAM transfected mutants. Furthermore, there was no change in the rapidity of calcium mobilisation following knockdown of any of the G α subunits (data not shown). Following knockdown and stimulation with 200 nM CCL3 there was considerable variation in the amount of calcium released compared to control transfections. Generally, single G α knockdowns released more calcium following stimulation compared to control, whereas dual knockdowns, where G α_q had been knocked down, resulted in a decrease in calcium mobilisation (Figure 6.4). Although trends were witnessed, no significant differences were measured at this concentration (Table 6.1). However, knockdown of G-proteins may affect receptor-CCL3 potency and efficacy rather than completely abolishing the signal, it is therefore paramount to perform concentration-response experiments.

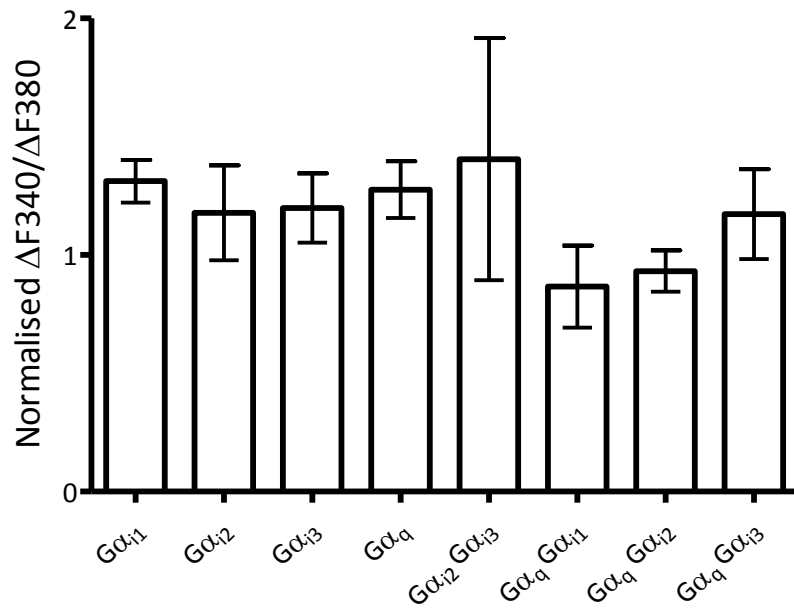


Figure 6.4 Calcium mobilisation is affected by G α knockdowns. Knockdown of single G α subunits results in an increase in calcium mobilisation following 200 nM CCL3 stimulation. Combination G α_q / G α_i knockdown resulted in lower calcium mobilisation for G α_q /G α_{i1} and G α_q /G α_{i2} knockdowns. Each bar represents the change in calcium levels normalised to the negative control, which was set to one for every assay. The points plotted are the mean and SEM of 2-5 independent experiments.

Knockdown	Mean	SEM	n
G α_{i1}	1.311698	± 0.090492	3
G α_{i2}	1.178028	± 0.20023	4
G α_{i3}	1.198684	± 0.146654	3
G α_q	1.276223	± 0.119457	5
G α_{i2} G α_{i3}	1.405027	± 0.511354	3
G α_q G α_{i1}	0.866546	± 0.173759	4
G α_q G α_{i2}	0.932072	± 0.087731	2
G α_q G α_{i3}	1.173047	± 0.189597	2

Table 6.1 Corresponding values for figure 4. Mean values represent data gathered from knockdown experiments and normalised to control samples set to one for each assay. Results for knockdown were analysed by Student's T-Test to negative control results, no significant differences were calculated.

6.2.2.2 $G\alpha_{i2}$ is not Involved in CCR5 Mediated Calcium Mobilisation

Knockdown of $G\alpha_{i2}$ with validated siRNA sequences was confirmed by western blot analysis (Figure 6.5). The effects of knockdown of $G\alpha_{i2}$ in HeLa RC-49 were further explored by measuring calcium mobilisation in a CCL3 concentration dependent way. No significant difference in log EC_{50} was found between control and $G\alpha_{i2}$ knockdown, with log EC_{50} values being -6.857 M (± 0.04917 M, n=4) and -6.922 M (± 0.03867 M, n=4), respectively. The intrinsic activity was likewise unaffected, with $G\alpha_{i2}$ knockdown cells having a calculated efficacy of 92.9% ($\pm 4.08\%$, n=4) of that of control (Figure 6.6).

6.2.2.3 Knockdown of $G\alpha_q$ Increases CCL3 Potency but not Efficacy

Knockdown of $G\alpha_q$ with validated siRNA sequences was confirmed by western blot analysis (Figure 6.7). The knockdown of $G\alpha_q$ was found to cause a leftwards shift in concentration response curve compared to control (Figure 6.8). The log EC_{50} for $G\alpha_q$ knockdowns was -7.045M (± 0.1181 M), compared to -6.615M (± 0.0473 M) for control, this represents a significant shift in potency ($p=0.0105$).

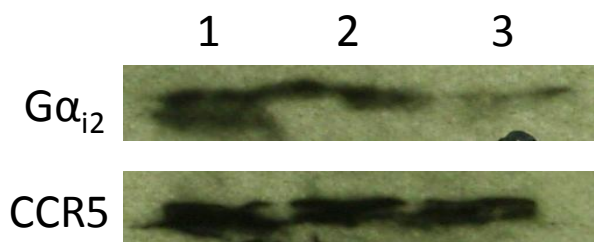


Figure 6.5 Western blots showing protein expression for CCR5 and $G\alpha_{i2}$. Lane 1 HeLa RC-49. Lane 2 Negative control. Lane 3 $G\alpha_{i2}$ knockdown.

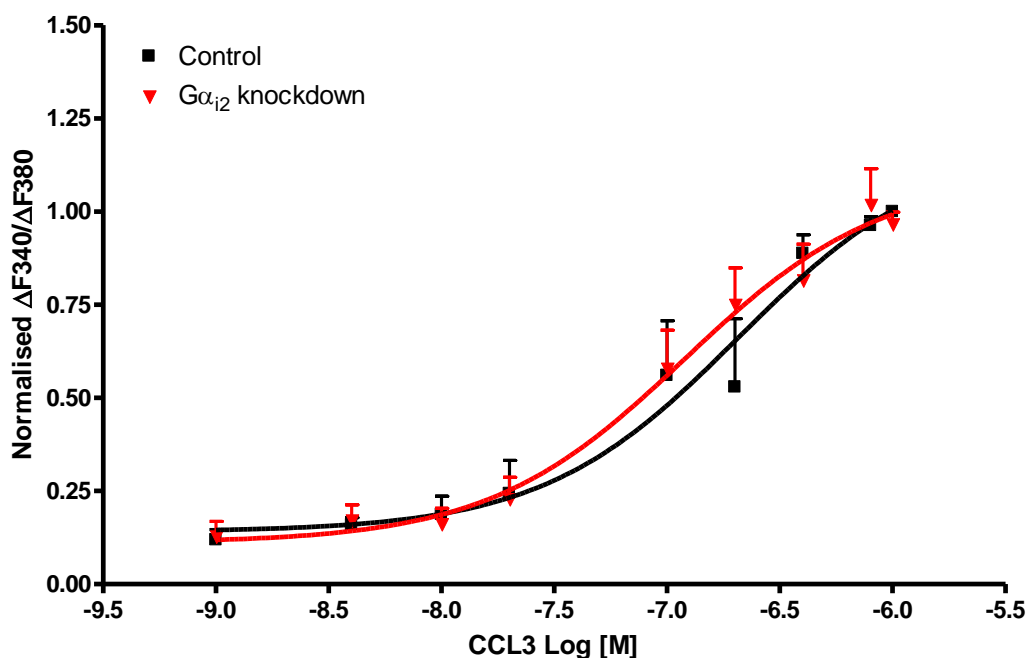


Figure 6.6 Concentration response curve for HeLa RC-49 $G\alpha_{i2}$ knockdown. No significant differences were recorded between any points measured, $\log EC_{50}$, or calculated efficacy (cE). Control cE=100%, $\log EC_{50}$ - 6.857M, (± 0.04917 M). $G\alpha_{i2}$ knockdown cE=92.9% \pm 4.08%, $\log EC_{50}$ -6.922 M (± 0.03867 M). The points plotted on the graph represent the mean and the SEM of 4 independent experiments.

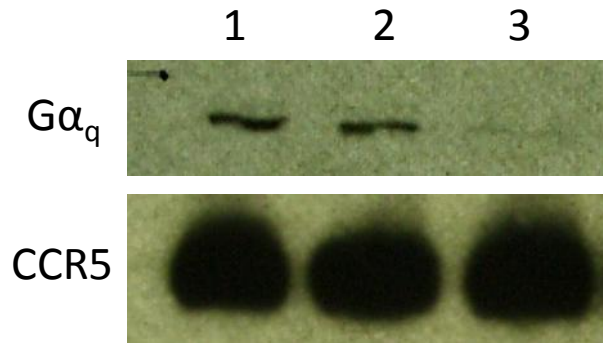


Figure 6.7 Western blots showing protein expression for CCR5 and $G\alpha_q$. Lane 1 HeLa RC-49. Lane 2 Negative control. Lane 3 $G\alpha_q$ knockdown.

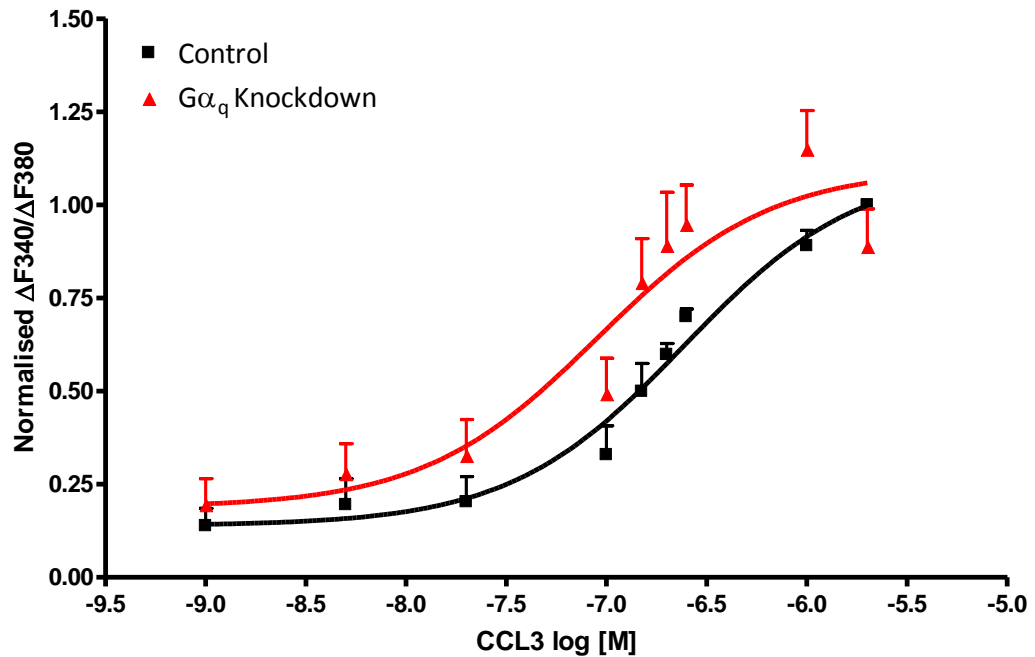


Figure 6.8 Concentration response curve for HeLa RC-49 $G\alpha_q$ knockdown. No significant differences were recorded between any points measured, log EC_{50} , or calculated efficacy (cE). Control cE=100%, log EC_{50} -6.615 M, (\pm 0.04737M). $G\alpha_q$ knockdown cE=99.6% \pm 12.34%, log EC_{50} -7.045 M (\pm 0.1181M). The points plotted represent the mean and the SEM of 5 independent experiments.

6.2.2.4 Combination Knockdown Results in a Decrease in Efficacy

Preliminary investigations into dual combination knockdowns of G α subunits have yielded some interesting results with respect to calcium release following stimulation of CCR5 with CCL3. Knockdown of G α_q in combination with G α_{i1} or G α_{i2} seems to decrease the ability of CCR5 to mediate typical calcium mobilisation. Knockdown of two G α_i subunits did not result in a decrease in maximum calcium mobilisation levels (Table 6.2). The most pronounced decrease in calcium mobilisation was observed in G α_q and G α_{i1} knockdown in combination. Log EC₅₀ values shifted significantly being -6.87M (\pm 0.0847 M, n=3) for control and -7.456 M (\pm 0.1093 M, n=2) for G α_q /G α_{i1} knockdowns (p =0.02959). The calculated efficacy for CCL3 acting on G α_q /G α_{i1} knockdowns was 52.2% (\pm 2.95%, n=2) when normalised to control values. Knockdown cells had severely attenuated calcium mobilisation at high CCL3 concentrations, yet similar responses to control at lower concentrations. Therefore, the shift in the log EC₅₀ recorded reports a relative change in the potency of CCL3 due to the effect knockdown has on CCR5-CCL3 intrinsic activity (Figure 6.9). Unfortunately, dual knockdowns could not be adequately characterised by western blot analysis, therefore these data represent preliminary findings.

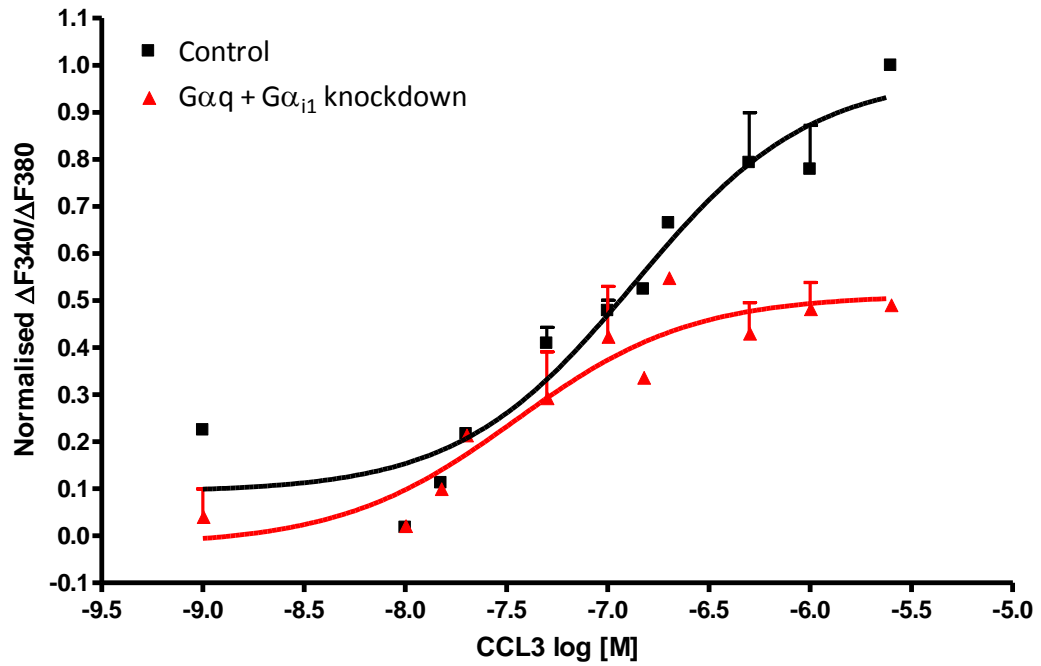


Figure 6.9 Concentration response curve for HeLa RC-49 Gα_q/Gα_{i1} knockdown. Control cE=100%, log EC₅₀ - 6.87M, (± 0.08477 M). Gα_q/Gα_{i1} knockdown cE=52.2% ± 2.95%, log EC₅₀ -7.456 M (±0.1093 M). cE values were normalised to the absolute calculated efficacy value for control in each independent experiment. The points plotted on the graph represent the mean and the SEM of 2 independent experiments.

Knockdown	$G\alpha_{i1}$ †	$G\alpha_{i2}$	$G\alpha_{i3}$ †	$G\alpha_q$
log EC ₅₀	-7.366	-6.922	-6.328	-7.045
SEM	0.1046	0.03867	0.07349	0.1181
p	ns	ns	ns	*
Cal. Efficacy %	125.725	92.893	159.549	99.637
Stdev	8.232	4.088	12.478	12.341
P	**	ns	***	ns
n	3	4	2	5
Knockdown	$G\alpha_{i2}$ $G\alpha_{i3}$ †	$G\alpha_q$ $G\alpha_{i1}$ †	$G\alpha_q$ $G\alpha_{i2}$ †	$G\alpha_q$ $G\alpha_{i3}$ †
log EC ₅₀	-6.961	-7.456	-7.175	-7.095
SEM	0.07902	0.1093	0.3479	0.2342
p	ns	*	ns	ns
Cal. Efficacy %	1.153	0.522	0.763	0.879
Stdev	6.252	2.959	4.418	3.278
P	ns	**	ns	ns
n	2	2	2	2

Table 6.2 Table comparing knockdown induced changes to CCL3 efficacy and potency in HeLa RC-49 cells.

Significance was determined by performing a two tailed unpaired t-test between control and knockdown samples. *=P<0.05, **=P<0.01, †=preliminary data.

6.3 Discussion

The aim of this chapter was to explore the possibility that CCR5 display could signal via G-protein heterotrimers, other than $G\alpha_{i2}$. Dominant negative mutants of $G\alpha$ subunits have been extensively utilised in other studies as a way to help delineate GPCR signalling pathways. The majority of this work has been carried out using $G\alpha_s$, with a small but significant proportion being performed with $G\alpha_{i2}$. Previous studies have indicated that $G\alpha_{i2}$ (G203T) has an important role to play in activation of cytosolic phospholipase A_2 and consequently the synthesis of arachidonic acid (Murray-Whelan *et al.*, 1995). The over expression of $G\alpha_{i2}$ (G203T) in CHO.CCR5 did not result in the abrogation of calcium release following stimulation with CCL3, strongly implying that CCR5 is capable of interacting with and activating other G-protein heterotrimers that act to raise cytosolic calcium levels. These data suggest the involvement of other members of the $G\alpha_i$ family and/or the $G\alpha_q$ family, but not of $G\alpha_{i2}$.

Counter intuitively, the over-expression of $G\alpha_{i2}$ (G203T) resulted in higher basal levels of cytosolic calcium, which was not anticipated before experiments were undertaken. This result directly contradicts a previous study where $G\alpha_{i2}$ (G203T) was over-expressed in CHO-K1 cells, with no effect upon resting calcium levels (Murray-Whelan *et al.*, 1995). One must draw the conclusion that the stable expression of CCR5 in conjunction with the expression of $G\alpha_{i2}$ (G203T) in some way accounts for this increase in basal calcium levels, although it is currently unclear as to how these changes are brought about. One possible explanation is that CCR5 pre-couples predominantly with $G\alpha_{i2}$ in its inactive state and the expression of $G\alpha_{i2}$ (G203T) results in a "space" for other G-proteins to interact with CCR5. Furthermore, other heterotrimers could potentially be spuriously activated by the inactive form of CCR5, resulting in the release of $G\beta\gamma$ and consequently a rise in basal calcium levels. Of course,

this theory is dependent upon $G\alpha_{i2}$ (G203T) being unable to interact with CCR5 specifically, as previous studies have indicated that the $G\alpha_{i2}$ (G203T) heterotrimer interacts with greater affinity to the α_2 -adrenergic receptor compared to wild type (Inoue *et al.*, 1995).

Previous studies have shown that $G\alpha_{i2}$ (G203T) has a similar affinity for $G\beta\gamma$ compared to wild type. Furthermore, it is capable of interacting with the α_2 -adrenergic receptor, has a faster GDP dissociation and GTP turnover than wild type, and upon GTP binding does not form an active conformation (Inoue *et al.*, 1995). Following stimulation of CHO.CCR5 with CCL3 there was a rapid increase in cytosolic calcium in cells transfected with $G\alpha_{i2}$ (G203T). Presuming that the $G\alpha_{i2}$ (G203T) heterotrimer does not undergo any sort of conformational shift and is incapable of releasing $G\beta\gamma$ subunits to activate downstream effectors which result in a release of cytosolic calcium, we must believe that CCR5 is activating different G protein heterotrimers. Work by Gales *et al* suggests that GPCR pre-couple to specific G-proteins, granting them a level of cellular signal specificity (Gales *et al.*, 2006). This work supports an earlier theory that CCR5 and members of the $G\alpha_i$ family are tightly associated in an inactive state (Mueller *et al.*, 2004a). The non-abrogation of calcium release following CCL3 treatment of CHO.CCR5 transfected with $G\alpha_{i2}$ (G203T) suggests that CCR5 induced calcium release is the effect of several G-protein heterotrimers being activated concomitantly and working in a coordinated fashion.

Data from this investigation demonstrate that there is a significant increase in calcium release following CCL3 stimulation in $G\alpha_{i2}$ (G203T) transfected cells. It is unknown whether $G\alpha_{i2}$ (G203T) interacts with CCR5 or leaves a “space” at the cytosolic tail free for other G-protein heterotrimers to bind in its place. Some recent contentious reports suggest that the $G\alpha_{i2}$ heterotrimer does not undergo full dissociation following activation (Bunemann *et al.*, 2003; Frank *et al.*, 2005). If this is the case, presumably the heterotrimer would predominantly target activate one downstream effector, corresponding either to $G\alpha$ or $G\beta\gamma$ subunit specificity. This could potentially provide an element of specificity to the signalling processes of GPCRs. There is a possibility that other G-protein heterotrimers that precouple to CCR5 in its inactive state are predominantly responsible for effects cumulating in the release of cytosolic calcium and that $G\alpha_{i2}$ heterotrimers may well target other downstream effectors. Without $G\alpha_{i2}$ heterotrimers binding to CCR5, the space once occupied by them could be occupied by other members of the $G\alpha_i$ family or even other G alpha family subunits. All members of the $G\alpha_i$ family share a strong homology (Suki *et al.*, 1987) and there are examples where all three members of the family interact with the GPCR in question (Mukhopadhyay *et al.*, 2005). An increase in the number of G-protein heterotrimers capable of activating PLC β associated with CCR5 could explain the significant increase in calcium released in these experiments.

The transfection of CHO.CCR5 with constitutively active $G\alpha_{i2}$ Q205L resulted in an increase in basal levels of calcium. Although it is unclear as to whether $G\alpha_{i2}$ undergoes dissociation following activation or not, the over expression of $G\alpha_{i2}$ Q205L does result in calcium release, suggesting the activation of PLC β by $G\beta\gamma$. Presuming the dissociation of the heterotrimer, this implicates $G\beta\gamma$ subunits are free from active $G\alpha_{i2}$. However, supposing the conformational change and non-dissociation of the heterotrimer, this result taken with

data from $G\alpha_{i2}$ G203T data suggests that following saturation of other downstream effectors the active $G\alpha_{i2}$ heterotrimer will also signal via its $G\beta\gamma$ pathway. The transfection of constitutively active $G\alpha_{i2}$ Q231L also resulted in an increase in basal levels of calcium. This is to be expected as $G\alpha_{i2}$ is a well characterised activator of PLC ϵ (Wing *et al.*, 2003).

In summary of the DNM and CAM experiments; the introduction of dominant negative and constitutively active forms of $G\alpha_{i2}$ does not abrogate CCL3 stimulated CCR5 mediated calcium release. Furthermore, the introduction of $G\alpha_{i2}$ G203T results in an enhanced release of calcium, strongly implying that other signalling mechanisms are primarily responsible in CCR5 mediated calcium mobilisation. The enhanced rapidity of calcium release also suggests a level of crosstalk between different signalling pathways, suggesting a role for $G\alpha_{i2}$ as a moderator of calcium release rather than an enhancer, although it is not apparent by what mechanism this may act by. These data indicate that CCR5 signalling, even with one ligand, is a multifaceted signalling network which relies upon the orchestrated activation and interactions of many signalling molecules, of which $G\alpha_{i2}$ is definitely a player.

The knockdown of individual $G\alpha$ subunits yielded some unexpected results. Knockdown of a single $G\alpha$ subunit tended to result in an increase in CCL3 stimulated efficacy and potency of calcium release. This could indicate interesting compensatory measures undertaken by cells to ensure important cellular processes are not perturbed. One such method that this could be achieved is crosstalk between signalling pathways. One method cells may utilise to achieve this level of cross talk in signalling pathways is by the formation of heterodimeric GPCRs. Many GPCR heterodimers have been reported (Gurevich *et al.*, 2008), and the act of

dimerisation can result in altered signalling properties (Milligan, 2006). Heterodimerization between the chemokine receptors CCR2 and CCR5 has been reported and was observed to synergistically increase in calcium mobilisation upon co-stimulation (Mellado *et al.*, 2001). Evidence that mixed complexes of receptors enhance coupling to $G\alpha_{q/11}$ has also been obtained in studies demonstrating that antagonism of either bradykinin B1 or B2 receptors reciprocally inhibits agonist mediated inositol phosphate production in prostate cancer PC3 cells (Barki-Harrington *et al.*, 2003). Despite a plethora of evidence of GPCR dimerization and an association of this with altered receptor function, including enhanced calcium signalling, the precise molecular mechanisms are still unclear. However, there are several consequences of dimerisation that could explain the unusual results seen in single knockdowns. One such method could be domain swapping (Gouldson *et al.*, 1998).

Domain swapping is a phenomenon by which a dimerised GPCR can undergo a conformational rearrangement in which receptors 'borrow' the transduction machinery of its dimeric partner (Maggio *et al.*, 1993). Therefore, activation of one GPCR may result in the activation of another GPCR's signalling machinery. Domain swapping and the activation of a dimerised GPCR's partner has been suggested as a way to prevent loss of function changes to a cell's signalling mechanism (Gouldson *et al.*, 1998). G-proteins are known to stabilise different GPCR conformations (Kobilka *et al.*, 2007), therefore it is fair to presume that the removal of a $G\alpha$ subunit that primarily interacts with a CCR5 may result in a destabilising effect and potentially a loss of normal function. Domain swapping could provide a method to functionally rescue compromised CCR5. In addition, it has been observed that calcium release can also be potentiated by a variant of this model in cells co-expressing angiotensin II AT1 and bradykinin B2 receptors. The bradykinin B2 receptors are thought to 'present' G-proteins to the AT1 receptors within a dimeric complex to facilitate

Ca²⁺ signalling in response to AT1 receptor agonists (AbdAlla *et al.*, 2000). Although we cannot be sure if CCR5 dimerises in HeLa RC-49, it is a possibility that should not be ignored.

Although CHO K1 and HeLa cells are known not to express chemokine receptors, a simple literature review of proteomic characterisation of CHO K1 cells reveals many endogenous GPCR that could potentially interact with CCR5 (Holdsworth *et al.*, 2005), as well as yet undefined orphan GPCRs (Kostenis, 2001). HeLa cells have also been shown to express several endogenous GPCR which may be able to interact with CCR5 as previously discussed (Steffen, 2008). For this reason caution must be exercised when trying to draw firm conclusions about CCR5 signalling mechanisms in model cell systems from the results gained from the individual knockdown of G-proteins.

In addition to hypotheses regarding dimerisation, there is plenty of evidence to suggest that GPCR couple to more than one sub-type, or even, family of G-proteins and that these interactions are physiologically relevant (Laugwitz *et al.*, 1996). It has been suggested that different conformational states in the same GPCR can alter the G-protein binding (Ahuja *et al.*, 1996). This phenomenon has been described in CXCR2, where a low affinity ligand binding form has been shown to be responsible for calcium mobilisation and a high affinity form responsible for chemotaxis (Ahuja *et al.*, 1996). Although the concept of precoupling is still a contentious issue, with equally strong supporting (Andressen *et al.*, 2006) and conflicting evidence (Qin *et al.*, 2008), it is possible that these GPCR binding states are stabilised by interactions with G-protein heterotrimers (Roka *et al.*, 1999). Removal of a subunit by knockdown would leave the receptor open to binding another subfamily in great

numbers, hence amplifying those subfamilies effects, which potentially may be the release of calcium.

Studies performed by Krumins *et al.* in HeLa cells investigated the effects targeted knockdown of G α subunits had upon the expression of non targeted G α and G β . They found that the knockdown of G α subunits often results in a compensatory up-regulation of other G-proteins (Krumins *et al.*, 2006). In particular, knockdown of G $\alpha_{q/11}$ resulted in a twofold increase in G α_{i1} subunits and knockdown of G α_{i3} resulted in an increase of G α_q , G α_{i1} and G α_{i2} . In fact, the only knockdown without effect was the knockdown of G α_{i1} . In relation to results seen in our experiments, this suggests that the increase of calcium following knockdown of a single G α subunit may be due to compensatory methods within the cell.

Knockdown of two G α subunits in combination may be more telling of the heterotrimer associated with and activated by CCR5 in response to CCL3 stimulation. Although caution must be used when inferring from these results; the greatest effect upon calcium mobilisation occurred with simultaneous knockdown of G α_q and G α_{i1} and G α_{i2} , indicating a role for these subunits in CCR5 mediated calcium release. Although calcium mobilisation was not completely abolished by combinational knockdown, these results strongly indicate that these subunits are somehow intertwined in the signalling response from CCR5. As with single knockdowns HeLa, cells could be undergoing compensatory mechanisms in order to prevent deleterious perturbations to the cells normal responses.

Taken together, this work provides additional data to support the hypothesis that GPCR associate with several discrete members of the G α family. Although results gained are far from absolute, they do indicate that signalling through CCR5 is a complex network that relies upon more than a single subfamily of G α proteins. Furthermore, these data also demonstrate that G-protein signalling is very resistant to change, and able to compensate for perturbations in the normal signalling machinery. The underlying methods for this are not clear and further work is needed in order to clarify the interactions and rescue mechanisms that underpin these findings.

Chapter Seven

Small Molecule Interference of G $\beta\gamma$ Subunits

7.1 Introduction

Expression of DNM G α_{i2} did not result in an inhibition of calcium release, suggesting that the G α_{i2} heterotrimer is not essential for chemokine stimulated release of calcium. As such it was decided to further investigate the activation mechanisms of calcium mobilisation following chemokine stimulation. The G $\beta\gamma$ subunit was once thought to be a negative regulator of G α signalling, acting to allow termination of G α signalling and facilitating the reassociation of the heterotrimer with the GPCR. However, in 1987 purified G $\beta\gamma$ was shown to be involved in the activation of a cardiac potassium channel *in vitro* (Logothetis *et al.*, 1987). It was not until 1987 that the first example of G $\beta\gamma$ dependent signalling, in a physiological mammalian system was identified. G $\beta\gamma$ was shown to regulate inwardly rectifying K_{Ach} channels (Logothetis *et al.*, 1987). We now know that the G $\beta\gamma$ subunit can modulate many downstream effectors (Clapham, 1996) and currently the functional properties of this subunit are under close scrutiny.

Gallein, a synthetic derivative of the naturally occurring dye haematoxylin, was until recently used only as a histological stain to mark cell nuclei. However, new research indicates that it may have a role to play in HIV treatment (Cruceanu *et al.*, 2006) and as a small molecule modulator of G $\beta\gamma$ function. Recent studies have shown gallein to inhibit G $\beta\gamma$ dependent chemotaxis and inflammation events in differentiated HL60 cells and *in vivo* in neutrophils (Lehmann *et al.*, 2008).

Gallein has been shown to bring about its disruptive effects by binding to an area of the G β γ subunit known as the “hot spot” (Lehmann *et al.*, 2008). The hot spot is an area on the G β γ subunit that has been shown to be a critical effector binding and signal transfer region (Davis *et al.*, 2005). However, recent reports indicate that the hot spot is not the only signal transfer region, G β γ may also activate downstream effectors through interactions with amino acids other than those in the hot spot area. The G β γ subunit has been shown to activate PLC β_2 , through a non hot spot region, independently of GPCR activation, upon binding activator of G protein signalling protein 8 (APS8) (Yuan *et al.*, 2007).

Gallein has only recently been characterised as a molecule capable of interacting with the G β γ subunit, as such it is still poorly characterised and understood. These experiments aim to illuminate the mechanisms by which gallein brings about its physiological changes, and through its unique G β γ modulating properties we hope to further elucidate CCR5 signalling pathways through G-protein heterotrimers.

7.2 Results

7.2.1 Gallein Enhances CCR5 Mediated Calcium Release

CHO.CCR5 were pre-treated for 30 minutes with varying concentrations of gallein prior to stimulation with CCL3 and the effects on cytosolic calcium mobilisation were monitored. Following stimulation with 100 nM CCL3, gallein treated cells exhibited enhanced levels of calcium mobilisation. The effect was concentration dependent; treatment with 20 mM gallein prior to experimentation resulted in the highest increases in calcium mobilisation (Figure 7.1). When analysed by Student's t-test (paired, two-tailed), treatment with 10 mM gallein did not result in a significant increase in calcium release. However, calcium release following 20 mM and 30 mM treatments did result in a significant increase, with P values of 0.0193 and 0.0129, respectively.

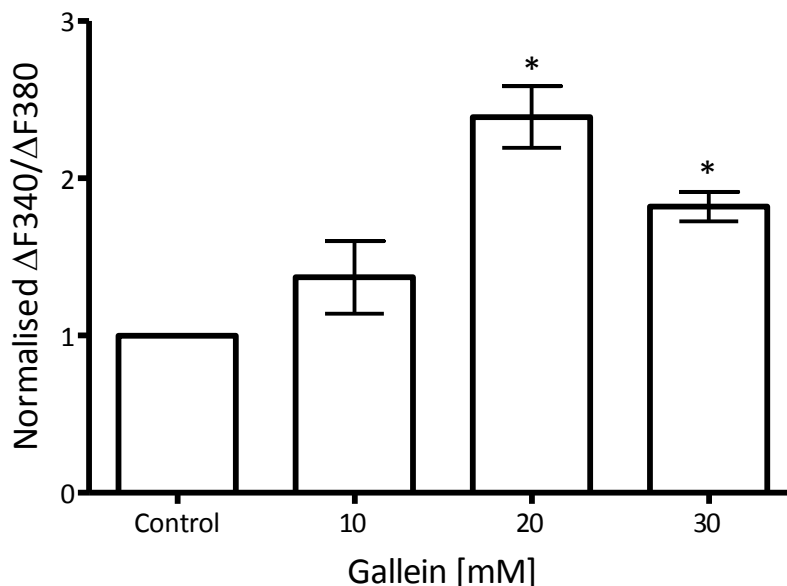


Figure 7.1 Gallein has a concentration dependent effect on CCR5 mediated calcium release. CHO.CCR5 were treated for 30 minutes with different concentrations of gallein, following fura2 loading cells were stimulated with 100nM CCL3 and calcium release measured. Results (mean, SEM) gallein 10 mM 1.371 (±0.2309, n=4, p=0.2498), 20 mM 2.390 (±0.1962, n=4, p=0.0193) and, 30 mM 1.820 (±0.0939, n=4, p=0.0129). Graph is data from four independent experiments

7.2.1.2 Gallein Treatment Results in Enhanced CCL3 Efficacy but not Potency

Concentration response assays were performed on CHO.CCR5 cells that had been treated with gallein at various concentrations. It was found that gallein treatment resulted in an increase in calcium mobilisation at all CCL3 concentrations. The intrinsic activity of CCL3-CCR5 signalling was increased almost 2.5 fold at some concentrations. However, the potency of CCL3 acting through CCR5 did not differ from that of control cells, with Log E_{50} values for control, 20 mM treatment and 30 mM treatment being, $-7.586 (\pm 0.08543 \text{ M}, n=4)$, $-7.516 (\pm 0.1110 \text{ M}, n=4)$ and $-7.606 (\pm 0.08398 \text{ M}, n=4)$, respectively (Figure 7.2).

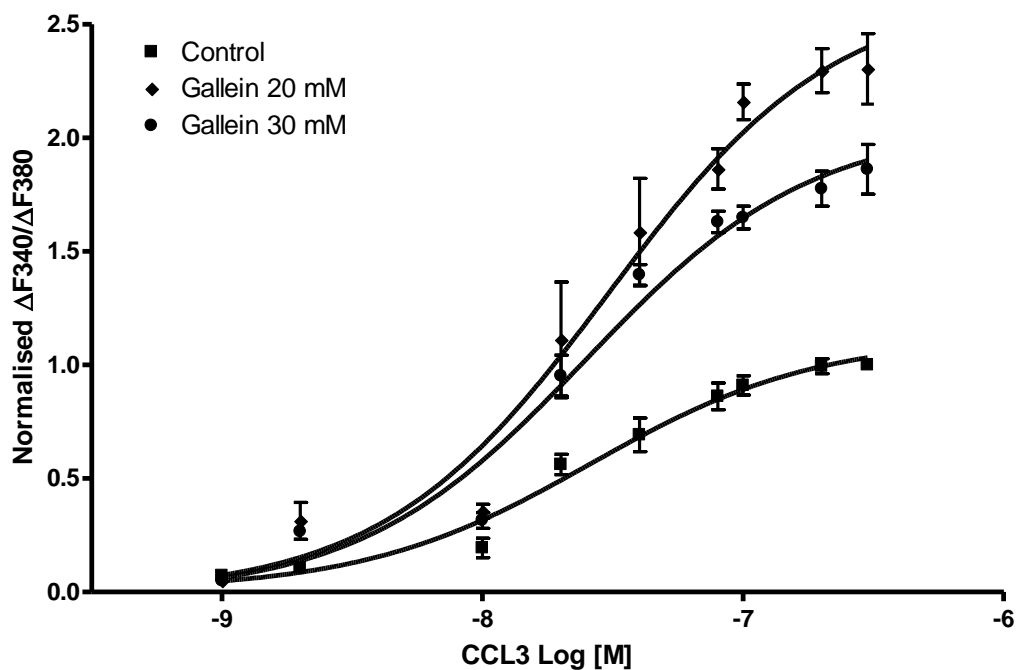


Figure 7.2 Gallein increases CCL3 efficacy through the CCR5 receptor. Control: Calculated Efficacy (cE) $cE=100\%$, $\text{Log}E_{50}=-7.586 \text{ M}$, 20 mM $cE=235.86\%$, $\text{Log}E_{50}=-7.516 \text{ M}$, 30 mM $cE=183.67\%$, $\text{Log}E_{50}=-7.606 \text{ M}$. Data points plotted are the mean and SEM of four independent experiments. Curves were plotted with a theoretical hill co-efficient of one.

7.2.2 Gallein's Effects are not Cell Type Specific.

To ensure that the unexpected results gathered in experiments with CHO.CCR5 were not due to cell specific expression of isozymes involved with the generation of second messengers, such as adenylyl cyclase (AC) and phospholipase C β (PLC β), further experiments were performed on HeLa RC-49 cells. Cells treated with gallein for 30 minutes prior to CCL3 stimulation also exhibited substantial increases in calcium mobilisation. The effect was concentration dependent, with the largest increase in calcium mobilisation seen following 30 mM gallein treatment (Figure 7.3). When analysed by student's t-test (paired, two tailed), treatment with 10 mM and 20 mM gallein did not result in a significant increase in calcium release, however 30 mM treatments did result in a significant increase with a P value of 0.0096.

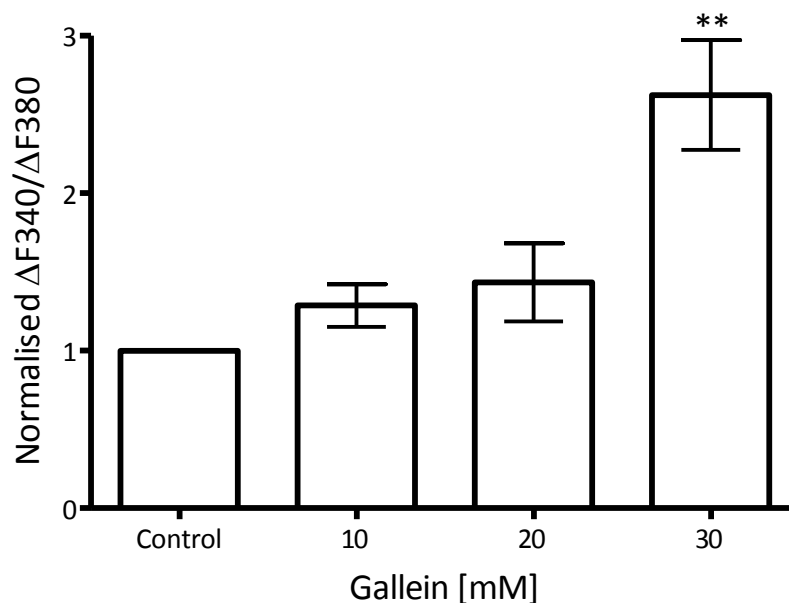


Figure 7.3 Gallein increases CCL3 stimulated calcium mobilisation in a concentrationdependent fashion in HeLa RC-49. HeLa RC-49 were treated for 30 minutes with different concentrations of gallein, following fura2-AM loading cells were stimulated with 100nM CCL3 and calcium release measured. Results; 10 mM gallein 1.287 (± 0.0496 , n=5, p=0.1020), 20 mM gallein 1.434 (± 0.2481 , n=5, p=0.1553), 30 mM gallein 2.623 (± 0.3485 , n=5, p=0.0096). The graph represents the mean and SEM from five independent experiments.

Concentration response assays were performed on HeLa RC-49 cells that had been treated with gallein at various concentrations. It was found that gallein treatment resulted in an increase in calcium mobilisation at all CCL3 concentrations. The intrinsic activity of CCL3-CCR5 signalling was increased 2.26 fold at saturating concentrations of CCL3. The potency of CCL3 acting through CCR5 was not found to differ from that of control cells (see Table 7.1), with Log E_{c50} values for control, 20 mM, and 30 mM gallein treatment being, -7.192 (± 0.06993 M, n=5) , -7.304(± 0.1899 M, n=5) and -7.225 (± 0.1557 M, n=5), respectively (Figure 7.4).

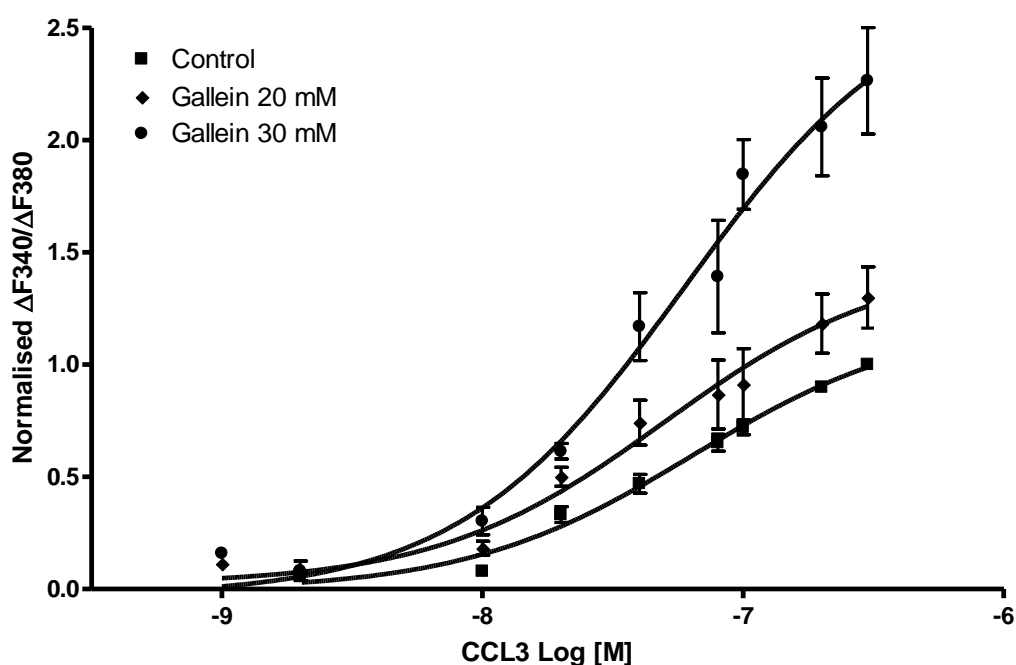


Figure 7.4 Gallein increases CCL3 efficacy through the CCR5 receptor. Control: cE=100%, Log E_{c50} -7.192 M, gallein 20 mM cE=121.96%, Log E_{c50} -7.304 M, gallein 30 mM cE=226.62%, Log E_{c50} -7.225 M. Data points plotted represent the mean and SEM of five independent experiments. Curves were plotted with a theoretical hill co-efficient of one.

7.2.3 Gallein Treatment Increases resting cAMP Levels

HeLa RC-49 cells were treated with 30 mM gallein and 10 μ M forskolin for 30 minutes prior to 3 minute stimulation with CCL3. Relative cAMP levels were measured using the cAMP-Glo™ assay kit (Promega). The relationship between cAMP concentration and bioluminescence is inversely proportional. Treated cells exhibited increased levels of cAMP and therefore reduced bioluminescence in the cAMP-Glo™ assay. Unstimulated cells had average luminescence values of 13724 (\pm 1545.14, n=3) for control, and 7451 (\pm 1088.36, n=3) for gallein treated. Cellular cAMP levels decreased in a concentration dependent way to CCL3 stimulation. Only at saturating concentrations of CCL3 did cAMP levels in gallein treated cells reach levels seen in unstimulated control cells (Figure 7.5).

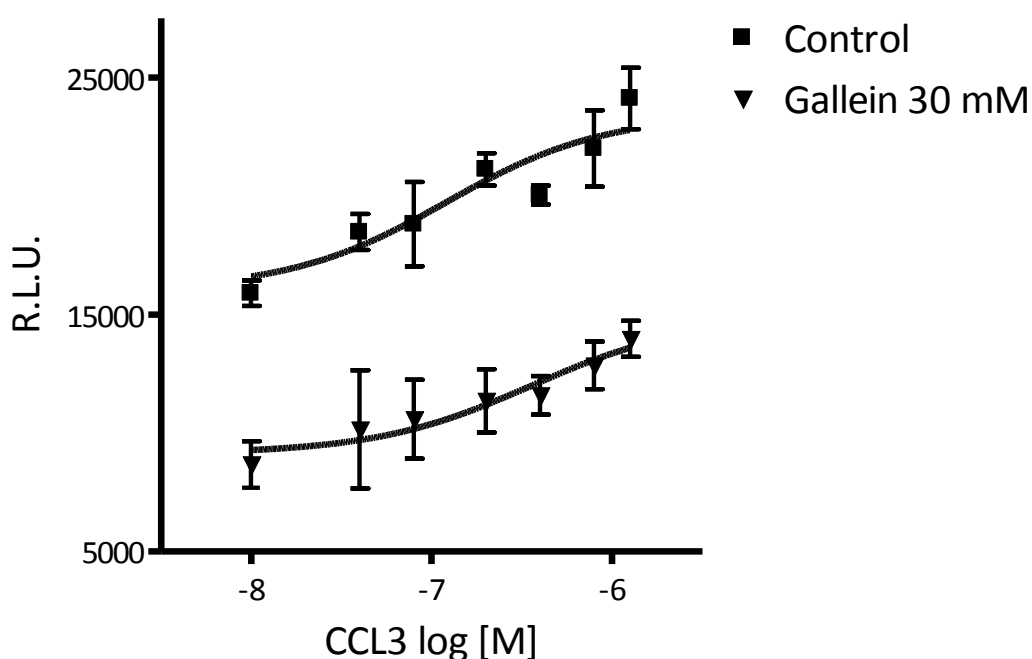


Figure 7.5 Gallein increases resting levels of cAMP in HeLa RC-49. Cells were treated with 30 mM gallein for 30 minutes before stimulation with CCL3. cAMP levels were measured using the Promega cAMP-Glo kit. Gallein increased resting levels of cAMP two-fold, but did not significantly affect CCL3 stimulated inhibition of adenylyl cyclase. Results; Control Log $E_{c_{50}}$ -6.918 M (\pm 0.1864 M), gallein Log $E_{c_{50}}$ -6.448 M (\pm 0.1475 M). Data points plotted represent the mean and SEM of three independent experiments.

HeLa Rc-49	Control	Gallein 10 mM	Gallein 20 mM	Gallein 30 mM
Log EC ₅₀ [M]	-7.192	-7.216	-7.304	-7.225
SEM [M]	±0.06993	±0.3849	±0.1899	±0.1557
P value	n/a	P>0.05	P>0.05	P>0.05
Cal. Efficacy	100%	138.44%	121.96%	226.62%
SEM	±4.501%	±22.828%	±10.689%	±9.783%
P value	n/a	*	P > 0.05	**
n	5	5	5	5
CHO.CCR5	Control	Gallein 10 mM	Gallein 20 mM	Gallein 30 mM
Log EC ₅₀ [M]	-7.586	-7.662	-7.516	-7.606
SEM [M]	±0.08543	±0.2074	±0.1110	±0.08398
P value	n/a	P>0.05	P>0.05	P>0.05
Cal. Efficacy	100%	126.76%	235.86%	183.67%
SEM	±4.110%	±26.164%	±5.926%	±12.943%
P value	n/a	P > 0.05	**	**
n	4	4	4	4

Table 7.1 Comparison of gallein induced changes to CCL3 concentration response.

7.3 Discussion

Interference of the G $\beta\gamma$ subunit by the small molecule gallein resulted in some unexpected and novel results. Gallein concentration dependent increases in calcium mobilisation were observed following stimulation with CCL3. No increase in basal calcium levels between gallein treated and non-treated cells was observed. These data suggest that the unique properties of gallein potentiate CCR5 mediated calcium mobilisation, although it is not clear how, mechanistically, this is achieved. Increases in calcium mobilisation was not cell line dependent, with studies carried out in CHO.CCR5, HeLa RC-49 and preliminary studies in HEK.CCR5 (data not shown) all following the same trend, thus ruling out differences in relative expression levels of different second messenger isozymes, such as adenylyl cyclase or PLC β accounting for these data. Interestingly, gallein treatment resulted in altered basal levels of cAMP production. Taken together, these data suggest that the binding of gallein to G-protein heterotrimer results in modulation of several second messenger pathways, without activation of the heterotrimer and disruption of the typical signalling mechanisms employed by CCR5 following CCL3 stimulation.

Gallein has also been shown to bind to the G $\beta\gamma$ hot spot (Smrcka *et al.*, 2008) and currently it is unknown what, if any, conformational change the G $\alpha\beta\gamma$ heterotrimer undergoes upon gallein binding. Data gained from these studies indicates that incubation with gallein alone does not result in enhanced calcium mobilisation, but potentiates the effect of CCL3 stimulation through CCR5. It is currently unclear how gallein brings about these effects. One plausible explanation is that gallein binding may modulate the traditional downstream effector targets of the active subunit. Several other compounds and proteins have also been shown to bind to the hot spot and induce atypical G $\beta\gamma$ binding (Seneviratne *et al.*, 2009). In particular, the protein activator of G-protein signalling 8 (AGS8) has been shown

to bind to the G $\beta\gamma$ hot spot, resulting in a conformational change in the G $\alpha\beta\gamma$ heterotrimer. This conformational change does not expose either the hot spot or the G α subunit binding face but results in an atypical G $\beta\gamma$ binding and activation of its downstream effectors. This is done without the dissociation of the G $\alpha\beta\gamma$ heterotrimer and without the activation of any GPCR (Yuan *et al.*, 2007). Mounting evidence suggests that not all subunits dissociate and assuming this is true for G α_{i2} , gallein could potentially block both traditional binding faces of the G α and G $\beta\gamma$ subunits thus preventing typical binding and the activation/inactivation of downstream effectors.

A potential downstream effector that may be affected by modulation of G $\beta\gamma$ binding patterns is PI3K γ . Data from gene knockouts of G $\beta\gamma$ effectors in murine models have indicated that PI3K γ is a common target for G $\beta\gamma$ subunits involved in inflammatory and chemotactic pathways (Li *et al.*, 2000), (Hirsch *et al.*, 2000). Activation of PI3K γ results in the phosphorylation of phosphatidylinositol 4,5 biphosphate (PIP₂) into phosphatidylinositol 3,4,5 biphosphate (PIP₃), which has been shown to increase calcium mobilisation by enhancing PLC γ and potentially PLC β synthesis of inositol 1,4,5-trisphosphate (IP3) (Lian *et al.*, 2005). The convergent point PI3K occupies in the signalling pathway has led to research into developing compounds capable of targeting PI3K γ activity with the hope they may be able to modulate the catalytic activity of PI3K γ , therefore preventing inflammatory events (Camps *et al.*, 2005). The activity of PI3K γ is directly regulated by G $\beta\gamma$ released from G α_i subunits activated by chemokine receptors (Stephens *et al.*, 1997) and the PI3K family, specifically PI3K α and γ , are also known to stimulate the mobilisation of calcium following activation (Hooshmand-Rad *et al.*, 1997), (Quignard *et al.*, 2001). A feasible mechanism for activation of PI3K γ by gallein bound G $\beta\gamma$ is through interaction with N-terminus residues in G $\beta\gamma$ (Yuan *et al.*, 2007).

Gallein treatment of HeLa RC-49 resulted in an increase in the relative rates of cAMP compared to control; however, it did not prevent CCL3 stimulated inactivation of AC. G $\beta\gamma$ has been shown to activate and inactivate specific AC isoforms (Tang *et al.*, 1991). The dramatic rise in cAMP levels observed suggests that gallein interferes with a cellular process that regulates basal levels of cAMP. However, we were unable to identify which G $\beta\gamma$ subtypes were responsible and at what AC subtype they were acting. It is unclear by what mechanism gallein affects a cell's ability to regulate cAMP levels.

However, the most evident participants when investigating enhancement calcium mobilisation through GPCR signalling are PLC β and PKA. Modulation of either of these proteins has been shown to affect calcium release (Harfi *et al.*, 2006). The modulation of PLC β is the most straight forward means of potentiating calcium signalling. Hydrolysis of PIP₂ by PLC results in IP₃ production, IP₃ receptor activation, and the release of calcium from intracellular stores (Ferris *et al.*, 1992). Clearly, enhancement of IP₃ production could enhance calcium mobilisation. Although PLC β isozyme expression can dictate the ability of G $\beta\gamma$ to mediate phosphoinositide and calcium signalling, results garnered from these experiments show gallein acts in a non cell type specific manner. This suggests that gallein interferes with general mechanisms that mediate second messenger synthesis.

PLC β has been shown to have distinct binding sites for G $\beta\gamma$ and G α_q (Smrcka *et al.*, 1993) and the dual occupation of these sites has been shown to be synergistic for its stimulation (Zhu *et al.*, 1996). Currently there is a lack of evidence to suggest G α_i family subunits have a synergistic effect through the same mechanism. However, there is evidence that G α_i subunit activation may enhance calcium mobilisation in the presence of G α_q activation (Chan *et al.*, 2000). CCR5 has been shown to associate with G α_q in previous studies (Mueller *et al.*, 2004a). A conformational change in G $\alpha\beta\gamma$ by gallein that results in the G $\beta\gamma$ binding site on PLC β becoming occupied may act to prime the enzyme ready for activation.

The rise in the basal cAMP levels may also play a part in enhancing calcium mobilisation through PLC β . Typically a rise in cAMP levels results in the activation of PKA, resulting in the phosphorylation and inactivation of PLC β (Yue *et al.*, 1998). However, active G $\beta\gamma$ subunits, specifically from G α_i , have been shown to inhibit phosphorylation of PLC β by PKA and even enhance calcium mobilisation from intracellular stores following activation of G $\alpha_{i/s}$ subunits (Litosch, 1997; Yue *et al.*, 2000). Generally PKA activation is viewed as inhibitory to PLC β , but there are examples where the opposite is true (Pittner *et al.*, 1989).

In addition to enhancing calcium mobilisation via stimulation of PLC it is possible that the same effects could be achieved through an increase in the PIP2 cytosolic pool. It is conceivable that in some circumstances the supply of PIP2 could limit PLC β activity. An enhanced pool of PIP2 could result in a quicker and larger production of IP3, resulting in a higher proportion of IP3 receptor activation and larger flux of calcium. Activation of src and Rho proteins have been shown to increase PIP2 production (Chong *et al.*, 1994; Stephens *et al.*, 1993). Src has also been shown to be stimulated by activation of the G α_i heterotrimer

(Arefieva *et al.*, 2005) and Rho is well characterised as being activated by CCR5 (Mueller *et al.*, 2004b). Although, from what is currently known about gallein binding to the $G\alpha\beta\gamma$ heterotrimer, this explanation is less likely than others. It is more likely is that enhanced calcium mobilisation is the result of potentiation of the IP3 receptor (DeSouza *et al.*, 2002); this is a possible mechanism by which calcium flux may be enhanced without an increase in the cytosolic PIP2 pool and subsequent production of IP3. cAMP stimulated PKA activation has been shown to sensitise the IP3 receptor through phosphorylation (Wojcikiewicz *et al.*, 1998). The potentiation of the IP3 receptor by this mechanism would increase calcium mobilisation without the requirement for additional PLC β activation.

Consideration must also be given to the long contested idea that a cell has a fixed amount of calcium stored in its intracellular stores (Blaustein *et al.*, 2001). The size of the calcium stores may well vary under certain circumstances (Short *et al.*, 2000). As gallein is currently poorly characterised, it is a possibility that enhancement of calcium release may be due to increases in specific intracellular calcium stores arbitrated by gallein. In conclusion, there are a myriad of potential ways gallein brings about these effects, so it is likely, due to the substantial increases in calcium mobilisation observed, that gallein interferes with more than one signalling mechanism (Figure 7.6).

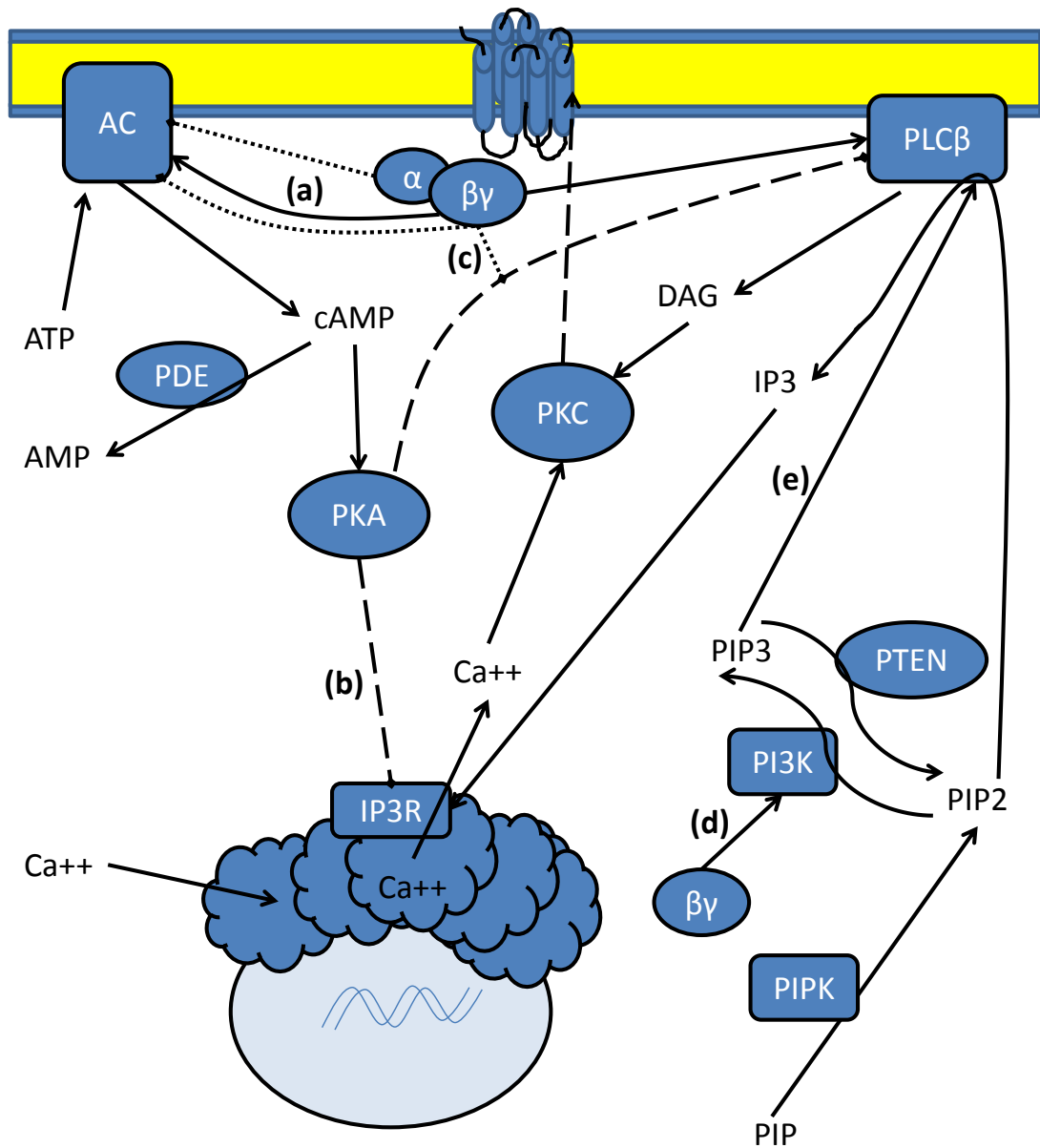


Figure 7.6 Schematic of interactions leading to calcium mobilisation and potential sites that gallein may interfere with. (a) Gallein may cause Gβγ activation of adenylyl cyclase results in enhanced cAMP accumulation. (b) PKA activation by raised cAMP levels could result in IP3R phosphorylation and potentiation. (c) Gβγ may prevent phosphorylation of PLCβ, resulting in longer activation of it. (d) Gβγ activation of PI3K. (e) PIP3 synthesis enhances PLCβ and potentially enhances PLCγ catalysis.

Chapter Eight

Summary

8.1 Exploring G-protein Interactions with Resonance Energy Transfer

Many research groups are interested in understanding the mechanisms of GPCR signalling, due to the multitude of physiological changes they are capable of bringing about. Recently there has been an influx of new, and sometimes controversial, knowledge regarding the signalling mechanisms that GPCR use to bring about the astonishing array of responses they are responsible for. As understanding of GPCR signalling pathways used to bring about cellular responses has increased, it has become clear, beyond doubt, that far from being the linear signal transduction routes they were once thought to be, GPCR signalling pathways are carefully orchestrated multi-protein events that rely on interactions with more than one family of G-proteins for correct transmission of signalling (Simmons, 2005). It has been known for some time that different cellular signalling pathways can interact, often providing specificity to GPCR responses and adding an additional layer of complexity to the process of signalling (Marinissen *et al.*, 2001). Modulations to GPCR signalling pathways are not well understood and clarification of stand-alone GPCR signalling pathways and exploration of the effects of cross talk between signalling pathways could yield new targets for treatment of physiological conditions ranging from HIV infection to blindness.

Isolation of CCR5 in a living system was achieved by use of stably transfected CHO K1, HEK293 and HeLa cell lines. All these cell lines are easy to transfect, resilient to the stresses of cell culture, and do not express endogenous CCR5 or any other chemokine receptor, as judged by an absence of response to chemokine treatment, thus providing an ideal model for studying CCR5 G-protein interactions. A novel assay system was created in HEK.CCR5 and CHO.CCR5 cell lines where G-protein subunits, tagged in such a way to permit fluorescence resonance energy transfer between the fluorescent protein tags were stably expressed. This system was used to recapitulate already identified G-protein heterotrimers that associate with and are activated by CCR5, namely the $G\alpha_{i2}\beta_1\gamma$ heterotrimer (Zhao *et al.*, 1998). Although this assay system was demonstrated to be reasonably successful, its further development was hampered by difficulties culturing triple transfected cell lines, ensuring adequate transgene expression and technical limitations with the equipment used. Problems were also encountered with the levels of cellular autofluorescence, probably due to increased levels of cellular stress resulting in the accumulation of fluorescent compound such as lipofuscin, NADPH, and FAD, which further hindered the exploitation of this innovative assay technology. For the time being, the measurement of protein-protein interactions will remain the preserve of live confocal microscopy imaging, but with current and future developments into plate reader technology equipment, limitations could soon be overcome. Promising recent studies have shown a confocal multiwell plate reader that allows high throughput screening of live cells (Talbot *et al.*, 2008). For the comprehensive development of this assay system, the creation of stable cell lines would also need to be refined. There has been an increase in demand for polycistronic expression vectors in recent years; as such, it is an exciting area of development with the potential to provide a method to overcome issues with the creation of stable cell lines. Recent advances have included the development of a multi-cDNA expression construct capable of robustly and stoichiometrically expressing cDNAs from a single plasmid (Nishiumi

et al., 2009). This, coupled with a lentiviral transfection method and fluorescence activated cell sorting approach to creating stable cell lines, could streamline the production of cells suitable for a high throughput assay FRET assay to measure G-protein interactions in real time.

A complementary approach to measuring protein-protein interactions by resonance energy transfer was attempted as a way to overcome issues encountered with the FRET assay. The use of a bioluminescent protein as the donor fluorophore in BRET allows for the removal of incidental autofluorescence caused by excitation of the donor fluorophore by an external light source. An increasing number of studies are using BRET as the choice method for studying protein-protein interactions in real time (Kocan *et al.*, 2009; Navarro *et al.*, 2009; Pflieger, 2009). BRET is still a rapidly evolving technology that over the last decade has been improved upon immensely from its first incarnation and is now a much more sensitive system capable of measuring previously undetectable signals (Kamal *et al.*, 2009). The system employed during this study was an early adaptation of the original BRET assays first carried out in mammalian cells by Angers *et al.* (Angers *et al.*, 2000). Unfortunately interactions between tagged $G\alpha_{i2}$ and $G\beta_1$ were unable to be characterised in this study using this BRET system. But with the creation of brighter isoforms of renilla luciferase and enhanced fluorescent proteins to act as acceptor molecules I believe a BRET based assay to measure the interactions of individual G-proteins within the heterotrimer will yield a trove of new interactome data. There are comparatively few publications where BRET has been used to explore the interaction of 'free' G-protein subunits with one another – often the $G\alpha$ subunit is immobilised by linkage to a receptor of interest (Hollins *et al.*, 2009). However, a recent publication demonstrates that these interactions can be measured in non immobilised G-protein subunits using YFP Venus tagged to the $G\gamma$ subunit (Ayoub *et al.*,

2009). The present study demonstrates that a high throughput screen for G-protein subunits using resonance energy transfer as a direct method to measure protein-protein interactions is a reality and could plausibly be a routine lab technique in the near future.

8.2 Interference of CCR5 G-protein signalling

The transient transfection of dominant negative and constitutively active $G\alpha_{i2}$ into cells expressing CCR5 showed that there is not a requirement for functional $G\alpha_{i2}$ for CCR5 mediated calcium release. Neither constitutively active nor dominant negative $G\alpha_{i2}$ resulted in the abrogation of calcium release following stimulation, strongly suggesting that CCR5 is functionally coupled to other members of the $G\alpha_i$ heterotrimer family or the $G\alpha_q$ heterotrimer family, both of which are capable of effecting the release of calcium upon activation (Berridge, 1987; Ghahremani *et al.*, 1999). The expression of the two opposing forms of $G\alpha_{i2}$ did result in a small increase in calcium mobilisation following stimulation. The mechanisms by which this increase occurred are currently unclear; however, it may suggest $G\alpha_{i2}\beta\gamma$ is not involved in calcium mobilisation following activation. Constitutively active $G\alpha_{12}$ was also transiently transfected and was found to have no effect on the release of calcium following stimulation, this is in keeping with current literature which does not describe any direct association of $G\alpha_{12}$ with CCR5, but is shown to be involved in cytoskeleton remodelling (Suzuki *et al.*, 2003).

Investigating CCR5 signalling using a dominant negative and constitutively active protein approach has certain limitations. The overexpression of a protein of interest may lead to effects on other cellular functions which may affect cellular behaviour (Lefrancois *et al.*, 2005). The effectiveness of these particular DNM and CAM proteins have not been extensively characterised and are regarded as having weak effects on normal function

(Barren *et al.*, 2007). In order to overcome any deficiencies associated with a dominant negative approach and determine if $G\alpha_{i2}$ heterotrimers play a role in calcium mobilisation, siRNA was used to reduce expression of $G\alpha_{i2}$ and several other $G\alpha$ subunits. Knockdown of $G\alpha_{i2}$ did not result in any change in calcium mobilisation following stimulation, supporting results seen with DNM work.

Published knockdown experiments on $G\alpha_i$ subunits show the bradykinin 2 receptor, another class A GPCR that is responsible for calcium mediated signalling (Hess *et al.*, 1992), relies on activation of both the $G\alpha_i$ family and the $G\alpha_q$ subunits to ensure normal signalling (Yang *et al.*, 1999). Similarly, knockdown of single $G\alpha$ subunits in HeLa RC-49 resulted in little change to normal calcium mobilisation. This was possibly due to recently defined compensatory measures characterised in HeLa cells in response to knockdown of G-protein subunits (Krumins *et al.*, 2006). However, upon knockdown of $G\alpha_q$ and a member of the $G\alpha_i$ family a significant decrease in calcium mobilisation at higher levels of stimulation was recorded. The preliminary data gathered in this investigation strongly support the notion that CCR5, like other GPCR, maintains its normal signalling pathways through concomitant activation of several combinations of G-protein heterotrimer. It is not clear from these experiments if the activation of $G\alpha_q$ is from direct association with CCR5 or if there is a crosstalk mechanism in place. An important step in confirming these results would be the characterisation of several second messenger pathways and the monitoring of any compensatory mechanisms cell lines may induce upon knockdown.

8.3 Small Molecule Disruption of G-Protein Interactions

Calcium mobilisation resulting from the activation of $G\alpha_i$ heterotrimers is predominantly due to the actions of the $G\beta\gamma$ subunit. Due to the ubiquitous nature of the $G\beta$ family, high sequence homology between subtypes, and a lack of compounds that suitably target $G\beta\gamma$ interactions, delineating $G\beta\gamma$ subunits interactions in a live cell system has not, until recently, been straightforward. A recent study identified gallein as a small molecule disruptor of $G\beta\gamma$ subunit signalling that inhibits chemotaxis in neutrophils (Lehmann *et al.*, 2008). Gallein is not completely characterised and this study, while not supporting currently published data regarding its effect on chemotaxis, does highlight the central role the $G\beta\gamma$ subunit plays in chemokine signal transduction (Dupre *et al.*, 2009).

Treatment of cells with gallein resulted in massively enhanced calcium mobilisation at high chemokine concentrations and a reduction in cAMP accumulation. These results alone suggest that gallein binding may actually be blocking heterotrimer interactions with adenylyl cyclase while enhancing or potentiating interactions with enzymes responsible for calcium mobilisation. It is currently unclear by which mechanism these effects are mediated. The $G\beta\gamma$ subunit, specifically $G\beta\gamma$ subunits in a $G\alpha_i$ heterotrimer, have been shown to target PI-3K (Hirsch *et al.*, 2000); further studies monitoring the effect gallein has on PIP3 levels may provide a more complete picture of its modulatory effects.

Biochemical studies have shown gallein binds to a region of the $G\beta\gamma$ subunit called the hotspot, this region is responsible for interactions with downstream effectors (Bonacci *et al.*, 2006). Small molecule binding to this region may have an effect comparable to AGS proteins, which bind to the intact heterotrimer conferring a conformational change to it

and creating a new active face on the G β γ subunit (Yuan *et al.*, 2007). This work supports the notion that small molecule disruptors alter the signalling properties of chemokine receptors and could potentially be used to target interactions downstream of the active heterotrimer.

8.4 Crosstalk in CCR5 Signalling Pathways

From this study it is clear that the signalling mechanisms CCR5 uses are resilient to change and rely upon a plethora of known protein-protein interactions and potentially other, as yet, unidentified protein-protein interactions. The original scope of this research was to disseminate the heterotrimers that are activated following stimulation of CCR5, with a view to tracing those interactions to disease states. Investigations have expanded from this original scope to include the effects CCR5 stimulation has upon second messenger system, especially calcium release, which is an incredibly important effector of cellular function and response.

In this study calcium release was measured and used as an indirect method to determine CCR5 activation of G α_i heterotrimers. However, it became clear that G α_q also plays a role in CCR5 mediated calcium release. The mechanisms by which this occur are not easily apparent, but are confirmed by combinational knockdown of subunits with siRNA. Currently there is little understanding regarding GPCR cross talk and no clear way to predict what modulations crosstalk brings about when it is in action. Nevertheless, there is a growing body of work that supports the notion of crosstalk as well as highlighting the potential physiological and pathological implications. It is well established that homodimerisation occurs between CCR5 and CCR2 and signals through the G α_q family

heterotrimers (Mellado *et al.*, 2001). Results garnered in this study relied upon presumed monomeric CCR5 and also noted a role for $G\alpha_q$ signalling. Taken together, this information suggests that a cell's individual GPCR expression profile may be one of the main causatives of signal pathway crosstalk. Thus, conferring specific functional selectivity, based on the location of expression. This notion is supported by previous research (Zlotnik *et al.*, 2000). Data gathered from this investigation forms the bedrock for exploring cooperative effects between chemokine receptors upon additional receptor activation.

It is clear that GPCR signalling is far more complex than the classical GPCR signalling model of "one ligand, one receptor, one G-protein per activation event". Understanding the interactions between canonical CCR5 signalling pathways and pathways that are intertwined through crosstalk mechanisms will contribute to the knowledge of therapeutic action, and potentially allow for better targeting of therapeutics by identifying common signalling bottle necks in signalling pathways.

8.5 Conclusions

The protein-protein interactions involved in the signalling pathways of GPCRs, although well studied, are only just beginning to be unravelled. The research contained in this thesis supports and confirms some established tenets about GPCR, such as activation of the $G\alpha_{i2}\beta_1\gamma$ heterotrimer by CCR5. But also exposes several avenues of investigation that could result in a greater understanding of interactions between GPCR and other GPCR as well as exploring the interactions GPCR have with heterotrimeric G-proteins.

The FRET based assay system developed and used to determine the activation of the $G\alpha_{i2}\beta_1\gamma$ heterotrimer is, to my knowledge, a novel technology which has been built upon the more cumbersome traditional FRET methods. Although the assay encountered problems that, unfortunately, didn't allow it to reach its full potential, it has contributed to the understanding of this experimental technology. Recent advances in stable cell line development and fluorometer technology mean that the development of a high throughput FRET assay to measure protein-protein interactions in real time is considerably more feasible than it was even four years ago.

Other research undertaken during the completion of this thesis has shown that the endogenous systems that control CCR5 signalling are very resilient to disruption of $G\alpha$ subunits by DNM, CAM, and siRNA disruption. Further research is needed to characterise cellular interactions that occur following this disruption. The difficulties associated with this approach further support the development of a direct assay system to measure protein-protein interactions.

Currently there is a surge of interest in understanding the role that the $G\beta\gamma$ subunit plays in GPCR signalling. The data gathered in this research, suggest that the $G\beta\gamma$ subunit is far more complex than anticipated and considerable work must be undertaken to decipher its role in CCR5 and other GPCR signalling pathways. It is clear from results in this research that disruption of its normal interactions results in modulation of GPCR effects. Further work should focus on the potential therapeutic benefits associated with selective $G\beta$ subunit targeting.

References

AbdAlla, S, Lothar, H, Quitterer, U (2000) AT1-receptor heterodimers show enhanced G-protein activation and altered receptor sequestration. *Nature* **407**(6800): 94-98.

Ahuja, SK, Lee, JC, Murphy, PM (1996) CXC chemokines bind to unique sets of selectivity determinants that can function independently and are broadly distributed on multiple domains of human interleukin-8 receptor B. Determinants of high affinity binding and receptor activation are distinct. *J Biol Chem* **271**(1): 225-232.

Andressen, KW, Norum, JH, Levy, FO, Krobert, KA (2006) Activation of adenylyl cyclase by endogenous G(s)-coupled receptors in human embryonic kidney 293 cells is attenuated by 5-HT(7) receptor expression. *Mol Pharmacol* **69**(1): 207-215.

Angers, S, Salahpour, A, Joly, E, Hilairet, S, Chelsky, D, Dennis, M, Bouvier, M (2000) Detection of beta 2-adrenergic receptor dimerization in living cells using bioluminescence resonance energy transfer (BRET). *Proc Natl Acad Sci U S A* **97**(7): 3684-3689.

Arefieva, TI, Kukhtina, NB, Antonova, OA, Krasnikova, TL (2005) MCP-1-stimulated chemotaxis of monocytic and endothelial cells is dependent on activation of different signaling cascades. *Cytokine* **31**(6): 439-446.

ATCC (2007) Technical Bulletin 7: Passage Number Effect in Cell Lines.

Ayoub, MA, Damian, M, Gespach, C, Ferrandis, E, Lavergne, O, De Wever, O, Baneres, JL, Pin, JP, Prevost, GP (2009) Inhibition of heterotrimeric G protein signaling by a small molecule acting on Galpha subunit. *J Biol Chem* **284**(42): 29136-29145.

Azpiazu, I, Gautam, N (2004) A fluorescence resonance energy transfer-based sensor indicates that receptor access to a G protein is unrestricted in a living mammalian cell. *J Biol Chem* **279**(26): 27709-27718.

Bader, N, Grune, T (2006) Protein oxidation and proteolysis. *Biol Chem* **387**(10-11): 1351-1355.

Baggiolini, M, Dewald, B, Moser, B (1997) Human chemokines: an update. *Annu Rev Immunol* **15**: 675-705.

Bajetto, A, Bonavia, R, Barbero, S, Schettini, G (2002) Characterization of chemokines and their receptors in the central nervous system: physiopathological implications. *J Neurochem* **82**(6): 1311-1329.

Barki-Harrington, L, Bookout, AL, Wang, G, Lamb, ME, Leeb-Lundberg, LM, Daaka, Y (2003) Requirement for direct cross-talk between B1 and B2 kinin receptors for the proliferation of androgen-insensitive prostate cancer PC3 cells. *Biochem J* **371**(Pt 2): 581-587.

- Barren, B, Artemyev, NO (2007) Mechanisms of dominant negative G-protein alpha subunits. *J Neurosci Res* **85**(16): 3505-3514.
- Bennett, TA, Maestas, DC, Prossnitz, ER (2000) Arrestin binding to the G protein-coupled N-formyl peptide receptor is regulated by the conserved "DRY" sequence. *J Biol Chem* **275**(32): 24590-24594.
- Benson, RC, Meyer, RA, Zaruba, ME, McKhann, GM (1979) Cellular autofluorescence--is it due to flavins? *J Histochem Cytochem* **27**(1): 44-48.
- Beqollari, D, Betzenhauser, MJ, Kammermeier, PJ (2009) Altered G-protein coupling in an mGluR6 point mutant associated with congenital stationary night blindness. *Mol Pharmacol* **76**(5): 992-997.
- Berridge, MJ (1995) Capacitative calcium entry. *Biochem J* **312** (Pt 1): 1-11.
- Berridge, MJ (1987) Inositol lipids and cell proliferation. *Biochim Biophys Acta* **907**(1): 33-45.
- Berridge, MJ, Lipp, P, Bootman, MD (2000) The versatility and universality of calcium signalling. *Nat Rev Mol Cell Biol* **1**(1): 11-21.
- Bertrand, L, Parent, S, Caron, M, Legault, M, Joly, E, Angers, S, Bouvier, M, Brown, M, Houle, B, Menard, L (2002) The BRET2/arrestin assay in stable recombinant cells: a platform to screen for compounds that interact with G protein-coupled receptors (GPCRS). *J Recept Signal Transduct Res* **22**(1-4): 533-541.
- Bettler, E, Krause, R, Horn, F, Vriend, G (2003) NRSAS: Nuclear Receptor Structure Analysis Servers. *Nucleic Acids Res* **31**(13): 3400-3403.
- Bhattacharya, S, Hall, SE, Li, H, Vaidehi, N (2008) Ligand-stabilized conformational states of human beta(2) adrenergic receptor: insight into G-protein-coupled receptor activation. *Biophys J* **94**(6): 2027-2042.
- Bird, AP, Wolffe, AP (1999) Methylation-induced repression--belts, braces, and chromatin. *Cell* **99**(5): 451-454.
- Blanpain, C, Lee, B, Vakili, J, Doranz, BJ, Govaerts, C, Migeotte, I, Sharron, M, Dupriez, V, Vassart, G, Doms, RW, Parmentier, M (1999) Extracellular cysteines of CCR5 are required for chemokine binding, but dispensable for HIV-1 coreceptor activity. *J Biol Chem* **274**(27): 18902-18908.
- Blanpain, C, Wittamer, V, Vanderwinden, JM, Boom, A, Renneboog, B, Lee, B, Le Poul, E, El Asmar, L, Govaerts, C, Vassart, G, Doms, RW, Parmentier, M (2001) Palmitoylation of CCR5 is critical for receptor trafficking and efficient activation of intracellular signaling pathways. *J Biol Chem* **276**(26): 23795-23804.
- Blaustein, MP, Golovina, VA (2001) Structural complexity and functional diversity of endoplasmic reticulum Ca(2+) stores. *Trends Neurosci* **24**(10): 602-608.

- Bonacci, TM, Mathews, JL, Yuan, C, Lehmann, DM, Malik, S, Wu, D, Font, JL, Bidlack, JM, Smrcka, AV (2006) Differential targeting of Gbetagamma-subunit signaling with small molecules. *Science* **312**(5772): 443-446.
- Bouabe, H, Fassler, R, Heesemann, J (2008) Improvement of reporter activity by IRES-mediated polycistronic reporter system. *Nucleic Acids Res* **36**(5): e28.
- Bugrim, AE (1999) Regulation of Ca²⁺ release by cAMP-dependent protein kinase. A mechanism for agonist-specific calcium signaling? *Cell Calcium* **25**(3): 219-226.
- Buhl, AM, Johnson, NL, Dhanasekaran, N, Johnson, GL (1995) G alpha 12 and G alpha 13 stimulate Rho-dependent stress fiber formation and focal adhesion assembly. *J Biol Chem* **270**(42): 24631-24634.
- Bunemann, M, Frank, M, Lohse, MJ (2003) Gi protein activation in intact cells involves subunit rearrangement rather than dissociation. *Proc Natl Acad Sci U S A* **100**(26): 16077-16082.
- Burzyn, D, Jancic, CC, Zittermann, S, Keller Sarmiento, MI, Fainboim, L, Rosenstein, RE, Chuluyan, HE (2002) Decrease in cAMP levels modulates adhesion to fibronectin and immunostimulatory ability of human dendritic cells. *J Leukoc Biol* **72**(1): 93-100.
- Camps, M, Ruckle, T, Ji, H, Ardisson, V, Rintelen, F, Shaw, J, Ferrandi, C, Chabert, C, Gillieron, C, Francon, B, Martin, T, Gretener, D, Perrin, D, Leroy, D, Vitte, PA, Hirsch, E, Wymann, MP, Cirillo, R, Schwarz, MK, Rommel, C (2005) Blockade of PI3Kgamma suppresses joint inflammation and damage in mouse models of rheumatoid arthritis. *Nat Med* **11**(9): 936-943.
- Candido, EP, Reeves, R, Davie, JR (1978) Sodium butyrate inhibits histone deacetylation in cultured cells. *Cell* **14**(1): 105-113.
- Chalfie, M, Tu, Y, Euskirchen, G, Ward, WW, Prasher, DC (1994) Green fluorescent protein as a marker for gene expression. *Science* **263**(5148): 802-805.
- Chan, JS, Lee, JW, Ho, MK, Wong, YH (2000) Preactivation permits subsequent stimulation of phospholipase C by G(i)-coupled receptors. *Mol Pharmacol* **57**(4): 700-708.
- Cherezov, V, Rosenbaum, DM, Hanson, MA, Rasmussen, SG, Thian, FS, Kobilka, TS, Choi, HJ, Kuhn, P, Weis, WI, Kobilka, BK, Stevens, RC (2007) High-resolution crystal structure of an engineered human beta2-adrenergic G protein-coupled receptor. *Science* **318**(5854): 1258-1265.
- Chernova, I, Lai, JP, Li, H, Schwartz, L, Tuluc, F, Korchak, HM, Douglas, SD, Kilpatrick, LE (2009) Substance P (SP) enhances CCL5-induced chemotaxis and intracellular signaling in human monocytes, which express the truncated neurokinin-1 receptor (NK1R). *J Leukoc Biol* **85**(1): 154-164.
- Chong, LD, Traynor-Kaplan, A, Bokoch, GM, Schwartz, MA (1994) The small GTP-binding protein Rho regulates a phosphatidylinositol 4-phosphate 5-kinase in mammalian cells. *Cell* **79**(3): 507-513.

- Clapham, DE (1996) Intracellular signalling: more jobs for G beta gamma. *Curr Biol* **6**(7): 814-816.
- Clapham, DE, Neer, EJ (1997) G protein beta gamma subunits. *Annu Rev Pharmacol Toxicol* **37**: 167-203.
- Coleman, DE, Berghuis, AM, Lee, E, Linder, ME, Gilman, AG, Sprang, SR (1994) Structures of active conformations of Gi alpha 1 and the mechanism of GTP hydrolysis. *Science* **265**(5177): 1405-1412.
- Conti, M, Richter, W, Mehats, C, Livera, G, Park, JY, Jin, C (2003) Cyclic AMP-specific PDE4 phosphodiesterases as critical components of cyclic AMP signaling. *J Biol Chem* **278**(8): 5493-5496.
- Cotecchia, S, Bjorklof, K, Rossier, O, Stanasila, L, Greasley, P, Fanelli, F (2002) The alpha1b-adrenergic receptor subtype: molecular properties and physiological implications. *J Recept Signal Transduct Res* **22**(1-4): 1-16.
- Dascal, N (2001) Ion-channel regulation by G proteins. *Trends Endocrinol Metab* **12**(9): 391-398.
- Davis, TL, Bonacci, TM, Sprang, SR, Smrcka, AV (2005) Structural and molecular characterization of a preferred protein interaction surface on G protein beta gamma subunits. *Biochemistry* **44**(31): 10593-10604.
- De Ruyck, J, Famerée, M, Wouters, J, Perpète, EA, Preat, J, Jacquemin, D (2007) Towards the understanding of the absorption spectra of NAD(P)H/NAD(P)+ as a common indicator of dehydrogenase enzymatic activity. *Chemical Physics Letters* **450**(1-3): 119-122.
- Dehmel, S, Wang, S, Schmidt, C, Kiss, E, Loewe, RP, Chilla, S, Schlondorff, D, Grone, HJ, Luckow, B (2009) Chemokine receptor Ccr5 deficiency induces alternative macrophage activation and improves long-term renal allograft outcome. *Eur J Immunol* **40**(1): 267-278.
- DeSouza, N, Reiken, S, Ondrias, K, Yang, YM, Matkovich, S, Marks, AR (2002) Protein kinase A and two phosphatases are components of the inositol 1,4,5-trisphosphate receptor macromolecular signaling complex. *J Biol Chem* **277**(42): 39397-39400.
- Di Marzio, P, Dai, WW, Franchin, G, Chan, AY, Symons, M, Sherry, B (2005) Role of Rho family GTPases in CCR1- and CCR5-induced actin reorganization in macrophages. *Biochem Biophys Res Commun* **331**(4): 909-916.
- Digby, GJ, Lober, RM, Sethi, PR, Lambert, NA (2006) Some G protein heterotrimers physically dissociate in living cells. *Proc Natl Acad Sci U S A* **103**(47): 17789-17794.
- Dorn, GW, 2nd, Oswald, KJ, McCluskey, TS, Kuhel, DG, Liggett, SB (1997) Alpha 2A-adrenergic receptor stimulated calcium release is transduced by Gi-associated G(beta gamma)-mediated activation of phospholipase C. *Biochemistry* **36**(21): 6415-6423.
- dos Remedios, CG, Moens, PD (1995) Fluorescence resonance energy transfer spectroscopy is a reliable "ruler" for measuring structural changes in proteins. Dispelling the problem of the unknown orientation factor. *J Struct Biol* **115**(2): 175-185.

- Dupre, DJ, Robitaille, M, Rebois, RV, Hebert, TE (2009) The role of Gbetagamma subunits in the organization, assembly, and function of GPCR signaling complexes. *Annu Rev Pharmacol Toxicol* **49**: 31-56.
- Farr, A, Roman, A (1992) A pitfall of using a second plasmid to determine transfection efficiency. *Nucleic Acids Res* **20**(4): 920.
- Farrens, DL, Altenbach, C, Yang, K, Hubbell, WL, Khorana, HG (1996) Requirement of rigid-body motion of transmembrane helices for light activation of rhodopsin. *Science* **274**(5288): 768-770.
- Farzan, M, Mirzabekov, T, Kolchinsky, P, Wyatt, R, Cayabyab, M, Gerard, NP, Gerard, C, Sodroski, J, Choe, H (1999) Tyrosine sulfation of the amino terminus of CCR5 facilitates HIV-1 entry. *Cell* **96**(5): 667-676.
- Ferris, CD, Snyder, SH (1992) IP3 receptors. Ligand-activated calcium channels in multiple forms. *Adv Second Messenger Phosphoprotein Res* **26**: 95-107.
- Fields, S, Song, O (1989) A novel genetic system to detect protein-protein interactions. *Nature* **340**(6230): 245-246.
- Fletcher, JE, Lindorfer, MA, DeFilippo, JM, Yasuda, H, Guilford, M, Garrison, JC (1998) The G protein beta5 subunit interacts selectively with the Gq alpha subunit. *J Biol Chem* **273**(1): 636-644.
- Forster, T (1949) Experimentelle und theoretische Untersuchung des zwischengmolekularen Ubergangs von Elektronenann. *Naturforschung* **4A**: 321-327.
- Foskett, JK, White, C, Cheung, KH, Mak, DO (2007) Inositol trisphosphate receptor Ca²⁺ release channels. *Physiol Rev* **87**(2): 593-658.
- Frank, M, Thumer, L, Lohse, MJ, Bunemann, M (2005) G Protein activation without subunit dissociation depends on a G{alpha}{i}-specific region. *J Biol Chem* **280**(26): 24584-24590.
- Friguet, B (2006) Oxidized protein degradation and repair in ageing and oxidative stress. *FEBS Letters* **580**(12): 2910-2916.
- Galarneau, A, Primeau, M, Trudeau, LE, Michnick, SW (2002) Beta-lactamase protein fragment complementation assays as in vivo and in vitro sensors of protein protein interactions. *Nat Biotechnol* **20**(6): 619-622.
- Gales, C, Rebois, RV, Hogue, M, Trieu, P, Breit, A, Hebert, TE, Bouvier, M (2005) Real-time monitoring of receptor and G-protein interactions in living cells. *Nat Methods* **2**(3): 177-184.
- Gales, C, Van Durm, JJ, Schaak, S, Pontier, S, Percherancier, Y, Audet, M, Paris, H, Bouvier, M (2006) Probing the activation-promoted structural rearrangements in preassembled receptor-G protein complexes. *Nat Struct Mol Biol* **13**(9): 778-786.

Galli, T, Haucke, V (2001) Cycling of synaptic vesicles: how far? How fast! *Sci STKE* **2001**(88): re1.

Ganesan, S, Ameer-Beg, SM, Ng, TT, Vojnovic, B, Wouters, FS (2006) A dark yellow fluorescent protein (YFP)-based Resonance Energy-Accepting Chromoprotein (REACH) for Forster resonance energy transfer with GFP. *Proc Natl Acad Sci U S A* **103**(11): 4089-4094.

Ganju, RK, Brubaker, SA, Meyer, J, Dutt, P, Yang, Y, Qin, S, Newman, W, Groopman, JE (1998) The alpha-chemokine, stromal cell-derived factor-1alpha, binds to the transmembrane G-protein-coupled CXCR-4 receptor and activates multiple signal transduction pathways. *J Biol Chem* **273**(36): 23169-23175.

Geisse, S, Gram, H, Kleuser, B, Kocher, HP (1996) Eukaryotic expression systems: a comparison. *Protein Expr Purif* **8**(3): 271-282.

Ghahremani, MH, Cheng, P, Lembo, PM, Albert, PR (1999) Distinct roles for Galphai2, Galphai3, and Gbeta gamma in modulation of forskolin- or Gs-mediated cAMP accumulation and calcium mobilization by dopamine D2S receptors. *J Biol Chem* **274**(14): 9238-9245.

Gouldson, PR, Snell, CR, Bywater, RP, Higgs, C, Reynolds, CA (1998) Domain swapping in G-protein coupled receptor dimers. *Protein Eng* **11**(12): 1181-1193.

Griesbeck, O, Baird, GS, Campbell, RE, Zacharias, DA, Tsien, RY (2001) Reducing the environmental sensitivity of yellow fluorescent protein. Mechanism and applications. *J Biol Chem* **276**(31): 29188-29194.

Gryczynski (2005) *Molecular Imaging FRET Microscopy and Spectroscopy*. Oxford University Press.

Guo, Y, Philip, F, Scarlata, S (2003) The Pleckstrin homology domains of phospholipases C-beta and -delta confer activation through a common site. *J Biol Chem* **278**(32): 29995-30004.

Gurevich, VV, Gurevich, EV (2008) How and why do GPCRs dimerize? *Trends Pharmacol Sci* **29**(5): 234-240.

Habasque, C, Aubry, F, Jegou, B, Samson, M (2002) Study of the HIV-1 receptors CD4, CXCR4, CCR5 and CCR3 in the human and rat testis. *Mol Hum Reprod* **8**(5): 419-425.

Harfi, I, Sariban, E (2006) Mechanisms and modulation of pituitary adenylate cyclase-activating protein-induced calcium mobilization in human neutrophils. *Ann N Y Acad Sci* **1070**: 322-329.

Harmar AJ, Hills RA, Rosser EM, Jones M, Buneman OP, Dunbar DR, Greenhill SD, Hale VA, Sharman JL, Bonner TI, Catterall WA, Davenport AP, Delagrèe P, Dollery CT, Foord SM, Gutman GA, Laudet V, Neubig RR, Ohlstein EH, Olsen RW, Peters J, Pin JP, Ruffolo RR, Searls DB, Wright MW and Spedding M. (2009) IUPHAR-DB: the IUPHAR database of G protein-coupled receptors and ion channels. *Nucl. Acids Res.* **37** (Database issue): D680-D685

Hayata, I (2002) Low frequency of spontaneous rearrangements during plasmid incorporation in CHO-K1 mutant cells defective in DNA repair. *Nukleonika* **47**(1): 7-11.

He, C, Yan, X, Zhang, H, Mirshahi, T, Jin, T, Huang, A, Logothetis, DE (2002) Identification of critical residues controlling G protein-gated inwardly rectifying K(+) channel activity through interactions with the beta gamma subunits of G proteins. *J Biol Chem* **277**(8): 6088-6096.

Hecht, I, Cahalon, L, Hershkovich, R, Lahat, A, Franitza, S, Lider, O (2003) Heterologous desensitization of T cell functions by CCR5 and CXCR4 ligands: inhibition of cellular signaling, adhesion and chemotaxis. *Int Immunol* **15**(1): 29-38.

Heim, R, Tsien, RY (1996) Engineering green fluorescent protein for improved brightness, longer wavelengths and fluorescence resonance energy transfer. *Curr Biol* **6**(2): 178-182.

Hein, P, Frank, M, Hoffmann, C, Lohse, MJ, Bunemann, M (2005) Dynamics of receptor/G protein coupling in living cells. *EMBO J* **24**(23): 4106-4114.

Henry, B (2004) GPCR allosterism and accessory proteins: new insights into drug discovery, 17 July 2004, Glasgow, Scotland. *IDrugs* **7**(9): 819-821.

Herlitze, S, Garcia, DE, Mackie, K, Hille, B, Scheuer, T, Catterall, WA (1996) Modulation of Ca²⁺ channels by G-protein beta gamma subunits. *Nature* **380**(6571): 258-262.

Hermouet, S, Merendino, JJ, Jr., Gutkind, JS, Spiegel, AM (1991) Activating and inactivating mutations of the alpha subunit of Gi2 protein have opposite effects on proliferation of NIH 3T3 cells. *Proc Natl Acad Sci U S A* **88**(23): 10455-10459.

Herr, I, Debatin, K-M (2001) Cellular stress response and apoptosis in cancer therapy. *Blood* **98**(9): 2603-2614.

Hess, JF, Borkowski, JA, Young, GS, Strader, CD, Ransom, RW (1992) Cloning and pharmacological characterization of a human bradykinin (BK-2) receptor. *Biochem Biophys Res Commun* **184**(1): 260-268.

Higashijima, T, Uzu, S, Nakajima, T, Ross, EM (1988) Mastoparan, a peptide toxin from wasp venom, mimics receptors by activating GTP-binding regulatory proteins (G proteins). *J Biol Chem* **263**(14): 6491-6494.

Hirsch, E, Katanaev, VL, Garlanda, C, Azzolino, O, Pirola, L, Silengo, L, Sozzani, S, Mantovani, A, Altruda, F, Wymann, MP (2000) Central role for G protein-coupled phosphoinositide 3-kinase gamma in inflammation. *Science* **287**(5455): 1049-1053.

Holdsworth, G, Slocombe, P, Hutchinson, G, Milligan, G (2005) Analysis of endogenous S1P and LPA receptor expression in CHO-K1 cells. *Gene* **350**(1): 59-63.

Hollins, B, Kuravi, S, Digby, GJ, Lambert, NA (2009) The c-terminus of GRK3 indicates rapid dissociation of G protein heterotrimers. *Cell Signal* **21**(6): 1015-1021.

Hooshmand-Rad, R, Claesson-Welsh, L, Wennstrom, S, Yokote, K, Siegbahn, A, Heldin, CH (1997) Involvement of phosphatidylinositide 3'-kinase and Rac in platelet-derived growth factor-induced actin reorganization and chemotaxis. *Exp Cell Res* **234**(2): 434-441.

Huang, Y, Paxton, WA, Wolinsky, SM, Neumann, AU, Zhang, L, He, T, Kang, S, Ceradini, D, Jin, Z, Yazdanbakhsh, K, Kunstman, K, Erickson, D, Dragon, E, Landau, NR, Phair, J, Ho, DD, Koup, RA (1996) The role of a mutant CCR5 allele in HIV-1 transmission and disease progression. *Nat Med* **2**(11): 1240-1243.

Huttenrauch, F, Nitzki, A, Lin, FT, Honing, S, Oppermann, M (2002) Beta-arrestin binding to CC chemokine receptor 5 requires multiple C-terminal receptor phosphorylation sites and involves a conserved Asp-Arg-Tyr sequence motif. *J Biol Chem* **277**(34): 30769-30777.

Hwang, JI, Choi, S, Fraser, ID, Chang, MS, Simon, MI (2005a) Silencing the expression of multiple Gbeta-subunits eliminates signaling mediated by all four families of G proteins. *Proc Natl Acad Sci U S A* **102**(27): 9493-9498.

Hwang, JI, Shin, KJ, Oh, YS, Choi, JW, Lee, ZW, Kim, D, Ha, KS, Shin, HS, Ryu, SH, Suh, PG (2005b) Phospholipase C-beta3 mediates the thrombin-induced Ca²⁺ response in glial cells. *Mol Cells* **19**(3): 375-381.

Hynes, TR, Yost, E, Mervine, S, Berlot, CH (2008) Multicolor BiFC analysis of competition among G protein beta and gamma subunit interactions. *Methods* **45**(3): 207-213.

Inoue, S, Hoshino, S, Kukimoto, I, Ui, M, Katada, T (1995) Purification and characterization of the G203T mutant alpha i-2 subunit of GTP-binding protein expressed in baculovirus-infected Sf9 cells. *J Biochem* **118**(3): 650-657.

Janetopoulos, C, Jin, T, Devreotes, P (2001) Receptor-mediated activation of heterotrimeric G-proteins in living cells. *Science* **291**(5512): 2408-2411.

Joost, P, Methner, A (2002) Phylogenetic analysis of 277 human G-protein-coupled receptors as a tool for the prediction of orphan receptor ligands. *Genome Biol* **3**(11): RESEARCH0063.

Kamal, M, Marquez, M, Vauthier, V, Leloire, A, Froguel, P, Jockers, R, Couturier, C (2009) Improved donor/acceptor BRET couples for monitoring beta-arrestin recruitment to G protein-coupled receptors. *Biotechnol J* **4**(9): 1337-1344.

Kammermeier, PJ, Ruiz-Velasco, V, Ikeda, SR (2000) A voltage-independent calcium current inhibitory pathway activated by muscarinic agonists in rat sympathetic neurons requires both Galpha q/11 and Gbeta gamma. *J Neurosci* **20**(15): 5623-5629.

Karasawa, S, Araki, T, Nagai, T, Mizuno, H, Miyawaki, A (2004) Cyan-emitting and orange-emitting fluorescent proteins as a donor/acceptor pair for fluorescence resonance energy transfer. *Biochem J* **381**(Pt 1): 307-312.

Katragadda, M, Maciejewski, MW, Yeagle, PL (2004) Structural studies of the putative helix 8 in the human beta(2) adrenergic receptor: an NMR study. *Biochim Biophys Acta* **1663**(1-2): 74-81.

Kimple, RJ, Kimple, ME, Betts, L, Sondek, J, Siderovski, DP (2002) Structural determinants for GoLoco-induced inhibition of nucleotide release by Galpha subunits. *Nature* **416**(6883): 878-881.

- Kingsbury, DJ, Griffin, TA, Colbert, RA (2000) Novel propeptide function in 20 S proteasome assembly influences beta subunit composition. *J Biol Chem* **275**(31): 24156-24162.
- Knight, AW, Goddard, NJ, Billinton, N, Cahill, PA, Walmsley, RM (2002) Fluorescence polarization discriminates green fluorescent protein from interfering autofluorescence in a microplate assay for genotoxicity. *J Biochem Biophys Methods* **51**(2): 165-177.
- Kobilka, BK, Deupi, X (2007) Conformational complexity of G-protein-coupled receptors. *Trends Pharmacol Sci* **28**(8): 397-406.
- Kocan, M, Pflieger, KD (2009) Detection of GPCR/beta-arrestin interactions in live cells using bioluminescence resonance energy transfer technology. *Methods Mol Biol* **552**: 305-317.
- Kocan, M, See, HB, Seeber, RM, Eidne, KA, Pflieger, KD (2008) Demonstration of improvements to the bioluminescence resonance energy transfer (BRET) technology for the monitoring of G protein-coupled receptors in live cells. *J Biomol Screen* **13**(9): 888-898.
- Kostenis, E (2001) Is Galpha16 the optimal tool for fishing ligands of orphan G-protein-coupled receptors? *Trends Pharmacol Sci* **22**(11): 560-564.
- Kretsinger, RH (2005) *Proteins and the flow of Information in Cellular Function*. Oxford University Press.
- Kristiansen, K (2004) Molecular mechanisms of ligand binding, signaling, and regulation within the superfamily of G-protein-coupled receptors: molecular modeling and mutagenesis approaches to receptor structure and function. *Pharmacol Ther* **103**(1): 21-80.
- Krumins, AM, Gilman, AG (2006) Targeted knockdown of G protein subunits selectively prevents receptor-mediated modulation of effectors and reveals complex changes in non-targeted signaling proteins. *J Biol Chem* **281**(15): 10250-10262.
- Kumar, P, Wu, Q, Chambliss, KL, Yuhanna, IS, Mumby, SM, Mineo, C, Tall, GG, Shaul, PW (2007) Direct Interactions with G alpha i and G betagamma mediate nongenomic signaling by estrogen receptor alpha. *Mol Endocrinol* **21**(6): 1370-1380.
- Lambright, DG, Sondek, J, Bohm, A, Skiba, NP, Hamm, HE, Sigler, PB (1996) The 2.0 A crystal structure of a heterotrimeric G protein. *Nature* **379**(6563): 311-319.
- Laugwitz, KL, Allgeier, A, Offermanns, S, Spicher, K, Van Sande, J, Dumont, JE, Schultz, G (1996) The human thyrotropin receptor: a heptahelical receptor capable of stimulating members of all four G protein families. *Proc Natl Acad Sci U S A* **93**(1): 116-120.
- Leduc, M, Breton, B, Gales, C, Le Gouill, C, Bouvier, M, Chemtob, S, Heveker, N (2009) Functional selectivity of natural and synthetic prostaglandin EP4 receptor ligands. *J Pharmacol Exp Ther* **331**(1): 297-307.
- Lee, C, Liu, QH, Tomkowicz, B, Yi, Y, Freedman, BD, Collman, RG (2003) Macrophage activation through CCR5- and CXCR4-mediated gp120-elicited signaling pathways. *J Leukoc Biol* **74**(5): 676-682.

Lefrancois, S, Canuel, M, Zeng, J, Morales, CR (2005) Inactivation of sortilin (a novel lysosomal sorting receptor) by dominant negative competition and RNA interference. *Biol Proced Online* **7**: 17-25.

Lehmann, DM, Seneviratne, AM, Smrcka, AV (2008) Small molecule disruption of G protein beta gamma subunit signaling inhibits neutrophil chemotaxis and inflammation. *Mol Pharmacol* **73**(2): 410-418.

Li, Z, Jiang, H, Xie, W, Zhang, Z, Smrcka, AV, Wu, D (2000) Roles of PLC-beta2 and -beta3 and PI3Kgamma in chemoattractant-mediated signal transduction. *Science* **287**(5455): 1046-1049.

Lian, L, Wang, Y, Draznin, J, Eslin, D, Bennett, JS, Poncz, M, Wu, D, Abrams, CS (2005) The relative role of PLC{beta} and PI3K{gamma} in platelet activation. *Blood* **106**(1): 110-117.

Lim, JK, Glass, WG, McDermott, DH, Murphy, PM (2006) CCR5: no longer a "good for nothing" gene--chemokine control of West Nile virus infection. *Trends Immunol* **27**(7): 308-312.

Ling, K, Wang, P, Zhao, J, Wu, YL, Cheng, ZJ, Wu, GX, Hu, W, Ma, L, Pei, G (1999) Five-transmembrane domains appear sufficient for a G protein-coupled receptor: functional five-transmembrane domain chemokine receptors. *Proc Natl Acad Sci U S A* **96**(14): 7922-7927.

Litosch, I (1997) G-protein betagamma subunits antagonize protein kinase C-dependent phosphorylation and inhibition of phospholipase C-beta1. *Biochem J* **326** (Pt 3): 701-707.

Logothetis, DE, Kurachi, Y, Galper, J, Neer, EJ, Clapham, DE (1987) The beta gamma subunits of GTP-binding proteins activate the muscarinic K⁺ channel in heart. *Nature* **325**(6102): 321-326.

Lohse, MJ, Nikolaev, VO, Hein, P, Hoffmann, C, Vilardaga, JP, Bunemann, M (2008) Optical techniques to analyze real-time activation and signaling of G-protein-coupled receptors. *Trends Pharmacol Sci* **29**(3): 159-165.

Mackay, CR (2001) Chemokines: immunology's high impact factors. *Nat Immunol* **2**(2): 95-101.

Maggio, R, Vogel, Z, Wess, J (1993) Coexpression studies with mutant muscarinic/adrenergic receptors provide evidence for intermolecular "cross-talk" between G-protein-linked receptors. *Proc Natl Acad Sci U S A* **90**(7): 3103-3107.

Mahadeo, DC, Janka-Junttila, M, Smoot, RL, Roselova, P, Parent, CA (2007) A chemoattractant-mediated Gi-coupled pathway activates adenylyl cyclase in human neutrophils. *Mol Biol Cell* **18**(2): 512-522.

Maki, AH, Co, T (1976) Study of triple-singlet energy transfer in an enzyme-dye complex using optical detection of magnetic resonance. *Biochemistry* **15**(6): 1229-1235.

Marc, T, Morad, Z, Jean-Claude, M, Marie-Jo, M, Maité, C-M (2006) Sensitivity of CFP/YFP and GFP/mCherry pairs to donor photobleaching on FRET determination by fluorescence

lifetime imaging microscopy in living cells. *Microscopy Research and Technique* **69**(11): 933-939.

Marinissen, MJ, Gutkind, JS (2001) G-protein-coupled receptors and signaling networks: emerging paradigms. *Trends Pharmacol Sci* **22**(7): 368-376.

Marmorstein, AD, Marmorstein, LY, Sakaguchi, H, Hollyfield, JG (2002) Spectral profiling of autofluorescence associated with lipofuscin, Bruch's Membrane, and sub-RPE deposits in normal and AMD eyes. *Invest Ophthalmol Vis Sci* **43**(7): 2435-2441.

Marrero, MB, Schieffer, B, Paxton, WG, Heerdt, L, Berk, BC, Delafontaine, P, Bernstein, KE (1995) Direct stimulation of Jak/STAT pathway by the angiotensin II AT1 receptor. *Nature* **375**(6528): 247-250.

Martin, JC, Bandres, JC (1999) Cells of the monocyte-macrophage lineage and pathogenesis of HIV-1 infection. *J Acquir Immune Defic Syndr* **22**(5): 413-429.

Massey, V (2002) The reactivity of oxygen with flavoproteins. *International Congress Series* **1233**: 3-11.

Massotte, D (2003) G protein-coupled receptor overexpression with the baculovirus-insect cell system: a tool for structural and functional studies. *Biochim Biophys Acta* **1610**(1): 77-89.

Matranga, C, Tomari, Y, Shin, C, Bartel, DP, Zamore, PD (2005) Passenger-strand cleavage facilitates assembly of siRNA into Ago2-containing RNAi enzyme complexes. *Cell* **123**(4): 607-620.

McCudden, CR, Hains, MD, Kimple, RJ, Siderovski, DP, Willard, FS (2005) G-protein signaling: back to the future. *Cell Mol Life Sci* **62**(5): 551-577.

Mellado, M, Rodriguez-Frade, JM, Vila-Coro, AJ, Fernandez, S, Martin de Ana, A, Jones, DR, Toran, JL, Martinez, AC (2001) Chemokine receptor homo- or heterodimerization activates distinct signaling pathways. *EMBO J* **20**(10): 2497-2507.

Milligan, G (2006) G-protein-coupled receptor heterodimers: pharmacology, function and relevance to drug discovery. *Drug Discov Today* **11**(11-12): 541-549.

Milligan, G (2003) High-content assays for ligand regulation of G-protein-coupled receptors. *Drug Discov Today* **8**(13): 579-585.

Mixon, MB, Lee, E, Coleman, DE, Berghuis, AM, Gilman, AG, Sprang, SR (1995) Tertiary and quaternary structural changes in Gi alpha 1 induced by GTP hydrolysis. *Science* **270**(5238): 954-960.

Moller, S, Vilo, J, Croning, MD (2001) Prediction of the coupling specificity of G protein coupled receptors to their G proteins. *Bioinformatics* **17 Suppl 1**: S174-181.

Monici, M (2005) Cell and tissue autofluorescence research and diagnostic applications. *Biotechnol Annu Rev* **11**: 227-256.

- Montecarlo, FS, Charo, IF (1996) The amino-terminal extracellular domain of the MCP-1 receptor, but not the RANTES/MIP-1 α receptor, confers chemokine selectivity. Evidence for a two-step mechanism for MCP-1 receptor activation. *J Biol Chem* **271**(32): 19084-19092.
- Mueller, A, Kelly, E, Strange, PG (2002a) Pathways for internalization and recycling of the chemokine receptor CCR5. *Blood* **99**(3): 785-791.
- Mueller, A, Mahmoud, NG, Goedecke, MC, McKeating, JA, Strange, PG (2002b) Pharmacological characterization of the chemokine receptor, CCR5. *Br J Pharmacol* **135**(4): 1033-1043.
- Mueller, A, Mahmoud, NG, Strange, PG (2006) Diverse signalling by different chemokines through the chemokine receptor CCR5. *Biochemical Pharmacology* **72**(6): 739-748.
- Mueller, A, Strange, PG (2004a) CCL3, acting via the chemokine receptor CCR5, leads to independent activation of Janus kinase 2 (JAK2) and Gi proteins. *FEBS Lett* **570**(1-3): 126-132.
- Mueller, A, Strange, PG (2004b) Mechanisms of internalization and recycling of the chemokine receptor, CCR5. *Eur J Biochem* **271**(2): 243-252.
- Mukhopadhyay, S, Howlett, AC (2005) Chemically distinct ligands promote differential CB1 cannabinoid receptor-Gi protein interactions. *Mol Pharmacol* **67**(6): 2016-2024.
- Mulholland, DJ, Cox, M, Read, J, Rennie, P, Nelson, C (2004) Androgen responsiveness of Renilla luciferase reporter vectors is promoter, transgene, and cell line dependent. *Prostate* **59**(2): 115-119.
- Murray-Whelan, R, Reid, JD, Piuze, I, Hezareh, M, Schlegel, W (1995) The guanine-nucleotide-binding protein subunit G α i2 is involved in calcium activation of phospholipase A2. Effects of the dominant negative G α i2 mutant, [G203T] G α i2, on activation of phospholipase A2 in Chinese hamster ovary cells. *FEBS Journal* **230**(1): 164.
- Nagai, T, Ibata, K, Park, ES, Kubota, M, Mikoshiba, K, Miyawaki, A (2002) A variant of yellow fluorescent protein with fast and efficient maturation for cell-biological applications. *Nat Biotechnol* **20**(1): 87-90.
- Natochin, M, Barren, B, Artemyev, NO (2006) Dominant negative mutants of transducin- α that block activated receptor. *Biochemistry* **45**(20): 6488-6494.
- Navarro, G, Aymerich, MS, Marcellino, D, Cortes, A, Casado, V, Mallol, J, Canela, EI, Agnati, L, Woods, AS, Fuxe, K, Lluís, C, Lanciego, JL, Ferré, S, Franco, R (2009) Interactions between calmodulin, adenosine A2A, and dopamine D2 receptors. *J Biol Chem* **284**(41): 28058-28068.
- Navenot, JM, Wang, ZX, Trent, JO, Murray, JL, Hu, QX, DeLeeuw, L, Moore, PS, Chang, Y, Peiper, SC (2001) Molecular anatomy of CCR5 engagement by physiologic and viral chemokines and HIV-1 envelope glycoproteins: differences in primary structural requirements for RANTES, MIP-1 α , and vMIP-II Binding. *J Mol Biol* **313**(5): 1181-1193.

- Neer, EJ, Lok, JM, Wolf, LG (1984) Purification and properties of the inhibitory guanine nucleotide regulatory unit of brain adenylate cyclase. *J Biol Chem* **259**(22): 14222-14229.
- Neer, EJ, Schmidt, CJ, Nambudripad, R, Smith, TF (1994) The ancient regulatory-protein family of WD-repeat proteins. *Nature* **371**(6495): 297-300.
- Neptune, ER, Bourne, HR (1997) Receptors induce chemotaxis by releasing the betagamma subunit of Gi, not by activating Gq or Gs. *Proc Natl Acad Sci U S A* **94**(26): 14489-14494.
- Neves, SR, Ram, PT, Iyengar, R (2002) G protein pathways. *Science* **296**(5573): 1636-1639.
- New, DC, Wong, YH (2003) CC chemokine receptor-coupled signalling pathways. *Sheng Wu Hua Xue Yu Sheng Wu Wu Li Xue Bao (Shanghai)* **35**(9): 779-788.
- Nguyen, AW, Daugherty, PS (2005) Evolutionary optimization of fluorescent proteins for intracellular FRET. *Nat Biotechnol* **23**(3): 355-360.
- Nibbs, RJ, Yang, J, Landau, NR, Mao, JH, Graham, GJ (1999) LD78beta, a non-allelic variant of human MIP-1alpha (LD78alpha), has enhanced receptor interactions and potent HIV suppressive activity. *J Biol Chem* **274**(25): 17478-17483.
- Nikolaev, VO, Boettcher, C, Dees, C, Bunemann, M, Lohse, MJ, Zenk, MH (2007) Live cell monitoring of mu-opioid receptor-mediated G-protein activation reveals strong biological activity of close morphine biosynthetic precursors. *J Biol Chem* **282**(37): 27126-27132.
- Nishiumi, F, Sone, T, Kishine, H, Thyagarajan, B, Kogure, T, Miyawaki, A, Chesnut, JD, Imamoto, F (2009) Simultaneous single cell stable expression of 2-4 cDNAs in HeLaS3 using psiC31 integrase system. *Cell Struct Funct* **34**(1): 47-59.
- Nobles, M, Benians, A, Tinker, A (2005) Heterotrimeric G proteins precouple with G protein-coupled receptors in living cells. *Proc Natl Acad Sci U S A* **102**(51): 18706-18711.
- Ohashi, T, Galiacy, SD, Briscoe, G, Erickson, HP (2007) An experimental study of GFP-based FRET, with application to intrinsically unstructured proteins. *Protein Sci* **16**(7): 1429-1438.
- Oldham, WM, Hamm, HE (2007) How do receptors activate G proteins? *Adv Protein Chem* **74**: 67-93.
- Onuffer, JJ, Horuk, R (2002) Chemokines, chemokine receptors and small-molecule antagonists: recent developments. *Trends Pharmacol Sci* **23**(10): 459-467.
- Oppermann, M (2004) Chemokine receptor CCR5: insights into structure, function, and regulation. *Cell Signal* **16**(11): 1201-1210.
- Pahl, HL (1999) Signal transduction from the endoplasmic reticulum to the cell nucleus. *Physiol Rev* **79**(3): 683-701.
- Parekh, AB, Putney, JW, Jr. (2005) Store-operated calcium channels. *Physiol Rev* **85**(2): 757-810.

- Patel, TB, Du, Z, Pierre, S, Cartin, L, Scholich, K (2001) Molecular biological approaches to unravel adenylyl cyclase signaling and function. *Gene* **269**(1-2): 13-25.
- Pfleger, KD (2009) Analysis of protein-protein interactions using bioluminescence resonance energy transfer. *Methods Mol Biol* **574**: 173-183.
- Piebler, J (2005) New methodologies for measuring protein interactions in vivo and in vitro. *Curr Opin Struct Biol* **15**(1): 4-14.
- Pittner, RA, Fain, JN (1989) Exposure of cultured hepatocytes to cyclic AMP enhances the vasopressin-mediated stimulation of inositol phosphate production. *Biochem J* **257**(2): 455-460.
- Platt, EJ, Wehrly, K, Kuhmann, SE, Chesebro, B, Kabat, D (1998) Effects of CCR5 and CD4 cell surface concentrations on infections by macrophagetropic isolates of human immunodeficiency virus type 1. *J Virol* **72**(4): 2855-2864.
- Pokorny, V, McQueen, F, Yeoman, S, Merriman, M, Merriman, A, Harrison, A, Highton, J, McLean, L (2005) Evidence for negative association of the chemokine receptor CCR5 d32 polymorphism with rheumatoid arthritis. *Ann Rheum Dis* **64**(3): 487-490.
- Pollok, BA, Heim, R (1999) Using GFP in FRET-based applications. *Trends Cell Biol* **9**(2): 57-60.
- Preininger, AM, Parello, J, Meier, SM, Liao, G, Hamm, HE (2008) Receptor-mediated changes at the myristoylated amino terminus of Galpha(il) proteins. *Biochemistry* **47**(39): 10281-10293.
- Puck, TT, Cieciura, SJ, Robinson, A (1958) Genetics of somatic mammalian cells. III. Long-term cultivation of euploid cells from human and animal subjects. *J Exp Med* **108**(6): 945-956.
- Qin, K, Sethi, PR, Lambert, NA (2008) Abundance and stability of complexes containing inactive G protein-coupled receptors and G proteins. *FASEB J* **22**(8): 2920-2927.
- Quignard, JF, Mironneau, J, Carricaburu, V, Fournier, B, Babich, A, Nurnberg, B, Mironneau, C, Macrez, N (2001) Phosphoinositide 3-kinase gamma mediates angiotensin II-induced stimulation of L-type calcium channels in vascular myocytes. *J Biol Chem* **276**(35): 32545-32551.
- Quitterer, U, Lohse, MJ (1999) Crosstalk between Galpha(i)- and Galpha(q)-coupled receptors is mediated by Gbetagamma exchange. *Proc Natl Acad Sci U S A* **96**(19): 10626-10631.
- Rizzo, MA, Springer, GH, Granada, B, Piston, DW (2004) An improved cyan fluorescent protein variant useful for FRET. *Nat Biotechnol* **22**(4): 445-449.
- Robishaw, JD, Berlot, CH (2004) Translating G protein subunit diversity into functional specificity. *Curr Opin Cell Biol* **16**(2): 206-209.

- Roka, F, Brydon, L, Waldhoer, M, Strosberg, AD, Freissmuth, M, Jockers, R, Nanoff, C (1999) Tight association of the human Mel(1a)-melatonin receptor and G(i): precoupling and constitutive activity. *Mol Pharmacol* **56**(5): 1014-1024.
- Rovati, GE, Capra, V, Neubig, RR (2007) The highly conserved DRY motif of class A G protein-coupled receptors: beyond the ground state. *Mol Pharmacol* **71**(4): 959-964.
- Rye, HS (2001) Application of fluorescence resonance energy transfer to the GroEL-GroES chaperonin reaction. *Methods* **24**(3): 278-288.
- Samson, M, LaRosa, G, Libert, F, Paindavoine, P, Detheux, M, Vassart, G, Parmentier, M (1997) The second extracellular loop of CCR5 is the major determinant of ligand specificity. *J Biol Chem* **272**(40): 24934-24941.
- Sangmi, LEE, Richard L, B, William, M (2009) Use of confocal laser scanning microscopy in systematics of insects with a comparison of fluorescence from different stains. *Systematic Entomology* **34**(1): 10-14.
- Savarese, TM, Wang, CD, Fraser, CM (1992) Site-directed mutagenesis of the rat m1 muscarinic acetylcholine receptor. Role of conserved cysteines in receptor function. *J Biol Chem* **267**(16): 11439-11448.
- Savitzky, A, Golay, MJE (1964) Smoothing and Differentiation of Data by Simplified Least Squares Procedures. *Analytical Chemistry* **36**(8): 1627-1639.
- Scheideler, L, Ninnemann, H (1988) Method for identification of intracellular free flavin species in the photosensitive fungus *Neurospora crassa*. *Analytical Biochemistry* **173**(1): 106-110.
- Schmidt, CJ, Thomas, TC, Levine, MA, Neer, EJ (1992) Specificity of G protein beta and gamma subunit interactions. *J Biol Chem* **267**(20): 13807-13810.
- Seneviratne, P, Wedekind, J, Burroughs, M, Smrcka, A (2009) Biophysical characterization of G{beta}{gamma} "hot spot" binding small molecules: explaining G{beta}{gamma} "hot spot" binding effector selectivity. *The FASEB Journal* **23**(1_MeetingAbstracts): 583.583.
- Sheng, M, Hoogenraad, CC (2007) The postsynaptic architecture of excitatory synapses: a more quantitative view. *Annu Rev Biochem* **76**: 823-847.
- Shibata, T, Suzuki, C, Ohnishi, J, Murakami, K, Miyazaki, H (1996) Identification of regions in the human angiotensin II receptor type 1 responsible for Gi and Gq coupling by mutagenesis study. *Biochem Biophys Res Commun* **218**(1): 383-389.
- Shimomura, O, Johnson, FH, Saiga, Y (1962) Extraction, purification and properties of aequorin, a bioluminescent protein from the luminous hydromedusan, *Aequorea*. *J Cell Comp Physiol* **59**: 223-239.
- Short, AD, Winston, GP, Taylor, CW (2000) Different receptors use inositol trisphosphate to mobilize Ca(2+) from different intracellular pools. *Biochem J* **351 Pt 3**: 683-686.

Simmons, MA (2005) Functional selectivity, ligand-directed trafficking, conformation-specific agonism: what's in a name? *Mol Interv* **5**(3): 154-157.

Simon, MI, Strathmann, MP, Gautam, N (1991) Diversity of G proteins in signal transduction. *Science* **252**(5007): 802-808.

Simonds, WF (1999) G protein regulation of adenylate cyclase. *Trends Pharmacol Sci* **20**(2): 66-73.

Skiba, NP, Bae, H, Hamm, HE (1996) Mapping of effector binding sites of transducin alpha-subunit using G alpha t/G alpha i1 chimeras. *J Biol Chem* **271**(1): 413-424.

Smrcka, AV, Lehmann, DM, Dessal, AL (2008) G protein betagamma subunits as targets for small molecule therapeutic development. *Comb Chem High Throughput Screen* **11**(5): 382-395.

Smrcka, AV, Sternweis, PC (1993) Regulation of purified subtypes of phosphatidylinositol-specific phospholipase C beta by G protein alpha and beta gamma subunits. *J Biol Chem* **268**(13): 9667-9674.

Sondek, J, Bohm, A, Lambright, DG, Hamm, HE, Sigler, PB (1996) Crystal structure of a G-protein beta gamma dimer at 2.1A resolution. *Nature* **379**(6563): 369-374.

Sprang, SR (1997) G proteins, effectors and GAPs: structure and mechanism. *Curr Opin Struct Biol* **7**(6): 849-856.

Spring, DJ, Neer, EJ (1994) A 14-amino acid region of the G protein gamma subunit is sufficient to confer selectivity of gamma binding to the beta subunit. *J Biol Chem* **269**(36): 22882-22886.

Steffen, ASaDL (2008) The Endogenous GPCR List. <http://www.tumor-gene.org/GPCR/qpcr.html>.

Stephens, L, Jackson, TR, Hawkins, PT (1993) Activation of phosphatidylinositol 4,5-bisphosphate supply by agonists and non-hydrolysable GTP analogues. *Biochem J* **296** (Pt **2**): 481-488.

Stephens, LR, Eguinoa, A, Erdjument-Bromage, H, Lui, M, Cooke, F, Coadwell, J, Smrcka, AS, Thelen, M, Cadwallader, K, Tempst, P, Hawkins, PT (1997) The G beta gamma sensitivity of a PI3K is dependent upon a tightly associated adaptor, p101. *Cell* **89**(1): 105-114.

Stryer, L, Haugland, RP (1967) Energy transfer: a spectroscopic ruler. *Proc Natl Acad Sci U S A* **58**(2): 719-726.

Suki, WN, Abramowitz, J, Mattera, R, Codina, J, Birnbaumer, L (1987) The human genome encodes at least three non-allelic G proteins with alpha i-type subunits. *FEBS Lett* **220**(1): 187-192.

Suzuki, N, Nakamura, S, Mano, H, Kozasa, T (2003) Galpha 12 activates Rho GTPase through tyrosine-phosphorylated leukemia-associated RhoGEF. *Proc Natl Acad Sci U S A* **100**(2): 733-738.

- Talbot, CB, McGinty, J, Grant, DM, McGhee, EJ, Owen, DM, Zhang, W, Bunney, TD, Munro, I, Isherwood, B, Eagle, R, Hargreaves, A, Dunsby, C, Neil, MA, French, PM (2008) High speed unsupervised fluorescence lifetime imaging confocal multiwell plate reader for high content analysis. *J Biophotonics* **1**(6): 514-521.
- Tang, WJ, Gilman, AG (1991) Type-specific regulation of adenylyl cyclase by G protein beta gamma subunits. *Science* **254**(5037): 1500-1503.
- Taussig, R, Tang, WJ, Gilman, AG (1994a) Expression and purification of recombinant adenylyl cyclases in Sf9 cells. *Methods Enzymol* **238**: 95-108.
- Taussig, R, Tang, WJ, Hepler, JR, Gilman, AG (1994b) Distinct patterns of bidirectional regulation of mammalian adenylyl cyclases. *J Biol Chem* **269**(8): 6093-6100.
- Tesmer, JJ, Berman, DM, Gilman, AG, Sprang, SR (1997a) Structure of RGS4 bound to AlF4--activated G(i alpha1): stabilization of the transition state for GTP hydrolysis. *Cell* **89**(2): 251-261.
- Tesmer, JJ, Sunahara, RK, Gilman, AG, Sprang, SR (1997b) Crystal structure of the catalytic domains of adenylyl cyclase in a complex with Galpha.GTPgammaS. *Science* **278**(5345): 1907-1916.
- Thaminy, S, Miller, J, Stagljar, I (2004) The split-ubiquitin membrane-based yeast two-hybrid system. *Methods Mol Biol* **261**: 297-312.
- Thelen, M (2001) Dancing to the tune of chemokines. *Nat Immunol* **2**(2): 129-134.
- Tohgo, A, Choy, EW, Gesty-Palmer, D, Pierce, KL, Laporte, S, Oakley, RH, Caron, MG, Lefkowitz, RJ, Luttrell, LM (2003) The stability of the G protein-coupled receptor-beta-arrestin interaction determines the mechanism and functional consequence of ERK activation. *J Biol Chem* **278**(8): 6258-6267.
- Vesuna, F, Winnard, P, Jr., Raman, V (2005) Enhanced green fluorescent protein as an alternative control reporter to Renilla luciferase. *Anal Biochem* **342**(2): 345-347.
- Wall, MA, Coleman, DE, Lee, E, Iniguez-Lluhi, JA, Posner, BA, Gilman, AG, Sprang, SR (1995) The structure of the G protein heterotrimer Gi alpha 1 beta 1 gamma 2. *Cell* **83**(6): 1047-1058.
- Watts, VJ, Neve, KA (1997) Activation of type II adenylate cyclase by D2 and D4 but not D3 dopamine receptors. *Mol Pharmacol* **52**(2): 181-186.
- Wess, J, Han, SJ, Kim, SK, Jacobson, KA, Li, JH (2008) Conformational changes involved in G-protein-coupled-receptor activation. *Trends Pharmacol Sci* **29**(12): 616-625.
- Williams, RS, Boeckeler, K, Graf, R, Muller-Taubenberger, A, Li, Z, Isberg, RR, Wessels, D, Soll, DR, Alexander, H, Alexander, S (2006) Towards a molecular understanding of human diseases using Dictyostelium discoideum. *Trends Mol Med* **12**(9): 415-424.

- Wing, MR, Bourdon, DM, Harden, TK (2003) PLC-epsilon: a shared effector protein in Ras-, Rho-, and G alpha beta gamma-mediated signaling. *Mol Interv* **3**(5): 273-280.
- Wojcikiewicz, RJ, Luo, SG (1998) Phosphorylation of inositol 1,4,5-trisphosphate receptors by cAMP-dependent protein kinase. Type I, II, and III receptors are differentially susceptible to phosphorylation and are phosphorylated in intact cells. *J Biol Chem* **273**(10): 5670-5677.
- Wurm, FM (2004) Production of recombinant protein therapeutics in cultivated mammalian cells. *Nat Biotechnol* **22**(11): 1393-1398.
- Xu, X, Soutto, M, Xie, Q, Servick, S, Subramanian, C, von Arnim, AG, Johnson, CH (2007) Imaging protein interactions with bioluminescence resonance energy transfer (BRET) in plant and mammalian cells and tissues. *Proc Natl Acad Sci U S A* **104**(24): 10264-10269.
- Xu, Y, Piston, DW, Johnson, CH (1999) A bioluminescence resonance energy transfer (BRET) system: application to interacting circadian clock proteins. *Proc Natl Acad Sci U S A* **96**(1): 151-156.
- Yamanaka, I, Koinuma, S, Shigeyoshi, Y, Uchiyama, Y, Yagita, K (2007) Presence of robust circadian clock oscillation under constitutive over-expression of mCry1 in rat-1 fibroblasts. *FEBS Lett* **581**(21): 4098-4102.
- Yang, X, Taylor, L, Polgar, P (1999) Effect of the G-protein, G alpha(i2), and G alpha(i3) subunit knockdown on bradykinin-induced signal transduction in rat-1 cells. *Mol Cell Biol Res Commun* **1**(3): 227-236.
- Yi, TM, Kitano, H, Simon, MI (2003) A quantitative characterization of the yeast heterotrimeric G protein cycle. *Proc Natl Acad Sci U S A* **100**(19): 10764-10769.
- Ying, W (2008) NAD⁺/NADH and NADP⁺/NADPH in cellular functions and cell death: regulation and biological consequences. *Antioxid Redox Signal* **10**(2): 179-206.
- Yoder, JA, Walsh, CP, Bestor, TH (1997) Cytosine methylation and the ecology of intragenomic parasites. *Trends Genet* **13**(8): 335-340.
- Yohannan, S, Faham, S, Yang, D, Whitelegge, JP, Bowie, JU (2004) The evolution of transmembrane helix kinks and the structural diversity of G protein-coupled receptors. *Proc Natl Acad Sci U S A* **101**(4): 959-963.
- Yu, B, Simon, MI (1998) Interaction of the xanthine nucleotide binding Galpha mutant with G protein-coupled receptors. *J Biol Chem* **273**(46): 30183-30188.
- Yuan, C, Sato, M, Lanier, SM, Smrcka, AV (2007) Signaling by a non-dissociated complex of G Protein betagamma and alpha subunits stimulated by a receptor-independent activator of G protein signaling, AGS8. *J Biol Chem* **282**(27): 19938-19947.
- Yue, C, Dodge, KL, Weber, G, Sanborn, BM (1998) Phosphorylation of serine 1105 by protein kinase A inhibits phospholipase Cbeta3 stimulation by Galphaq. *J Biol Chem* **273**(29): 18023-18027.

Yue, C, Ku, CY, Liu, M, Simon, MI, Sanborn, BM (2000) Molecular mechanism of the inhibition of phospholipase C beta 3 by protein kinase C. *J Biol Chem* **275**(39): 30220-30225.

Zagar, Y, Chaumaz, G, Lieberherr, M (2004) Signaling cross-talk from Gbeta4 subunit to Elk-1 in the rapid action of androgens. *J Biol Chem* **279**(4): 2403-2413.

Zeng, FY, McLean, AJ, Milligan, G, Lerner, M, Chalmers, DT, Behan, DP (2003) Ligand specific up-regulation of a Renilla reniformis luciferase-tagged, structurally unstable muscarinic M3 chimeric G protein-coupled receptor. *Mol Pharmacol* **64**(6): 1474-1484.

Zhao, J, Ma, L, Wu, YL, Wang, P, Hu, W, Pei, G (1998) Chemokine receptor CCR5 functionally couples to inhibitory G proteins and undergoes desensitization. *J Cell Biochem* **71**(1): 36-45.

Zhu, X, Birnbaumer, L (1996) G protein subunits and the stimulation of phospholipase C by Gs- and Gi-coupled receptors: Lack of receptor selectivity of G α (16) and evidence for a synergic interaction between G β and the α subunit of a receptor activated G protein. *Proc Natl Acad Sci U S A* **93**(7): 2827-2831.

Zlotnik, A, Yoshie, O (2000) Chemokines: a new classification system and their role in immunity. *Immunity* **12**(2): 121-127.